Molecular Surveillance and Drug Target Discovery for Human Filarial Nematodes

By

Kendra Joy Dahmer

A dissertation submitted in partial fulfillment of the requirements for the degree of

Doctor of Philosophy

(Comparative Biomedical Sciences)

at the

UNIVERSITY OF WISCONSIN-MADISON

2023

Date of final oral examination: 07/21/2023

The dissertation is approved by the following members of the Final Oral Committee: Mostafa Zamanian, Associate Professor, Pathobiological Sciences
Lyric C. Bartholomay, Professor, Pathobiological Sciences
Tony L. Goldberg, Professor, Pathobiological Sciences
Ahna Skop, Professor, Genetic and Life Science Communications
Jennifer E. Golden, Associate Professor, Pharmaceutical Sciences

ABSTRACT

Vector-borne parasitic nematodes (roundworms) cause diseases associated with poverty endemic to underdeveloped and exploited countries, infecting 100's of millions of people globally. These nematode diseases are often overlooked and understudied providing ample room for improving treatment and the understanding of these parasites basic biology. In my dissertation research. I implement and establish surveillance strategies for vector-borne parasitic nematodes and develop and optimize methods to characterize a prominent family of cell surface receptors that serve as promising drug targets. In chapter two, I describe one of the most prevalent under-studied vector-borne parasite infections. mansonellosis, comparatively benchmark classical and molecular diagnostics. We perform genomic analysis to confirm species identity and determine close clustering with sequenced isolates from neighboring countries. We explore associations between parasite infection and other demographic and clinical variables using statistical modeling. Additionally, we successfully establish cryopreservation and revitalization of Mansonella ozzardi microfilariae, advancing the prospects of rearing infective larvae in laboratory settings. Together, these data suggest a severe underestimation of true mansonellosis prevalence in Colombia, and we expect that these methods will help facilitate the study of mansonellosis in both endemic and laboratory settings. In chapter three and four, I transition my focus from surveillance to molecular parasitology. Since current control mechanisms for lymphatic filariasis (LF) infections rely upon mass drug administration with suboptimal antiparasitic drugs (anthelmintics), we need new treatments with novel targets. I focus on a family of biogenic amine G protein-coupled receptors (BA-GPCRs) that have remained unexploited as potential anthelmintic targets. In chapter three, I establish experimental and computational pipelines to explore the druggability and pharmacology of GPCRs. I focus my research on spatio-temporal expression patterns and the pharmacological profile of Bma-GAR-3, an acetylcholine receptor. In chapter four, I expand my characterization of BA-GPCRs using high throughput phenotypic assays. Dopamine and dopaminergic compounds negatively affected fitness phenotypes and I prioritized 12 dopaminergic compounds from a neurotransmitter library that have strong microfilarial and mixed adulticidal effects. Using homology-based searches, I identify BA-GPCRs and ion channel receptors that could be mediating the observed effects. Fundamental knowledge of novel helminth drug targets is crucial for the future control and elimination of LF and other neglected diseases. These approaches progress the characterization and screening of a promising class of proteins with anthelmintic target potential.

DEDICATION

To Lydia, Zhora, and Clementine.



ACKNOWLEDGEMENTS

The University of Wisconsin Madison occupies ancestral Ho-Chunk land, a place their nation has called Teejop (day-JOPE) since time immemorial. In an 1832 treaty, the Ho-Chunk were forced to cede this territory. Decades of ethnic cleansing followed when both the federal and state government repeatedly, but unsuccessfully, sought to forcibly remove the Ho-Chunk from Wisconsin. We acknowledge the circumstances that led to the forced removal of the Ho-Chunk people, and honor their legacy of resistance and resilience. This history of colonization informs our work and vision for a collaborative future. We recognize and respect the inherent sovereignty of the Ho-Chunk Nation and the other 11 Native Nations within the boundaries of the state of Wisconsin.

I want to acknowledge and thank the indigenous people from the Departamento del Amazonas Colombia who voluntarily allowed us into their communities to study *Mansonella*. Without the indigenous people in the Amazon region of Colombia, part of my research would not have been possible.

I would also like to thank my family for their unwavering support. My brother, Atlas, thank you for always being there for me and making me laugh more than anyone else. Thank you for always being yourself and showing me what true bravery and resilience is throughout this chaotic life! Thank you for always taking care of the cats when I would spend long days in the lab, field, or hiking. I want to thank my two sisters, Kamlyn and Shani. Kamlyn, I wouldn't have accomplished any of my successes if it wasn't for your persistent guidance and the sacrifices you made. Thank you for ensuring I always prioritized my education. Shani, thank you for always listening to me complain and having such strength and tenacity throughout everything life has thrown at us! You are truly a role model with huge aspirations! I want to thank my mom, Julie, for being a model for overcoming seemingly impossible challenges. To my dad, Brian, thank you for making difficult decisions while also letting me explore my own path in life. Thank you for believing that college was something attainable and realistic for me to pursue. To my Grandma and Grandpa Dahmer, thank you for always accepting me, without judgment, and having your home open to me throughout my life.

To the members of the Zamanian lab, you've made this journey fun and exciting even when faced with some of the most complicated scientific challenges. Clair, thank you for bringing a positive disposition to the lab and encouraging me to keep going even after numerous failed experiments. Katie, thank you for the touch of chaos you brought to the lab and helping me establish some work-life balance by getting out of the lab and hiking. Thank you both for prioritizing friendship and grabbing a few gin drinks after celebrations or after an exceptionally frustrating week. You both are truly life long friends. Dr. Zamanian, thank you for believing in me and giving me the opportunity to grow as a scientist. Thank you for encouraging me and giving me opportunities to define projects that drive my scientific curiosity.

To my committee members, thank you for all your advice and guidance during the last five years. I have benefited tremendously from the plethora of knowledge and the diverse expertise that has helped guide my research.

To myself, "In spite of it all. Life is beautiful." (IDLES 2021).

Table of Contents

ABSTRACT	i
DEDICATION	ii
ACKNOWLEDGEMENTS	iii
CHAPTER 1: INTRODUCTION	1
Introduction	2
Dissertation Synopsis	13
Literature Cited	15
Figures	22
CHAPTER 2: Molecular surveillance detects high prevalence of the neglecte	ed parasite
Mansonella ozzardi in the Colombian Amazon	24
Abstract	25
Introduction	26
Methods	27
Results	33
Discussion	37
Acknowledgments	39
Funding	39
Conflicts of interest	40
Literature Cited	40
Figures	45
Supplementary materials	51
CHAPTER 3: Pharmacological Profiling of a Brugia malayi Muscarinic Acety	Icholine Receptor
as a Putative Antiparasitic Target	54
Abstract	55

	Introduction	56
	Results and Discussion	58
	Conclusion	67
	Methods	68
	Acknowledgments	76
	Funding	77
	Literature Cited	78
	Figures	87
	Supplementary materials	95
CHAP	TER 4: High throughput aminergic library screen prioritizes dopaminergic recept	ors for
antheli	mintic discovery	97
	Abstract	98
	Introduction	99
	Results and Discussion	101
	Conclusion and future directions	105
	Methods	107
	Acknowledgments	111
	Funding	112
	Literature Cited	112
	Figures	118
	Supplementary materials	126
CHAP	TER 5: CONCLUSION	130
	Conclusion	131
	Literature Cited	134

Chapter 1: INTRODUCTION

1.1 Arthropod-borne nematodes of significance

Neglected tropical diseases (NTDs) are infectious diseases of poverty caused by viruses, microbes, and parasites. Nearly half of the 26 million disability-adjusted life years (DALYs) associated with NTDs are a result of parasitic worm (helminth) infections with parasitic nematode (roundworm) infections alone accounting for around 8 million DALYs [1]. (One DALY is equivalent to the loss of one year of prime health.) Roundworms infect nearly two billion humans [1,2] in addition to companion animals and wildlife. Soil-transmitted helminths (STH) account for the majority of roundworm infections with the remaining caused by vector-borne parasitic nematodes.

Eradication of these parasitic nematodes has been difficult but some progress has been made towards this end. For instance, Dracunculiasis, or Guinea worm, afflicts individuals in Africa who do not have reliable access to clean water and thus ingest copepods containing infectious stage larvae. Progress towards global elimination of Guinea worm has been highly successful however, dogs have recently been identified as reservoirs complicating eradication programs [3,4].

Members of the Filarioidea superfamily are arthropod-borne, clade IIIc, parasitic nematodes [5] that infect vertebrate hosts. These parasites share a common lifecycle, differing mainly in the invertebrate vector (intermediate host) and locations of development in both the vector and mammalian definitive host (**Fig 1**). Several species of these filarial parasites are of global veterinary and medical importance. *Dirofilaria spp.* (*immitis, repens*), *Brugia pahangi*, and *Acanthocheilonema reconditum* are significant parasites in global veterinary medicine and companion animals (dogs, cats) may serve as reservoirs for zoonotic arthropod-borne nematodes [6–8]. Both *Dirofilaria spp.* (heartworm) and *B. pahangi* are mosquito transmitted while *A. reconditum* is primarily transmitted by fleas or lice.

NTDs in humans caused by arthropod-borne nematodes include lymphatic filariasis (*Wuchereria bancrofti, Brugia malayi, Brugia timori*), onchocerciasis (*Onchocerca volvulus*) and dracunculiasis (*Dracunculus medinensis*) [9]. Lymphatic filariasis (LF) is a chronic infection that can lead to disability and disfigurement and nearly one billion individuals are at risk of infection across 57 countries [10]. *Wuchereria bancrofti, Brugia malayi,* and *Brugia timori* are transmitted by several different genera of mosquitoes restricted by geographic distribution across Africa, Asia, South America, and Caribbean and Pacific islands [11]. Onchocerciasis, or river blindness, is mainly transmitted in sub-Saharan Africa by black flies and currently infects over 20 million individuals worldwide with over one million suffering from visual impairment [12,13].

Despite lacking the title of NTD, other less well studied species of filarial parasites are projected to infect hundreds of millions of individuals worldwide [14,15] and cause diseases such as mansonellosis (Mansonella streptocerca, Mansonella perstans, Mansonella ozzadi) and loiasis (Loa loa). Mansonellosis and loiasis are both severely under-mapped and many questions surrounding their biology are unresolved. Mansonella parasites infect hundreds of millions of people throughout Africa and Central and South America [14]. The vector responsible for transmitting Mansonella is likely dependent on both species and geographic distributions, and both Simulium (black flies) and Culicoides (biting midges) species have been implicated in transmission dynamics. Symptoms for mansonellosis are not well resolved and variable pathologies (ranging from asymptomatic to more chronic symptoms including headache, fatique, itching) have been reported requiring further study to investigate clinical and subclinical impacts [16]. Loa loa, or eye worm, is transmitted by Chrysops (deer flies) and infects around 13 million individuals in western and central Africa causing symptoms and complications ranging from complete absence to severe cardiac, cerebral, and neurologic pathologies [15,17]. Over 30 million individuals are at risk of exposure and infection of L. loa. Both loiasis and mansonellosis complicate diagnostics and treatment for other filarial parasites in co-endemic areas.

These parasitic nematode infections, regardless of their distinction as NTDs or not, perpetuate poverty in endemic counties. Social stigmatism, health loss, and secondary economic impacts from both deterred tourism and the cost of treatment interventions are common detrimental effects not portrayed by DALY measures [1]. The true deleterious effects of arthropod-borne parasitic nematodes are profusely underestimated and further study as well as improved interventions, prophylactics, and therapeutics can reduce this gross human and animal suffering.

1.2 Treatment discovery and control interventions

1.2.1 Anthelmintic discovery and pitfalls

Current control mechanisms for human helminth infections almost entirely rely upon mass drug administration (MDA) with a limited arsenal of drugs. Historically, there are two standard methods for anthelmintic drug discovery [18]. One approach, whole-organism screening, measures endpoint phenotypes such as motility and mortality of parasites in culture. This approach is advantageous because *a priori* knowledge of targets or drug mechanisms of action are not required; all endogenous tissue and receptor types are present in the parasite [19,20]. Furthermore, exposure or permeability can be determined sufficiently in whole-organism screens if phenotypes are observed in response to the compound [21]. However, obtaining enough parasite tissue can be difficult due to complex life-cycles and lack of adequate animal models, leading to many whole-organism screens being low-throughput or done in the microfilariae (mf) lifestage [19,22,23]. Showing efficacy in mf often does not translate to efficacy in the L3 infectious stage or adult stage parasites [19]. Moreover, whole-organism screens tend to result in both false negative and false positive leads.

Effective drugs may be overlooked due to lack of whole-organism phenotypes.

Ivermectin, a frontline drug in both veterinary and human medicine, rapidly reduces and often clears microfilaremia in the host but *in vitro* there are no motility or mortality phenotypes

associated with application of drug directly to parasites in culture [24–26]. On the other hand, drugs that caused phenotypes from whole-organism screens have been pursued which did not translate to any efficacy *in vivo* [21]. This may be due to the pharmacokinetics and pharmacodynamics (i.e. drug metabolism) in the host making the compound not biologically available or active at the location harboring parasites [20]. In this same vein, off-target effects can be deleterious to the host. Additionally, host-parasite interaction may complicate *in vivo* studies. Parasites modulate the host's immune system and knowledge surrounding the drug-host-parasite interface has not been thoroughly investigated [27–29]. Praziquantel (PZQ), a drug used to treat the helminth disease schistosomiasis, has a paralyzing effect on parasites and clearance may be mediated by a direct effect of PZQ upregulating the host's immune cells [23,30]. Lack of new drugs being developed from whole-organism screens has pushed researchers towards a lower cost, high-throughput approach [31].

This second approach, target-based screening, utilizes a surrogate cell line for heterologous parasitic receptor expression. Target-based screens can be used to prioritize receptors that regulate critical biological processes in the parasite but this approach also has limitations. Many potential therapeutic targets have not been deophanized and limited molecular tools are available to begin characterizing these targets outside of bioinformatic analysis which are often based on developing gene models [20,23]. And, while it is advantageous to directly perturb a specific known receptor, it is not guaranteed that all receptors express properly in cell types derived from distant phylogenetic lineages [32]. The combinations of potential subunit combinations, accessory proteins, molecular chaperones, and membrane determinants required for the successful trafficking and signaling of parasite receptors in surrogate systems have not been comprehensively identified [33]. Direct target perturbation via cell line expression overcomes the hindrance of permeability making the target easily accessible by test compounds but this may not translate to whole-organism or *in vivo* screens [31].

Concentrations needed for compounds to be bioavailable may not be reached in whole-organism screens or may have toxic effects on the host *in vivo* [21]. Furthermore, culture conditions for target-based screens are even further removed from host conditions than that of whole-organism screens. However, a key advantage of target-based screens is the high-throughput capacity and ability to follow up on compound hits in a more cost effective manner. Compounds of interest from initial screens can be used in counter-screens to reduce the risk of off-target effects *in vivo* and to assays for broad spectrum nematode efficacy [21]. Further, these leads can be used in low throughput whole-organism screens before moving to *in vivo* animal model screening further improving the probability of a successful *in vivo* screen [21].

Both whole-organism and target-based approaches overcome the labor, time and cost intensiveness of *in vivo* animal screening which has historically been used [19,21]. However, neither of these approaches have brought a new antihelminthic to market for human use [20]. The ability to predict *in vivo* efficacy based on *in vitro* screens has proved difficult due to off-target effects on the host, uncharacterized drug-host-parasite interaction, drug metabolism and bioavailability, inefficient target expression and lack of deorphanized targets of interest [20,23,34]. Ideally, target based screens combined with whole-organism screening could lead to new promising leads.

Nearly all anthelmintics approved for human use were initially used in veterinary medicine and discovered from *in vivo* screens in animals [21,35,36]. *Post hoc* determination of the mechanism of action and potential receptor targets for all major antinematodal compounds used a model nematode, *Caenorhabditis elegans* [37–40] (**Table 1**). In fact, *C. elegans*, a clade IV free-living nematode, has been used to advance our understanding of the mechanism of action for anthelmintics and is an important organism for identifying putative anthelmintic targets due to the range of molecular tools available to manipulate its genetics which are unavailable in intractable parasitic nematodes.

1.2.2 Current treatment options

In veterinary medicine, heartworm is prevented with prophylactic intervention using macrocyclic lactones (MLs) and milbemycins [41]. Heartworm prevention is often coupled with pyrantel and PZQ for prevention of other roundworms and flatworms (tapeworms). With ML resistance in *D. immitis*. being documented [41], novel prophylactics and safer, less toxic, adulticide drugs are needed for preventing and treating patent infections. Current treatment for animals, mainly canines, with adult heartworm infections relies on the arsenic based drug melarsomine paired with doxycycline (tetracycline antibiotic) and MLs [42,43]. There are no efficacious adulticidal anthelmintics in human medicine although the antibiotic, doxycycline, has been shown to have some adulticidal effects. Doxycycline is a broad spectrum antibiotic that targets the endosymbiotic bacteria *Wolbachia* that, in most filarial parasites, is required for development and survival [44]. In human medicine doxycycline has been shown to be an effective adulticidal treatment for LF, onchocerciasis, and potentially *M. perstans* but the treatment regime requires daily dosages for up to six weeks which is difficult to implement and ensure compliance, and is more costly than current MDA [44].

MDA for arthropod-borne parasitic nematode infections in humans currently include ivermectin (IVM, ML), albendazole (ABZ, benzimidazole), and diethylcarbamazine (DEC). IVM targets invertebrate specific glutamate-gated chloride channels leading to worm paralysis and is used in MDA campaigns for LF and onchocerciasis [35,45–47]. Despite IVM rapidly clearing blood-circulating mf from the host, it does not kill or clear adult worms from infected individuals [26,48]. Furthermore, due to severe adverse reactions, IVM is contraindicated in areas co-endemic with loiasis [49]. ABZ targets β-tubulins and inhibits microtubule polymerization leading to mf death and is the key anthelmintic used in MDA for STH as well as LF and onchocerciasis and can be used in *L. loa* endemic regions [35,45,50]. DEC exhibits strong efficacy against mf despite its mechanism of action not being well understood [48]. DEC is contraindicated in areas co-endemic with onchocerciasis due to Mazzotti adverse reactions [51].

Currently, there is no treatment regime established for dracunculiasis or mansonellosis. A new and exciting anthelmintic, Emodepside, is used in veterinary medicine for STH treatment and prevention and is currently in clinical trials for treatment of river blindness [44,49,52,53]. Due to its broad anthelmintic efficacy and novel target, emodepside is being pursued for other filarial parasite and STH infections in humans [37,54–56].

1.2.3 Anthelmintic resistance

Currently, most anthelmintic drugs primarily target ligand-gated ion channels (LGICs) in both veterinary and human medicine and almost all drugs that target ion channels, including anthelmintics, were discovered via *in vivo* animal screens without a priori knowledge of the mechanism of action (MOA) [21,35,57]. Ion channels are typically multimeric, fast-acting, have different gating-mechanisms, and are both functionally and structurally diverse receptors. LGICs targeted by anthelmintics regulate many critical physiological processes and dysregulation of these receptors leads to pathophysiology in the parasite making them good drug targets [57,58]. Furthermore, some LGICs are solely found in invertebrates and can be selectively targeted such as glutamate-gated ion channels, the target of ivermectin [59]. LGICs make up the second largest class of drug targets in human medicine and there are still unexplored LGICs predicted in parasite genomes that could act as promising drug targets [57–59].

Unfortunately, with the field moving toward *in vitro* screening approaches LGICs have become more difficult to study. LGICs cloned into cell lines are often unstable, overexpressed, and detrimental to the cell [57]. If a cell survives cloning, LGICs often do not fold or associate with their subunits properly leading to non-native pharmacology and cell toxicity [57]. Another issue with cloning LGICs is the lack of fundamental knowledge of endogenous parasite receptor subunit composition. For cell line expression and native pharmacology to be preserved, each subunit of the channel needs to be expressed and interact properly. Furthermore, if a stable cell line is developed, measuring receptor function in a high-throughput screen is difficult [57,60].

Ligand binding and fluorescence-based assays measuring receptor activation have been successful but have mild functional relevance to actual receptor function [57,60]. The patch-clamp method of measuring channel activity remains the gold standard but is a low-throughput, expensive, and time consuming assay [60]. Furthermore, the fast acting nature of these receptors may also lead to fast recovery in the parasite. Anthelmintics, such as ivermectin, that act on LGICs typically lead to quick paralysis and clearance of larval stages but do not lead to clearance of adult parasites from the host [47,59,61]. Additionally, the rapid killing of larval stages has led to adverse effects in the host [13,51]. Overall, LGICs are good drug targets but due to rapidly developing resistance, lack of adulticidal drugs, and difficulties studying these receptors via high-throughput screens other druggable targets need to be examined.

1.2.4 G protein-coupled receptors

A group of drug targets prevalent in human medicine are the G protein-coupled receptors (GPCRs). GPCRs are cell surface receptors that transduce extracellular stimuli from ligand binding to intracellular signals. All GPCRs share common structural characteristics including a seven transmembrane (7-TM) hydrophobic helical regions with an extracellular N-terminus, three extracellular (ECL) and three intracellular loops (ICL) with and an intracellular C-terminus [62]. Activation of a GPCR via extracellular ligand binding leads to a confirmation change and the intracellular exchange of GDP to GTP by way of a guanine nucleotide exchange factor (GEF) resulting in a GTP bound α -subunit. The GTP- α subunit detaches from the $\beta\gamma$ - subunits and regulates downstream pathways. Four families of α -subunits regulate different pathways typically through effector molecules and second messengers. These pathways can involve LGICs, transient receptor potential channels (TRPs), transporter proteins, and enzymes which can lead to a cascade of inhibition or activation of hundreds to thousands of downstream molecules [63–65].

GPCRs constitute over one third of all FDA approved druggable targets in human medicine yet not a single anthelmintic drug has been discovered that primarily targets GPCRs in helminths [66,67]. In fact, GPCRs have not been thoroughly characterized in parasitic nematodes and much of what is known about nematode GPCRs derives from knowledge about *C. elegans* receptor biology. In *C. elegans* biogenic amine GPCRs (BA-GPCRs) regulate many of the same biological functions as the LGICs targeted by current anthelmintics and BA-GPCRs have been shown to be essential for growth, development, and neuromuscular function in *C. elegans* [67–71]. Despite the critical role of BA-GPCRs in *C. elegans* [32,57,58,60,72], little attention has been given to the study of this group of receptors in parasitic nematodes as potential anthelmintic targets.

In contrast to LGICs, GPCRs are monomeric receptors and thus overcome issues of subunit association seen in heterologous expression of LGICs. However, heterologous expression of GPCRS can lead to promiscuous alph-protein coupling and non-native second messenger cascades, but for initial high-throughput screens receptor activation is the gold standard and G protein-coupling can be characterized post hoc [32]. Moreover, helminth GPCRs have not been under selective pressure by MDA and drug resistance to these receptors is less likely to emerge as quickly as seen with drugs targeting LGICs [20,35]. GPCRs acting slower than LGICs can be a key advantage. Signal amplification, pleiotropic effects (polypharmacology) and downstream indirect modulation of LGICs through activation of GPCRs may lead to adulticidal action over time and cure parasite infection without adverse effects on the host [73,74].

1.3 Diagnostics

1.3.1 Classical methods

The gold standard diagnostic for most vector-transmitted nematode parasites remains microscopy and morphological species identification [75]. For Onchocerciasis bloodless skin

snips followed by microscopy for mf identification with replication for higher sensitivity is the gold standard [76,77]. Blood smear microscopy is standard for lymphatic filariasis, loiasis, and mansonellosis [16,75,78–80]. Loiasis diagnostics can also involve visualization of adult worms in the eye or subcutaneously [79]. In areas where multiple filarial species are co-endemic, the periodicity of circulating mf may require multiple samples to be acquired at different times. Although for *Mansonella spp.* periodicity has not been observed, this may reflect lack of data and not lack of periodicity for these mf. Microscopy requires both head space and tail nuclei characterization for species identification after Giemsa staining [75]. In non-sterile field settings fibers, fungi, and other contaminants may make species identification difficult which then may complicate treatment due to potential adverse effects.

1.3.2 Molecular methods

Veterinary diagnostics for heartworm primarily focus on blood antigen tests but microscopy for detection of mf can also provide ample information for diagnosis [43]. For human filaria diagnostics, molecular tests are not routine in endemic settings and are typically restricted to laboratory settings. Lab based serology and PCR-based tests are available but with limited utility. Both serology and PCR based tests offer higher sensitivity than microscopy which can help confirm mf species after microscopy exams. For lymphatic filariasis rapid test strips, immunochromatographic test (ICTs), and point-of-care antibody tests are widely used for mapping and transmission surveys [78,80]. Nested PCR assays are both sensitive and species specific but adaptation to a field setting has been hindered due to the complexity of reagents and equipment required for amplification and distinguishing amplicon sizes [81–83].

Loop-mediated isothermal amplification (LAMP) assays have been used in laboratory settings showing highly sensitive and specific detection of all the discussed vector-transmitted nematode parasites and while this method is poised for adaptation to field settings, no point of care LAMP assays are currently available [84–89]. More sensitive and species specific point-of-care

molecular diagnostics will facilitate MDA and elimination of these parasites in endemic countries.

1.4 Summary of existing Challenges and emerging solutions

No new anthelmintics for human filarial infections have been brought to market in decades and with the growing threat of anthelmintic resistance, new drugs are in dire need [5,24,35,47]. Current anthelmintics for filarial nematodes are inadequate and do not cure or prevent reinfection. Continued MDA is costly and it's difficult to ensure compliance and availability in remote settings. Additionally, reports of anthelmintic resistance have only emphasized the need for novel druggable targets (receptors, enzymes, transporters, structural proteins) and therapies [90,91]. Resistance to anthelmintics is well established in veterinary medicine and continues to threaten disease control [35]. However, realization of new anthelmintics is hampered by the sparse information available on druggable targets in filarial parasites. Current anthelmintics are poorly understood and their antiparasitic activities have all been discovered via in vivo experiments [21,26,48]. New drugs are needed with novel targets to continue control efforts and cure adult filarial infections. The field has recently moved toward more cost effective, in vitro target-based high throughput screening (HTS) but difficulties prioritizing targets due to lack of fundamental knowledge about druggable targets in filarial parasites has hindered our ability to achieve true target-based HTS [20,23,35]. To date, no novel drugs have been discovered from these approaches [20,23,35]. We need a better understanding of the basic biology and the repertoire and interactions of current and potential drug targets to continue to control and make progress towards elimination of these vector-borne filarial parasites.

On the diagnostic front, sensitive molecular diagnostics that are species specific are needed in field settings especially in co-endemic regions. Microscopy based diagnostic, which requires trained individuals to morphologically differentiate mf of different species, often misses occult or low amicrofilaremic infections [92,93]. Molecular diagnostic assays can provide a

highly sensitive, specific, and potentially cost-effective approach for the surveillance of filarial nematode infections and their vectors. Additionally, a method that has the potential for point of care diagnostics in endemic settings can facilitate MDA efforts and help map disease prevalence and transmission dynamics.

Eradication of these filarial parasites will ultimately require climate stability and socio-economic improvements including better sanitation and access to clean potable water [94]. Climate change currently threatens our progress towards elimination and re-emergence may be imminent in areas previously deemed eradicated [95–97]. With warming climates and rising sea levels, it is predicted that vectors responsible for transmission of these parasites will expand or shift their range, doubling the number of at-risk individuals [95–98]. Support for communities that will be most impacted by climate change and will face increased risk for infectious diseases is being provided through scientific collaborations [99]. Empowering autonomy for health care providers and community leaders and researchers in endemic countries is necessary for successful control and elimination of vector-borne parasitic nematodes as well as other infectious diseases. Combined approaches of MDA, climate initiatives, vector control, and more sensitive diagnostic combined with training for individuals in endemic areas will facilitate control and elimination of these vector-borne parasitic nematodes.

1.5 Dissertation synopsis

The lack of 1) accurate mapping of vectors and infections 2) basic knowledge about these parasites biology and transmission dynamics and 3) curative treatment have motivated my thesis research.

In this dissertation, I address these needs by improving our understanding of severely understudied arthropod-borne human infective parasites through implementing field surveillance studies, computational approaches, and molecular laboratory techniques. My research expands our understanding of the basic biology of *Mansonella* and *Brugia* parasites and provides a

framework for cell surface receptor deorphanization and characterization with potential to serve as novel anthelmintic targets.

In chapter two, I describe my research on field surveillance and molecular diagnostics for *M. ozzardi* in the Colombian Amazon. We sought to establish both classical and molecular diagnostics methods to estimate community prevalence. Blood samples were taken from ~235 individuals residing in communities along the Amazon river in Colombia. We determined a community-wide prevalence of 40% using molecular diagnostics and were able to confirm species identity (*M. ozzardi*) using bioinformatic approaches as well as determine close clustering with sequenced isolates from neighboring countries. We began to disentangle clinical and sub-clinical impacts of *M. ozzardi* on infected individuals using statistical modeling. Finally, we established a cryopreservation protocol to allow for further studies of these parasites in laboratory settings.

In chapter three, I deorphanize and pharmacologically characterize a G protein-coupled receptor (GPCR), GAR-3, expressed by *B. malayi*. I optimize and establish experimental and computational pipelines to explore the druggability and pharmacology of GAR-3. I establish that the endogenous ligand for GAR-3 is acetylcholine and use RNAscope to localize expression of the receptor to highly diverse and important tissues including neurons, muscle, and reproductive organs. Finally, I establish a high-throughput screen using a transgenic model nematode (*C. elegans*) expressing GAR-3 from *B. malayi* and measure phenotypic modulation under drug perturbation.

In chapter four, I expand my characterization of GPCRs to include the repertoire of biogenic amine receptors (BARs) in *B. malayi* with a focus on dopaminergic GPCRs. Using multivariate phenotypic screening assays, I prioritize a set of dopaminergic compounds that have strong antiparasitic effects on *B. malayi* mf and screen this subset of compounds for adulticidal effects.

In chapter five, I conclude my findings with a summary of major impacts and future directions as well as remaining needs for the field.

Literature Cited

- Hotez PJ, Alvarado M, Basáñez M-G, et al. The global burden of disease study 2010: interpretation and implications for the neglected tropical diseases. PLoS Negl Trop Dis. 2014; 8(7):e2865.
- 2. Pullan RL, Smith JL, Jasrasaria R, Brooker SJ. Global numbers of infection and disease burden of soil transmitted helminth infections in 2010. Parasit Vectors. **2014**; 7:37.
- 3. Richards RL, Cleveland CA, Hall RJ, et al. Identifying correlates of Guinea worm (Dracunculus medinensis) infection in domestic dog populations. PLoS Negl Trop Dis. **2020**; 14(9):e0008620.
- 4. WHO Collaborating Center for Dracunculiasis Eradication, Guinea Worm Wrap-Up #284, 2022, Centers for Disease Control and Prevention (CGH): Atlanta. Available from: https://www.cartercenter.org/resources/pdfs/news/health_publications/guinea_worm/wrap-up/2023/295.pdf
- 5. International Helminth Genomes Consortium. Comparative genomics of the major parasitic worms. Nat Genet. **2019**; 51(1):163–174.
- 6. Dantas-Torres F, Otranto D. Dogs, cats, parasites, and humans in Brazil: opening the black box. Parasit Vectors. **2014**; 7:22.
- 7. Nguyen V-L, Dantas-Torres F, Otranto D. Canine and feline vector-borne diseases of zoonotic concern in Southeast Asia. Current Research in Parasitology & Vector-Borne Diseases. **2021**; 1:100001.
- 8. Bhumiratana A, Nunthawarasilp P, Intarapuk A, Pimnon S, Ritthison W. Emergence of zoonotic Brugia pahangi parasite in Thailand. Vet World. **2023**; 16(4):752–765.
- 9. Hotez PJ, Aksoy S, Brindley PJ, Kamhawi S. What constitutes a neglected tropical disease? PLoS Negl Trop Dis. **2020**; 14(1):e0008001.
- 10. Kalyanasundaram R, Khatri V, Chauhan N. Advances in Vaccine Development for Human Lymphatic Filariasis. Trends Parasitol. **2020**; 36(2):195–205.
- 11. CDC-Centers for Disease Control, Prevention. CDC Lymphatic Filariasis General Information Vectors of Lypmhatic Filaraisis. **2010** [cited 2023 Jun 2]; . Available from: https://www.cdc.gov/parasites/lymphaticfilariasis/gen_info/vectors.html
- Jawahar S, Tricoche N, Bulman CA, Sakanari J, Lustigman S. Drugs that target early stages of Onchocerca volvulus: A revisited means to facilitate the elimination goals for onchocerciasis. PLoS Negl Trop Dis. 2021; 15(2):e0009064.
- 13. Tyagi R, Bulman CA, Cho-Ngwa F, et al. An Integrated Approach to Identify New Anti-Filarial Leads to Treat River Blindness, a Neglected Tropical Disease. Pathogens

- [Internet]. 2021; 10(1). Available from: http://dx.doi.org/10.3390/pathogens10010071
- Bélard S, Gehringer C. High Prevalence of Mansonella Species and Parasitic Coinfections in Gabon Calls for an End to the Neglect of Mansonella Research. J Infect Dis. 2021; 223(2):187–188.
- 15. Dieki R, Nsi-Emvo E, Akue JP. The Human Filaria Loa loa: Update on Diagnostics and Immune Response. Res Rep Trop Med. **2022**; 13:41–54.
- 16. Ta-Tang T-H, Crainey JL, Post RJ, Luz SL, Rubio JM. Mansonellosis: current perspectives. Res Rep Trop Med. **2018**; 9:9–24.
- 17. Metzger WG, Mordmüller B. Loa loa-does it deserve to be neglected? Lancet Infect Dis. **2014**; 14(4):353–357.
- Lage OM, Ramos MC, Calisto R, Almeida E, Vasconcelos V, Vicente F. Current Screening Methodologies in Drug Discovery for Selected Human Diseases. Mar Drugs [Internet].
 2018; 16(8). Available from: http://dx.doi.org/10.3390/md16080279
- 19. Paveley RA, Bickle QD. Automated imaging and other developments in whole-organism anthelmintic screening. Parasite Immunol. **2013**; 35(9-10):302–313.
- 20. Nixon SA, Welz C, Woods DJ, Costa-Junior L, Zamanian M, Martin RJ. Where are all the anthelmintics? Challenges and opportunities on the path to new anthelmintics. Int J Parasitol Drugs Drug Resist. **2020**; 14:8–16.
- 21. Geary TG. Mechanism-based screening strategies for anthelmintic discovery. Parasitic Helminths. Weinheim, Germany: Wiley-VCH Verlag GmbH & Co. KGaA; 2012. p. 121–134.
- 22. Hahnel SR, Dilks CM, Heisler I, Andersen EC, Kulke D. Caenorhabditis elegans in anthelmintic research Old model, new perspectives. Int J Parasitol Drugs Drug Resist [Internet]. **2020**; Available from: http://www.sciencedirect.com/science/article/pii/S2211320720300312
- 23. Zamanian M, Chan JD. High-content approaches to anthelmintic drug screening. Trends Parasitol. **2021**; 37(9):780–789.
- 24. Geary TG, Woo K, McCarthy JS, et al. Unresolved issues in anthelmintic pharmacology for helminthiases of humans. Int J Parasitol. **2010**; 40(1):1–13.
- 25. Blair LS, Williams E, Ewanciw DV. Efficacy of ivermectin against third-stage Dirofilaria immitis larvae in ferrets and dogs. Res Vet Sci. **1982**; 33(3):386–387.
- 26. Laing R, Gillan V, Devaney E. Ivermectin Old Drug, New Tricks? Trends Parasitol. **2017**; 33(6):463–472.
- 27. Brindley PJ, Mitreva M, Ghedin E, Lustigman S. Helminth genomics: The implications for human health. PLoS Negl Trop Dis. **2009**; 3(10):e538.
- 28. Moreno Y, Nabhan JF, Solomon J, Mackenzie CD, Geary TG. Ivermectin disrupts the function of the excretory-secretory apparatus in microfilariae of Brugia malayi. Proc Natl Acad Sci U S A. **2010**; 107(46):20120–20125.

- 29. Evans CC, Day KM, Chu Y, Garner B, Sakamoto K, Moorhead AR. A rapid, parasite-dependent cellular response to Dirofilaria immitis in the Mongolian jird (Meriones unguiculatus). Parasit Vectors. **2021**; 14(1):25.
- 30. Eyoh E, McCallum P, Killick J, Amanfo S, Mutapi F, Astier AL. The anthelmintic drug praziquantel promotes human Tr1 differentiation. Immunol Cell Biol. **2019**; 97(5):512–518.
- 31. Geary TG, Sakanari JA, Caffrey CR. Anthelmintic drug discovery: into the future. J Parasitol. **2015**; 101(2):125–133.
- 32. Law W, Wuescher LM, Ortega A, Hapiak VM, Komuniecki PR, Komuniecki R. Heterologous Expression in Remodeled C. elegans: A Platform for Monoaminergic Agonist Identification and Anthelmintic Screening. PLoS Pathog. **2015**; 11(4):e1004794.
- 33. Kubiak TM, Larsen MJ, Bowman JW, Geary TG, Lowery DE. FMRFamide-like peptides encoded on the flp-18 precursor gene activate two isoforms of the orphan Caenorhabditis elegans G-protein-coupled receptor Y58G8A. 4 heterologously expressed in mammalian cells. Pept Sci. Wiley Online Library; **2008**; 90(3):339–348.
- 34. Duque-Correa MA, Maizels RM, Grencis RK, Berriman M. Organoids New Models for Host-Helminth Interactions. Trends Parasitol. **2020**; 36(2):170–181.
- 35. Abongwa M, Martin RJ, Robertson AP. A BRIEF REVIEW ON THE MODE OF ACTION OF ANTINEMATODAL DRUGS. Acta Vet . **2017**; 67(2):137–152.
- 36. Sasaki T, Takagi M, Yaguchi T, Miyadoh S, Okada T, Koyama M. A new anthelmintic cyclodepsipeptide, PF1022A. J Antibiot . **1992**; 45(5):692–697.
- 37. Martin RJ, Buxton SK, Neveu C, Charvet CL, Robertson AP. Emodepside and SL0-1 potassium channels: a review. Exp Parasitol. **2012**; 132(1):40–46.
- 38. Guest M, Bull K, Walker RJ, et al. The calcium-activated potassium channel, SLO-1, is required for the action of the novel cyclo-octadepsipeptide anthelmintic, emodepside, in Caenorhabditis elegans. Int J Parasitol. **2007**; 37(14):1577–1588.
- 39. Driscoll M, Dean E, Reilly E, Bergholz E, Chalfie M. Genetic and molecular analysis of a Caenorhabditis elegans beta-tubulin that conveys benzimidazole sensitivity. J Cell Biol. **1989**; 109(6 Pt 1):2993–3003.
- 40. Cully DF, Vassilatis DK, Liu KK, et al. Cloning of an avermectin-sensitive glutamate-gated chloride channel from Caenorhabditis elegans. Nature. **1994**; 371(6499):707–711.
- 41. Wolstenholme AJ, Evans CC, Jimenez PD, Moorhead AR. The emergence of macrocyclic lactone resistance in the canine heartworm, Dirofilaria immitis. Parasitology. **2015**; 142(10):1249–1259.
- 42. Jacobson LS, DiGangi BA. An Accessible Alternative to Melarsomine: "Moxi-Doxy" for Treatment of Adult Heartworm Infection in Dogs. Front Vet Sci. **2021**; 8:702018.
- 43. Noack S, Harrington J, Carithers DS, Kaminsky R, Selzer PM. Heartworm disease Overview, intervention, and industry perspective. Int J Parasitol Drugs Drug Resist. **2021**; 16:65–89.

- 44. Panic G, Duthaler U, Speich B, Keiser J. Repurposing drugs for the treatment and control of helminth infections. Int J Parasitol Drugs Drug Resist. **2014**; 4(3):185–200.
- 45. Holden-Dye L, Walker RJ. Anthelmintic drugs and nematicides: studies in Caenorhabditis elegans. WormBook. **2014**; :1–29.
- 46. Burg RW, Miller BM, Baker EE, et al. Avermectins, new family of potent anthelmintic agents: producing organism and fermentation. Antimicrob Agents Chemother. **1979**; 15(3):361–367.
- 47. Campbell WC. Efficacy of the avermectins against filarial parasites: a short review. Vet Res Commun. Springer; **1982**; 5(3):251–262.
- 48. Martin RJ, Robertson AP, Bjorn H. Target sites of anthelmintics. Parasitology. **1997**; 114 Suppl:S111–24.
- 49. Geary TG. Are new anthelmintics needed to eliminate human helminthiases? Curr Opin Infect Dis. **2012**; 25(6):709–717.
- 50. Matamoros G, Rueda MM, Rodríguez C, et al. High Endemicity of Soil-Transmitted Helminths in a Population Frequently Exposed to Albendazole but No Evidence of Antiparasitic Resistance. Trop Med Infect Dis [Internet]. **2019**; 4(2). Available from: http://dx.doi.org/10.3390/tropicalmed4020073
- 51. Francis H, Awadzi K, Ottesen EA. The Mazzotti reaction following treatment of onchocerciasis with diethylcarbamazine: clinical severity as a function of infection intensity. Am J Trop Med Hyg. **1985**; 34(3):529–536.
- 52. Krücken J, Holden-Dye L, Keiser J, et al. Development of emodepside as a possible adulticidal treatment for human onchocerciasis-The fruit of a successful industrial-academic collaboration. PLoS Pathog. **2021**; 17(7):e1009682.
- 53. Emodepside Phase II Trial for Treatment of Onchocerciasis [Internet]. [cited 2023 Jun 4]. Available from: https://www.clinicaltrials.gov/ct2/show/NCT05180461
- 54. Hübner MP, Townson S, Gokool S, et al. Evaluation of the in vitro susceptibility of various filarial nematodes to emodepside. Int J Parasitol Drugs Drug Resist. **2021**; 17:27–35.
- 55. Kashyap SS, Verma S, Voronin D, et al. Emodepside has sex-dependent immobilizing effects on adult Brugia malayi due to a differentially spliced binding pocket in the RCK1 region of the SLO-1 K channel. PLoS Pathog. **2019**; 15(9):e1008041.
- 56. Montresor A, Gabrielli AF. Emodepside A Promising Drug for the Treatment of Soil-Transmitted Helminthiases. N Engl J Med. **2023**; 388(20):1907–1908.
- 57. Clare JJ. Targeting ion channels for drug discovery. Discov Med. 2010; 9(46):253–260.
- 58. Komuniecki RW, Hobson RJ, Rex EB, Hapiak VM, Komuniecki PR. Biogenic amine receptors in parasitic nematodes: what can be learned from Caenorhabditis elegans? Mol Biochem Parasitol. **2004**; 137(1):1–11.
- 59. Wolstenholme AJ. Ion channels and receptor as targets for the control of parasitic nematodes. Int J Parasitol Drugs Drug Resist. Elsevier; **2011**; 1(1):2–13.

- 60. Yu H-B, Li M, Wang W-P, Wang X-L. High throughput screening technologies for ion channels. Acta Pharmacol Sin. **2016**; 37(1):34–43.
- 61. Sakimura K. Ionotropic Receptor. In: Binder MD, Hirokawa N, Windhorst U, editors. Encyclopedia of Neuroscience. Berlin, Heidelberg: Springer Berlin Heidelberg; 2009. p. 2056–2060.
- 62. Lefkowitz RJ. Historical review: a brief history and personal retrospective of seven-transmembrane receptors. Trends Pharmacol Sci. **2004**; 25(8):413–422.
- 63. Syrovatkina V, Alegre KO, Dey R, Huang X-Y. Regulation, Signaling, and Physiological Functions of G-Proteins. J Mol Biol. **2016**; 428(19):3850–3868.
- 64. Leurs R, Bakker RA, Timmerman H, Esch IJP de. The histamine H3 receptor: from gene cloning to H3 receptor drugs. Nat Rev Drug Discov. **2005**; 4(2):107–120.
- 65. Zhou Q, Yang D, Wu M, et al. Common activation mechanism of class A GPCRs. Elife [Internet]. **2019**; 8. Available from: http://dx.doi.org/10.7554/eLife.50279
- 66. Hauser AS, Attwood MM, Rask-Andersen M, Schiöth HB, Gloriam DE. Trends in GPCR drug discovery: new agents, targets and indications. Nat Rev Drug Discov. **2017**; 16(12):829–842.
- 67. Mani T, Bourguinat C, Prichard RK. G-protein-coupled receptor genes of Dirofilaria immitis. Mol Biochem Parasitol. **2018**; 222:6–13.
- 68. Kozlova AA, Lotfi M, Okkema PG. Crosstalk with the GAR-3 Receptor Contributes to Feeding Defects in Caenorhabditis eleganseat-2 Mutants. Genetics [Internet]. **2019**; . Available from: http://dx.doi.org/10.1534/genetics.119.302053
- 69. Greenberg RM. Ion channels and drug transporters as targets for anthelmintics. Curr Clin Microbiol Rep. **2014**; 1(3-4):51–60.
- 70. Avery L, You Y-J. C. elegans feeding. WormBook. 2012; :1-23.
- 71. Park YS, Lee YS, Cho NJ, Kaang BK. Alternative splicing of gar-1, a Caenorhabditis elegans G-protein-linked acetylcholine receptor gene. Biochem Biophys Res Commun. **2000**; 268(2):354–358.
- 72. Hobson RJ, Hapiak VM, Xiao H, Buehrer KL, Komuniecki PR, Komuniecki RW. SER-7, a Caenorhabditis elegans 5-HT7-like receptor, is essential for the 5-HT stimulation of pharyngeal pumping and egg laying. Genetics. **2006**; 172(1):159–169.
- 73. Silbering AF, Benton R. Ionotropic and metabotropic mechanisms in chemoreception: "chance or design"? EMBO Rep. **2010**; 11(3):173–179.
- 74. Roth BL. Molecular pharmacology of metabotropic receptors targeted by neuropsychiatric drugs. Nat Struct Mol Biol. **2019**; 26(7):535–544.
- 75. Mathison BA, Couturier MR, Pritt BS. Diagnostic Identification and Differentiation of Microfilariae. J Clin Microbiol [Internet]. **2019**; 57(10). Available from: http://dx.doi.org/10.1128/JCM.00706-19

- 76. CDC-Centers for Disease Control, Prevention. CDC Onchocerciasis Resources for Health Professionals. **2010** [cited 2023 Jun 7]; . Available from: https://www.cdc.gov/parasites/onchocerciasis/health_professionals/index.html
- 77. Unnasch TR, Golden A, Cama V, Cantey PT. Diagnostics for onchocerciasis in the era of elimination. Int Health. **2018**; 10(suppl 1):i20–i26.
- 78. Diagnosis and treatment [Internet]. [cited 2023 Jun 7]. Available from: https://www.who.int/teams/control-of-neglected-tropical-diseases/lymphatic-filariasis/diagnosis-and-treatment
- 79. CDC-Centers for Disease Control, Prevention. CDC Loiasis Diagnosis. **2010** [cited 2023 Jun 7]; . Available from: https://www.cdc.gov/parasites/loiasis/diagnosis.html
- 80. CDC-Centers for Disease Control, Prevention. CDC Lymphatic Filariasis Diagnosis. **2010** [cited 2023 Jun 7]; . Available from: https://www.cdc.gov/parasites/lymphaticfilariasis/diagnosis.html
- 81. Jiménez M, González LM, Carranza C, et al. Detection and discrimination of Loa loa, Mansonella perstans and Wuchereria bancrofti by PCR-RFLP and nested-PCR of ribosomal DNA ITS1 region. Exp Parasitol. **2011**; 127(1):282–286.
- 82. Tang T-HT, López-Vélez R, Lanza M, Shelley AJ, Rubio JM, Luz SLB. Nested PCR to detect and distinguish the sympatric filarial species Onchocerca volvulus, Mansonella ozzardi and Mansonella perstans in the Amazon Region. Mem Inst Oswaldo Cruz. **2010**; 105(6):823–828.
- 83. Fischer P, Büttner DW, Bamuhiiga J, Williams SA. Detection of the filarial parasite Mansonella streptocerca in skin biopsies by a nested polymerase chain reaction-based assay. Am J Trop Med Hyg. **1998**; 58(6):816–820.
- 84. Drame PM, Fink DL, Kamgno J, Herrick JA, Nutman TB. Loop-mediated isothermal amplification for rapid and semiquantitative detection of Loa loa infection. J Clin Microbiol. **2014**; 52(6):2071–2077.
- 85. Poole CB, Li Z, Alhassan A, et al. Colorimetric tests for diagnosis of filarial infection and vector surveillance using non-instrumented nucleic acid loop-mediated isothermal amplification (NINA-LAMP). PLoS One. **2017**; 12(2):e0169011.
- 86. Poole CB, Sinha A, Ettwiller L, et al. In Silico Identification of Novel Biomarkers and Development of New Rapid Diagnostic Tests for the Filarial Parasites Mansonella perstans and Mansonella ozzardi. Sci Rep. **2019**; 9(1):10275.
- 87. Avendaño C, Patarroyo MA. Loop-Mediated Isothermal Amplification as Point-of-Care Diagnosis for Neglected Parasitic Infections. Int J Mol Sci [Internet]. **2020**; 21(21). Available from: http://dx.doi.org/10.3390/ijms21217981
- 88. Ta-Tang T-H, Berzosa P, Rubio JM, et al. Evaluation of LAMP for the diagnosis of Loa loa infection in dried blood spots compared to PCR-based assays and microscopy. Mem Inst Oswaldo Cruz. **2022**: 116:e210210.
- 89. Amambo GN, Innocentia N, Abong RA, et al. Application of loop mediated isothermal

- amplification (LAMP) assays for the detection of Onchocerca volvulus, Loa loa and Mansonella perstans in humans and vectors. Frontiers in Tropical Diseases [Internet]. **2023**; 3. Available from: https://www.frontiersin.org/articles/10.3389/fitd.2022.1016176
- 90. Ismail M, Botros S, Metwally A, et al. Resistance to praziquantel: direct evidence from Schistosoma mansoni isolated from Egyptian villagers. Am J Trop Med Hyg. **1999**; 60(6):932–935.
- 91. Osei-Atweneboana MY, Awadzi K, Attah SK, Boakye DA, Gyapong JO, Prichard RK. Phenotypic evidence of emerging ivermectin resistance in Onchocerca volvulus. PLoS Negl Trop Dis. **2011**; 5(3):e998.
- 92. Crainey JL, Costa CHA, Oliveira Leles LF de, et al. Deep Sequencing Reveals Occult Mansonellosis Coinfections in Residents From the Brazilian Amazon Village of São Gabriel da Cachoeira. Clin Infect Dis. **2020**; 71(8):1990–1993.
- 93. Hoseini M, Jalousian F, Hoseini SH, Gerami Sadeghian A. A cross sectional study on Dirofilaria immitis and Acanthocheilonema reconditum in sheepdogs in a western region in Iran. Vet Res Forum. **2020**; 11(2):185–190.
- 94. Lustigman S, Prichard RK, Gazzinelli A, et al. A research agenda for helminth diseases of humans: the problem of helminthiases. PLoS Negl Trop Dis. **2012**; 6(4):e1582.
- 95. Okulewicz A. The impact of global climate change on the spread of parasitic nematodes. Ann Parasitol. **2017**; 63(1):15–20.
- 96. Short EE, Caminade C, Thomas BN. Climate Change Contribution to the Emergence or Re-Emergence of Parasitic Diseases. Infect Dis. **2017**; 10:1178633617732296.
- 97. Blum AJ, Hotez PJ. Global "worming": Climate change and its projected general impact on human helminth infections. PLoS Negl Trop Dis. **2018**; 12(7):e0006370.
- 98. Couper LI, Farner JE, Caldwell JM, et al. How will mosquitoes adapt to climate warming? Elife [Internet]. **2021**; 10. Available from: http://dx.doi.org/10.7554/eLife.69630
- 99. Collaboration [Internet]. [cited 2023 Jun 8]. Available from: https://www.who.int/teams/control-of-neglected-tropical-diseases/collaboration

Figures

Figure 1) General life cycle of vector-borne nematode parasites. Microfilariae (mf), L3's, and adults reside in human hosts (shown in orange). Typically, mf are consumed by a vector and develop to infectious stage L3 larvae. L3 larvae are transmitted to human hosts via subsequent interactions with the vector. For dracunculiasis L1's infect copepods which act as the intermediate host and consumption of contaminated water or undercooked infected aquatic animals leads to human infection. For LF, onchocerciasis, loiasis, and mansonellosis dipteran vectors (mosquitoes, black flies, biting midges) interact via blood repeated meals.

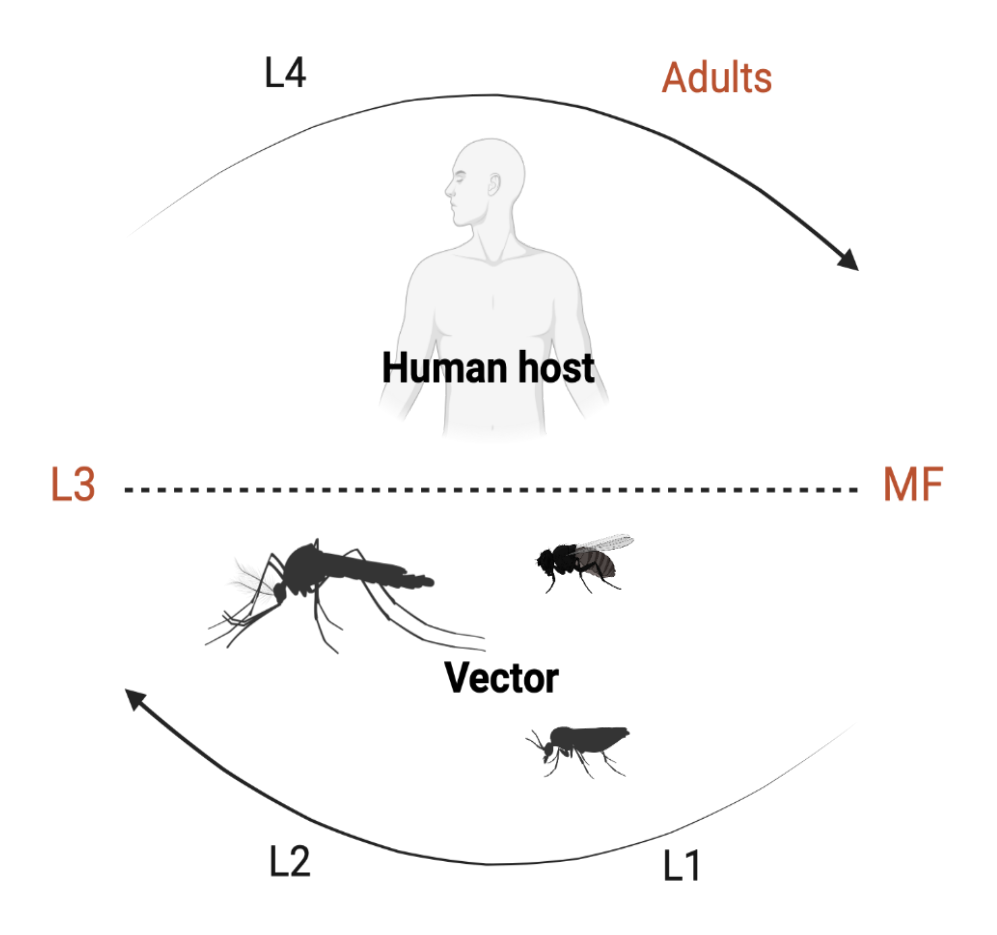


Table 1. Current anthelmintics used in veterinary and human medicine detailing the mechanism of action (MOA) and reports of resistance in the field.

Drug Class	Year	МОА	Use	Resistance
Benzimidazoles (BZs)	1961	β-tubulin, inhibits microtubule polymerization	Human and animal, broad scope anthelmintic	Yes
Imidazothiazoles	1967	nACHR, paralysis	Ruminants	Yes
Tetrahydropyrimidines	1966	nACHR	Domestic Animals for roundworms, whipworms, and hookworms	Yes
Macrocyclic Lactones	1980's	GluCls, paralysis and inhibition of pharyngeal pumping	Humans and Animals, Broad scope	Yes
Amino-acetonitrile derivatives	~2009	nACHR	animals	Yes
Spiroindoles	2010	nACHR, flaccid paralysis	Ruminants, broad-scope anthelmintic	Yes
Tribendimidine	1980's	nACHR	Humans and animals, effective against nematodes, cestodes, and trematodes	?
Cyclooctadepsipeptides	1990's	calcium-activated potassium channel, locomotion inhibition, feeding inhibition	Animals, pending human use, Broad scope anthelmintic	

Chapter 2: Molecular surveillance detects high prevalence of the neglected parasi	te
Mansonella ozzardi in the Colombian Amazon	

Dahmer KJ, Palma-Cuero M, Ciuoderis K, Patiño C, Roitman S, Li Z, Sinha A, Hite JL, Bellido Cuellar O, Hernandez-Ortiz JP, Osorio JE, Christensen BM, Carlow CKS, Zamanian M. Molecular surveillance detects high prevalence of the neglected parasite *Mansonella ozzardi* in the Colombian Amazon. medRxiv 2023.05.10.23289806; doi:

https://doi.org/10.1101/2023.05.10.23289806

In review at The Journal of Infectious Diseases ISSN: 0022-1899 (print); 1537-6613 (web)

Abstract

Mansonellosis is an under-mapped insect-transmitted disease caused by filarial nematodes that are estimated to infect hundreds of millions of people. Despite their prevalence, there are many outstanding questions regarding the general biology and health impacts of the responsible parasites. Historical reports suggest that the Colombian Amazon is endemic for mansonellosis and may serve as an ideal location to pursue these questions. We deployed molecular and classical approaches to survey Mansonella prevalence among adults belonging to indigenous communities along the Amazon River and its tributaries near Leticia, Colombia. Loop-mediated isothermal amplification (LAMP) assays on whole blood samples detected a much higher prevalence of Mansonella ozzardi infection (~40%) compared to blood smear microscopy or LAMP performed using plasma, likely reflecting greater sensitivity and the ability to detect low microfilaremias and occult infections. Mansonella infection rates increased with age and were higher among males. Genomic analysis confirmed the presence of M. ozzardi that clusters closely with strains sequenced in neighboring countries. We successfully cryopreserved M. ozzardi microfilariae, advancing the prospects of rearing infective larvae in controlled settings. These data suggest an underestimation of true mansonellosis prevalence, and we expect that these methods will help facilitate the study of mansonellosis in endemic and laboratory settings.

Summary: Sensitive molecular diagnostics reveal a high prevalence of *Mansonella ozzardi* infection in Colombian Amazon communities, adding to growing evidence that classical diagnostic approaches underestimate disease prevalence. We establish a cryopreservation protocol to facilitate future lab studies of this neglected parasite.

Introduction

Mansonellosis is a highly prevalent but undermapped [1] and understudied parasitic disease that infects hundreds of millions of people throughout Africa and Central and South America [2]. Three species of insect-transmitted parasitic nematodes (*Mansonella ozzardi, M. perstans* and *M. streptocerca*) are responsible for the majority of human cases although other *Mansonella* species have the potential to infect humans, including the recently discovered *Mansonella* sp. "DEUX" which has revitalized demands for allocating resources to study this severely neglected disease [2–5].

There are major gaps in our understanding of the basic biology and clinical or subclinical impacts of mansonellosis in human populations. *Mansonella* infections underlie variable clinical presentations that are likely underrecognized [4] and may alter host immunity in ways that alter vaccine responses and susceptibility to other pathogens [6–8]. Drugs used in mass drug administration campaigns for lymphatic filariasis and onchocerciasis are not as effective against *Mansonella spp.* [9–13] suggesting a unique genetic basis for anthelmintic resistance [14–16]. Additionally, *Mansonella* infections can introduce diagnostic challenges related to species mis-identification [17,18], cross-reactivity of immunochromatographic tests [19,20], and the inability to easily discern occult or amicrofilaremic infections [21]. Together, these limitations can potentially confound parasite elimination and surveillance programs focused on more prominent filarial worm parasites in co-endemic regions [9–13,16].

To address these challenges, we deployed both classical and molecular diagnostic approaches to carry out more precise epidemiological surveys of *Mansonella* prevalence in adults from villages along the Amazon River and its tributaries around the capital city of Leticia in the Amazonas Department of Colombia. The Amazon basin is historically associated with "new world" *M. ozzardi* [22–25] and is ideally situated to pursue fundamental questions about *Mansonella* biology, clinical presentations, and interactions with other pathogens that are

endemic in the region. Parasite surveys in this region are outdated [22–24], but incidental findings from community health workers in the course of malaria screening and estimates from communities in neighboring countries [4,21,26] suggest a high prevalence.

The gold standard diagnostic for *M. perstans* and *M. ozzardi* is blood smear microscopy, which requires morphological differentiation of the circulating microfilariae (mf) stage [4,17]. Molecular diagnostic approaches including real-time PCR (qPCR) [27–29] are largely restricted to laboratory settings. However, more recently developed loop-mediated isothermal amplification (LAMP) assays with a simple colorimetric readout are more amenable to field studies [30]. We comparatively profiled LAMP assays with classical microscopy-based techniques to evaluate potential underestimation of parasite prevalence among a cluster of indigenous communities in the Colombian Amazon region. Microfilariae were isolated for population genomic analyses of *Mansonella* with respect to previously characterized field isolates, as well as for the establishment of a cryopreservation protocol to enable laboratory studies. Lastly, we probed associations of *Mansonella* infection status with other clinical and demographic variables. We expect that these data and methods will help facilitate future studies of *Mansonella*.

Methods

Study design and sampling procedure

This study was conducted between 2021 and 2023 in the Amazonas Department of Colombia in areas surrounding the capital city of Leticia and Puerto Nariño municipalities (**Figure 1A**). This region of vast biodiversity is largely populated by indigenous communities situated near the Amazon River and its tributaries. The study protocol was reviewed and approved by the UW-Madison IRB (study # 2019-1107) and Corporación para Investigaciones Biológicas (CIB

#17022021). The study population (n = 235) from 13 communities was recruited by convenience and individuals ≥18 years of age were invited to participate. Community leaders and health promoters described the study to the community and individuals interested in participating were enrolled after providing written informed consent. Peripheral (venous) blood samples were collected into ethylenediaminetetraacetic acid (EDTA) tubes and thin and thick blood smears were prepared and examined for the presence of filarial parasites and malaria. Serum/plasma were extracted and aliquoted along with whole blood into 1.5 mL tubes and stored at -80°C for detection of *Mansonella* and other pathogens (**Figure 1B**). Self-reported socio-demographic and epidemiological data were collected using a structured questionnaire through verbal face-to-face interviews by trained study staff at the enrollment site. Recorded data included demographics (age, sex, ethnicity, occupation, place of residence), housing conditions, travel history, medical history (pre-existing diseases), and clinical symptoms. Symptoms were reported as present or absent at the time blood was drawn. Symptoms queried were: fever, headache, muscle pain, joint pain, eye pain, chills, abdominal pain, weakness, skin rash, dizziness, vomit, diarrhea, cough, red eyes, anosmia/ageusia, weight loss, jaundice.

Microscopy smears and microfilariae quantification

Routine thin and thick smears were prepared at field sites at the time of blood draws. Slides were allowed to dry at room temperature, Giemsa stained and examined microscopically. For quantitative microscopy, 40 µL of thawed whole blood was mixed with equal amounts of water and microfilaria (mf) were counted using light microscopy. For filtration of thawed whole blood aliquots, 1 mL of whole blood mixed with 4 ml of phosphate-buffered saline (PBS), was added to a Millipore syringe (Sigma-Aldrich, Z268429) with a 5 µm filter membrane (Millipore Sigma, TMTP02500). Filter membranes were imprinted in a microscope slide, allowed to dry before methanol fixation and Giemsa staining for microscopical observation.

Cryopreservation and recovery of microfilariae

Blood samples were transported on ice from Puerto Nariño to Leticia, where they were mixed with 5% dimethyl sulfoxide (DMSO) at a 1:1 ratio, aliquoted in cryogenic tubes and stored at -80°C [31]. Processed samples were then shipped to Medellin and stored at -80°C. Samples were thawed in a water bath at 37°C for 5 minutes and washed twice with sterile PBS (at 37°C), followed by centrifugation at 2,000 rpm for 10 minutes. The mf pellet was gently mixed with 2 mL of RPMI-1640 + 1x Antibiotic-Antimycotic (Gibco, 15240096). 1 mL aliquots were added to wells in a 6-well cell culture plate and the plate was incubated at 37°C and 5% CO₂. Movement patterns of mf were recorded using an inverted microscope (40X objective). Movement levels were quantified using a customized optical flow pipeline[32].

DNA extraction from blood and plasma samples

DNA was extracted from whole blood and plasma using the Quick-DNA 96-plus kit (Zymo, D4070/71) with minor adjustments to the protocol. For whole blood samples, the "solid tissue protocol" was followed by adding 50 μ L of whole blood in place of water and tissue. After incubation for 2.5 hours, samples were spun at 3,500g for 2 minutes and supernatant lysate was transferred to the Zymo-spin 96-XL plate. For plasma samples, the "biological fluid and cells" protocol was followed. Final DNA was eluted with 15 μ L of water and concentrations were assessed via NanoDrop for quality assurance.

Loop-mediated isothermal amplification assays

LAMP reactions were carried out as previously described [30] with slight modifications. Briefly, each LAMP reaction contained 1.6 μM each of primers FIP (5'-CGCAAACAGAAGCCCGAAAC-GCTCGCAATTTCATAGTGG-3') and BIP (5'-CTTGCGCGTAGCATTAGATCC-TCCGAAATGTATACGACAGAT-3'), 0.2 μM each of F3

(5'-GCACGAAATGTTTTTGTACG-3') and B3 (5'-CGTATCACCGTTGATGACG-3'), 0.4 μM each of LF (5'-AAGCCTAAGCCTGA-3') and LB (5'-GCACATCTTCAATCTCCTCTTGC-3'), 2 μl 10X GuHCL, 10 μl of WarmStart Colorimetric LAMP 2x Master Mix (NEB, M1804L), 4 μl water and 2 μl of template DNA, or 2 μl water for non-template controls for a total volume of 20 μl per reaction. For a colorimetric readout, reactions were incubated at 63°C for 30 minutes in a SimpliAmp Thermocycler (Applied Biosystems, A24811) and images were acquired using an ImageQuant 800 (Cytiva). A post amplification color of yellow indicated detection of *M. ozzardi*, and pink (or orange) indicated no detection.

For semi-quantitative LAMP (sq-LAMP), simultaneous colorimetric and fluorescent readouts were obtained by adding SYTOTM 9 green (Invitrogen, S34854) to a final concentration of 1 μ M in the colorimetric LAMP reaction. Reactions were performed in a Bio-Rad CFX Opus 96 Real-Time PCR instrument at 65°C with total fluorescence read in the SYBR/FAM channel every 15 seconds for 150 "cycles" (~53 minutes with each "cycle" corresponding to 21.2 seconds of reaction time, 15 seconds combined with plate reading time). A cut-off time threshold (Tt) value of 30 minutes was used to differentiate positive/negative reactions, with Tt defined as the time (min) to reach the fluorescence detection threshold. A Tt ≤ 30 minutes indicated the detection of the target, whereas a Tt > 30 minutes or N/A, indicated no detection. Plates were scanned using the Epson Perfection v600 Photo Scanner.

DNA extraction and Illumina library construction and sequencing

DNA was extracted from 200 uL of whole blood using the MagAttract HMW DNA kit (Qiagen, 67563) following the manufacturer's instructions. The NEBNext Microbiome DNA enrichment kit (NEB, E2612) was used as directed to enrich *Mansonella* DNA and reduce human DNA prior to library construction. The Illumina libraries were constructed using the NEBNext Ultra II DNA Library Prep Kit for Illumina (NEB, E7645) as described by the manufacturer. The quality and concentration of each library were determined using a 2100 Bioanalyzer with a high-sensitivity

DNA chip (Agilent Technologies). Libraries were diluted to 1 nM with 10 mM Tris, 0.1 mM EDTA pH 8. Phi X DNA (5%) was added to balance base pair composition in these A:T rich filarial libraries prior to sequencing on a NovaSeq platform (paired end, 150 bps).

Bioinformatic analysis

Raw Illumina reads were processed to remove adapters and poor-quality reads using the BBTools package (https://igi.doe.gov/data-and-tools/bbtools/). For each isolate, the reads were mapped to a combined reference sequence set comprising a *M. ozzardi* reference genome from Brazil [16], a reference mitogenome KX822021.1 [33] and the *Wolbachia w*Moz assembly GCF_020278625.1 [34] using bowtie2 [35]. Reads mapping to mitochondria were extracted from the bam alignment files using samtools [36] and assembled into circular mitochondrial genomes using GetOrganelle v1.7.7.0 [37]. The average nucleotide identity scores between pairs of all assembled mitogenomes and published mitogenomes, namely the accessions KX822021.1 and MN416134.1 for *M. ozzardi* [21,33] and MT361687.1 and MN432521.1 for *M. perstans* [21,38] were calculated using the OrthoANIu tool [39]. Multiple sequence alignments of all *M. ozzardi* and *M. perstans* mitogenomes were obtained using mafft v7.149b [40]. The phylogenetic tree based on this alignment was generated using the iqtree online server [41], which performs automatic best fit substitution model selection using ModelFinder [42]. Bootstrap support values were calculated based on ultrafast bootstrap [43] with 1000 replicates. The tree was annotated on the iTOL webserver [44].

Serological tests for viral infections

Serum samples were used for antibody detection against several pathogens. Anti-dengue immunoglobulin G (IgG) and IgM were detected using SD BIOLINE Dengue Duo rapid test (Abbott), following manufacturer's instructions. Anti-Human Immunodeficiency Virus (HIV).

Hepatitis B Virus (HBV), and Hepatitis C Virus (HCV) as well as anti-IgM against Severe Acute Respiratory Syndrome Coronavirus 2 (SARS-COV-2) were detected by chemiluminescence immunoassay using the Architect I1000 system (Abbott), following manufacturer's instructions.

Data analysis

Self-reported data were recorded on printed surveys by study personnel and completed forms were entered into Microsoft Excel by double entry. Excel spreadsheets were used for data inspection, cleaning, and quality control before data analysis using R Studio software v4.2.2 (42). To examine sex- and age-based differences of M. ozzardi infections, we used a linear model (lm) to get the residuals and assess the normality of our data. We determined our data did not follow a normal distribution (Shapiro-Wilk test, male age: W = 0.93224, p-value = 0.0002649, female age: W = 0.89475, p-value = 8.05e-09). Based on these results, we ran a non-parametric Wilcox rank sum test with a p-value < 0.05 considered statistically significant. Next, to examine differences between infection prevalence across demographic variables and analyses on reported symptoms and serology results, we used generalized linear models (GLMs) with binomial distributions and log link functions [45]. We conducted model selection analyses using the aictab function in the R package AlCcmodavg [46]. We built candidate models starting with the full model with all combinations of main effects among relevant biological and methodological factors, while avoiding overfitting. We compared candidate models using Akaike's information criterion and Δ AIC (the difference in AIC values for the focal model and the model with the lowest AIC, i.e., the 'winning' model) [47]. We also calculated the Akaike weight (w), which further quantifies the probability that a model is the most appropriate model relative to the candidate models (Supplementary Table 1). \triangle AIC less than two and a higher w generally indicates that a model has substantial support while a suite of best models with low weights ($w \sim 0$) indicates that no single variable plays a substantial role in mediating

infection dynamics [47]. Using the *Anova* function in the R package car [48], we assessed significance of the effects using Wald $\chi 2$ statistics for the winning model.

Protocol and data availability

All pipelines for statistical analysis and data visualization are available at https://github.com/zamanianlab/Mansonella-ms.

Raw read data used for assembly of mitogenomes of *M. ozzardi* isolates Moz-Col-195, Moz-Col-204, Moz-Col-220 and Moz-Col-239 are submitted under NCBI BioProject PRJNA981507, PRJNA981522, PRJNA981514, and PRJNA981525, respectively. The accession numbers of the assembled mitogenomes are OR271611, OR288092, OR296456, OR296457, respectively. The mitogenomes of isolates Moz-Brazil-1 and Moz-Venz-1 were assembled from previously reported raw read datasets [16] available from NCBI BioProject PRJNA917722 and PRJNA917766 respectively. The corresponding GenBank accessions for these mitogenomes are OR296458 for Moz-Brazil-1 and OR296459 for Moz-Venz-1.

Results

Parasite Prevalence

To assess *Mansonella* prevalence within our study population, we deployed a species-specific loop-mediated isothermal amplification (LAMP) assay [30] and compared diagnostic results with microscopic examination of thin blood smears. Across the first survey (samples 1-117), whole blood LAMP results show a higher prevalence of *M. ozzardi* infections (54/115, 46.9%) than single thin smear microscopy (16/104, 15.3%) and LAMP carried out using DNA from matched plasma (31/115, 26.9%) (**Figure 2 A**). Consensus whole blood LAMP results were derived from

experiments involving DNA extractions from independent aliquots of whole blood as well as replicates of LAMP assays carried out in two laboratories using DNA from a single extraction (Supplementary Figure 1 A).

Treating the whole blood LAMP as the truth case, thin smear microscopy shows a 31% sensitivity and plasma LAMP shows a 50% sensitivity. For the 30 samples where whole blood LAMP was positive and microscopy was negative, lower time (Tt) which is indicative of more parasite material being present in semi-quantitative LAMP (sq-LAMP) were observed (Supplementary Figure 1 B-C). We therefore hypothesized that the discrepancy between LAMP results and microscopy is likely associated with lower titers of microfilariae in venous blood leading to thin smear false negatives [49] or occult (amicrofilaremic) infections [21] that can only be detected using molecular methods. In both cases, we would expect the whole blood LAMP assay to display better sensitivity.

Subsequent surveys (samples 118-186; samples 187-244) were used to probe potential associations between microfilaremia and *Mansonella* diagnostic results by incorporating quantitative microscopy. Whole blood LAMP assays showed an *M. ozzardi* prevalence of 33% (40/120). Among the 14 samples which tested positive in microscopy, 13 also tested positive in LAMP. Plasma LAMP (16%) and thin smear microscopy detected a lower prevalence (12%), reflecting the pattern observed in the first survey (**Figure 2 B**). Quantitative microscopy detected mf in 23/122 samples (19%), ranging from 0-11 mf/40 µL blood spot (**Figure 2 C**). Samples with the highest mf titers were most likely to be positive across whole blood and plasma LAMP assays and thin smears, while samples with lower mf titers were more likely to be negative in blood smears and only detected in the whole blood LAMP assay (**Figure 2 D**). This lends support to the hypothesis that low mf titers is a driver of false negatives in both thin smears and plasma LAMP assays.

To explore whether occult infections could also be a factor contributing to the positive whole blood LAMP samples which had negative microscopy results, we re-sampled blood from

six individuals that fit this pattern. A larger volume of blood (1 mL) was filtered to identify mf that could be circulating at titers not routinely detectable via thick and thin smear microscopy. All six samples were still microscopy negative, supporting the likelihood of occult infections. It is possible that the freeze-thaw process preceding filtration of these samples reduced the sensitivity of this approach. Whole blood LAMP was the most sensitive diagnostic test and identified a prevalence of 40% for *M. ozzardi* across all three surveys (**Table 1**).

Population Demographics

The three surveys consisted of individuals who reside in thirteen different communities situated between -02°50'14.9496" north latitude and -03°52'39.1980" south latitude; and -069°44'10.7880" and -070°35'52.2240" west longitude (**Figure3 A**). A majority of our sampled population were centered in Puerto Nariño (n = 136) (Table 2), where the prevalence of M. ozzardi as determined by whole blood LAMP is 44%. The next largest sampled communities in our survey, 12 de Octubre (24%; n = 25) and San Pedro de Tipisca (14%; n = 21), had lower prevalence. There was a higher prevalence of *M. ozzardi* mf identified via blood LAMP in males (49%; n = 84; mean age = 40.1 years) compared to females (32%; n = 148; mean age = 34.7 years). The mean age of M. ozzardi positive individuals was higher than the mean age of negative individuals in females (Wilcox: p = 0.026) but not males (Wilcox: p = 0.07) (Figure 3 B). To further examine differences between infection prevalence across demographic variables, we assessed significance of the fixed effects using Wald x2 statistics and identified education and place of residence as drivers of prevalence (education binomial GLM: $\chi 2 = 16.2647$, p = 0.01240, case origin GLM: $\chi 2 = 13.6850$, p = 0.03336). However, given the limitation of the data we were unable to confirm significant differences within these groups due to unequal and small sample sizes amongst subsets.

To explore potential associations between clinical symptoms and infections with other pathogens, clinical histories were collected and additional serological tests were carried out for

survey two and three samples (n = 117) (**Figure 3 C**) and compared across *M. ozzardi* whole blood LAMP positive and negative individuals (**Figure 3 D**). Symptoms and serology results that were differentially reported (abdominal pain, fever, joint pain, muscle pain, Hepatitis B antibodies, and Hepatitis C antibodies) between whole blood LAMP positive and negative individuals were examined further to determine if fixed effects or *M. ozzardi* infections were more likely to explain these data. We assessed significance of the fixed effects and whole blood LAMP results using Wald $\chi 2$ statistics and determined that *M. ozzardi* infection status did not significantly correlate to reported symptoms or serology results. Fixed effects including sex and age were identified as potential drivers of some of the reported symptoms and serology results but unequal and small sample sizes amongst subsets of data limited our post-hoc analysis.

Genomic Analysis

Whole genome sequencing was performed on 4 samples (ID numbers 195, 204, 220 and 239) which tested positive in the *M. ozzardi* specific whole blood LAMP assay and where larger volumes of whole blood were available for DNA extractions. Only sample 239 had detectable microfilariae in the quantitative microscopy assay. While a mapping analysis of the sequencing data showed that over 94% of the reads were from the human host, 1 to 6 % of reads mapped to the reference *M. ozzardi* genome assembly and to the *Wolbachia w*Moz genome assembly, although at a low coverage (**Supplementary Figure 2**).

Sufficient read coverage was obtained for successful assembly of complete, circular mitogenomes for each isolate. The assembled mitogenomes displayed more than 99.6% sequence identity to each other and to previously reported *M. ozzardi* mitogenomes from Brazil [21,33], as well as to the newly assembled mitogenomes from isolates Moz-Brazil-1 and Moz-Venz-1 obtained from Brazil and Venezuela respectively [16]. A phylogenetic analysis of all *M. ozzardi* mitogenomes in conjunction with *M. perstans* mitogenomes from Brazil [21] and Cameroon [38] showed a distinct *M. ozzardi* clade with very short branch lengths between

various isolates and a clear separation from the *M. perstans* clade (**Figure 4**). Together, these results confirm the presence of *M. ozzardi* infection in these individuals.

Cryopreservation of Blood-Dwelling Parasite Stage

As a first step towards establishing the lifecycle of *M. ozzardi* in a laboratory environment, we sought to functionally cryopreserve microfilariae and observe viable and active worms after thawing samples. We collected peripheral blood from individuals who were positive for *M. ozzardi* via blood LAMP assay and thin smear microscopy in our initial survey. Blood samples were mixed with dimethyl sulfoxide (DMSO) and kept at -80°C. We observed revitalization of microfilariae upon thawing at 37°C, whereby motility increased over the first 24 hour incubation period before steadily declining (**Figure 5 A**). Videos showed viable and healthy microfilariae (**Figure 5 B**) that may allow for membrane feeding of lab colonies of *Culicoides* and the production of infective-stage larvae (L3) in a laboratory setting.

Discussion

We conducted three seroprevalence surveys to better map the distribution of *Mansonella* infections among indigenous communities in the Amazon basin of Colombia. Blood smear microscopy identified microfilariae in 12.7% of sampled individuals, which falls within the range of historical studies in the region [23,24,50]. Whole blood LAMP assays detected *M. ozzardi* DNA in 40% of sampled individuals, in closer agreement with more recent PCR-based surveys in the Amazon region of neighboring countries [26,28,51,52]. Our survey data adds to the growing body of evidence that microscopy-based approaches can drastically underestimate the true prevalence of global mansonellosis [5,14,26–30,51–53].

Molecular diagnostic assays can be leveraged to capture a broader range of infection states, including low microfilaremias or afilaremic (occult) infections [21]. The recovery of complete mitogenomes confirms the presence of *M. ozzardi* DNA in blood samples that previous microscopy diagnostics could not detect, providing further confidence in LAMP diagnostic results. The distribution of *M. ozzardi* adults within the human body is not fully resolved [54], but it is presumed that they commonly take residence in subcutaneous tissues and possibly the serous cavities. These larger stages are the likely source of blood-detectable nucleic acids in molecular diagnostic assays. LAMP assays provide a sensitive, specific, and potentially cost-effective approach for the surveillance of filarial nematode infections in human and vector populations [30,55–57]. The development of direct LAMP assays [58] not reliant on DNA extraction will add to the convenience of this approach in endemic settings.

The establishment of a cryopreservation protocol can potentially facilitate the eventual rearing of *M. ozzardi* in laboratory settings, including through the controlled blood-feeding of reanimated microfilariae to susceptible colonies of biting midges or via intra-thoracic infection of mosquitoes (Lowrie and Eberhard 1985; Lowrie et al. 1982). In vitro phenotyping of *Mansonella* drug responses [59] can help resolve the genetic and molecular basis for observed differences in antifilarial drug susceptibility across species [9,10,12,13,15,60] and open avenues for the screening and discovery of new therapeutic leads for mansonellosis.

Mansonella is neglected even among neglected pathogens due to a lack of investment in studying its biology and potential health impacts [4,8,61]. More complete demographic and clinical data are needed to determine *M. ozzardi* pathogenicity and assess risk factors.

Non-specific clinical effects and the potentially skewed baseline health of our study population may have hampered our ability to resolve associations with infection status. Adult worms disperse somewhat randomly into various tissues and body cavities, the consequences of which can vary considerably across individuals but have historically been summarized as relatively non-pathogenic. Although there are growing clinical case reports suggesting appreciable

pathogenicity [4], it is difficult to streamline causal associations with more subtle health impacts. The current established threshold for addressing human filariasis is a causal association with significant morbidity, including blindness and physical disfigurement. Investigation of subclinical or secondary impacts of infection would shift the threshold of potential human clinical concern in mansonellosis-endemic regions to the same threshold that often triggers action as it relates to subclinical nematode infections of livestock and companion animals. We expect that improved diagnostic tools, growing genomic resources, and methods to study *Mansonella* in laboratory settings will facilitate this goal.

Acknowledgements

The authors thank the communities, the Secretaria de Salud Departamental del Amazonas, Alcaldia de Puerto Nariño, E.S.E Hospital San Rafael de Puerto Nariño, and the Laboratorio Departamental de Salud Pública de Leticia for their contributions to this study. We sincerely thank Julian Rodriguez and Corporacion Corpotropica for their assistance and coordination of activities at the study sites. In addition, we would like to thank the staff of One Health lab and auxiliary personnel at all the study sites for their assistance. Thanks to the Abbott Pandemic Defense Coalition for the provision of laboratory testing kits. **Author contributions**: Study design: Dahmer KJ, Hernandez-Ortiz JP, Osorio JE, Christensen BM, Carlow CKS, Zamanian M. Execution: Dahmer KJ, Palma-Cuero M, Ciuoderis K, Patiño C, Roitman S, Li Z, Sinha A, Bellido Cuellar O, Christensen BM. Analysis and interpretation: Dahmer KJ, Patiño C, Roitman S, Li Z, Sinha A, Hite JL. Writing and proofing: Dahmer KJ, Palma-Cuero M, Ciuoderis K, Patiño C, Roitman S, Li Z, Sinha A, Hite JL, Bellido Cuellar O, Hernandez-Ortiz JP, Osorio JE, Christensen BM, Carlow CKS, Zamanian M.

Funding

KJD was supported by a UW-SciMed GRS Fellowship (scimedgrs.wisc.edu) and NIH Parasitology and Vector Biology Training grant number T32 Al007414 (NIH.gov). This work was supported by a seed grant from the University of Wisconsin-Madison Global Health Institute (GHI) to MZ. CKSC, ZL, AS and SR gratefully acknowledge funding and support from New England Biolabs.

Conflicts

CKSC, ZL, AS and SR are employed by New England Biolabs, a manufacturer and vendor of molecular biology reagents. This affiliation does not affect the authors' impartiality, adherence to journal standards and policies or availability of data. All other authors report no potential conflicts of interest.

References

- 1. Schluth CG, Standley CJ, Bansal S, Carlson CJ. Spatial parasitology and the unmapped human helminthiases. Parasitology. **2023**; :1–9.
- Bélard S, Gehringer C. High Prevalence of Mansonella Species and Parasitic Coinfections in Gabon Calls for an End to the Neglect of Mansonella Research. J Infect Dis. 2021; 223(2):187–188.
- 3. Mourembou G, Fenollar F, Lekana-Douki JB, et al. Mansonella, including a Potential New Species, as Common Parasites in Children in Gabon. PLoS Negl Trop Dis. **2015**; 9(10):e0004155.
- 4. Ta-Tang T-H, Crainey JL, Post RJ, Luz SL, Rubio JM. Mansonellosis: current perspectives. Res Rep Trop Med. **2018**; 9:9–24.
- 5. Sandri TL, Kreidenweiss A, Cavallo S, et al. Molecular Epidemiology of Mansonella Species in Gabon. J Infect Dis. **2021**; 223(2):287–296.
- 6. Stensgaard A-S, Vounatsou P, Onapa AW, et al. Ecological Drivers of Mansonella perstans Infection in Uganda and Patterns of Co-endemicity with Lymphatic Filariasis and Malaria. PLoS Negl Trop Dis. **2016**; 10(1):e0004319.

- 7. Phillips RO, Frimpong M, Sarfo FS, et al. Infection with Mansonella perstans Nematodes in Buruli Ulcer Patients, Ghana. Emerg Infect Dis. **2014**; 20(6):1000–1003.
- 8. Ritter M, Ndongmo WPC, Njouendou AJ, et al. Mansonella perstans microfilaremic individuals are characterized by enhanced type 2 helper T and regulatory T and B cell subsets and dampened systemic innate and adaptive immune responses. PLoS Negl Trop Dis. **2018**; 12(1):e0006184.
- 9. Bregani ER, Rovellini A, Mbaïdoum N, Magnini MG. Comparison of different anthelminthic drug regimens against Mansonella perstans filariasis. Trans R Soc Trop Med Hyg. **2006**; 100(5):458–463.
- 10. Van Hoegaerden M, Ivanoff B, Flocard F, Salle A, Chabaud B. The use of mebendazole in the treatment of filariases due to Loa loa and Mansonella perstans. Ann Trop Med Parasitol. **1987**; 81(3):275–282.
- 11. Simonsen PE, Onapa AW, Asio SM. Mansonella perstans filariasis in Africa. Acta Trop. **2011**; 120 Suppl 1:S109–20.
- 12. Gonzalez AA, Chadee DD, Rawlins SC. Ivermectin treatment of mansonellosis in Trinidad. West Indian Med J. **1999**; 48(4):231–234.
- 13. Simonsen PE, Fischer PU, Hoerauf A, Weil G. Manson's Tropical Diseases, 23rd Edition: The Filariases. Manson's Tropical Diseases. unknown; 2014. p. 737–765.
- 14. Ta-Tang T-H, Luz SLB, Merino FJ, et al. Atypical Mansonella ozzardi Microfilariae from an Endemic Area of Brazilian Amazonia. Am J Trop Med Hyg. **2016**; 95(3):629–632.
- 15. Coulibaly YI, Dembele B, Diallo AA, et al. A randomized trial of doxycycline for Mansonella perstans infection. N Engl J Med. **2009**; 361(15):1448–1458.
- Sinha A, Li Z, Poole CB, et al. Genomes of the human filarial parasites Mansonella perstans and Mansonella ozzardi [Internet]. bioRxiv. 2023 [cited 2023 Jan 17]. p. 2023.01.06.523030. Available from: https://www.biorxiv.org/content/10.1101/2023.01.06.523030v1
- 17. Mathison BA, Couturier MR, Pritt BS. Diagnostic Identification and Differentiation of Microfilariae. J Clin Microbiol [Internet]. **2019**; 57(10). Available from: http://dx.doi.org/10.1128/JCM.00706-19
- 18. Crainey JL, Bessa Luz SL. Light Microscopic Detection of Mansonella ozzardi Parasitemias. Clin. Infect. Dis. 2019. p. 2156.
- 19. Coulibaly YI, Soumaoro L, Dembele B, Hodges M, Zhang Y. POTENTIAL CROSS REACTIVITY OF MANSONELLA PERSTANS WITH WUCHERERIA BANCROFTI BY FILARIASIS TEST STRIPS. AMERICAN JOURNAL OF TROPICAL MEDICINE AND HYGIENE. AMER SOC TROP MED & HYGIENE 8000 WESTPARK DR, STE 130, MCLEAN, VA 22101 USA; 2019. p. 160–160.
- 20. Wanji S, Amvongo-Adjia N, Koudou B, et al. Cross-Reactivity of Filariais ICT Cards in Areas of Contrasting Endemicity of Loa loa and Mansonella perstans in Cameroon: Implications for Shrinking of the Lymphatic Filariasis Map in the Central African Region. PLoS Negl Trop

- Dis. **2015**; 9(11):e0004184.
- 21. Crainey JL, Costa CHA, Oliveira Leles LF de, et al. Deep Sequencing Reveals Occult Mansonellosis Coinfections in Residents From the Brazilian Amazon Village of São Gabriel da Cachoeira. Clin Infect Dis. **2020**; 71(8):1990–1993.
- 22. Kozek WJ, Palma G, Valencia W, Montalvo C, Spain J. Filariasis in Colombia: prevalence of Mansonella ozzardi in the Departamento de Meta, Intendencia del Casanare, and Comisaría del Vichada. Am J Trop Med Hyg. **1984**; 33(1):70–72.
- 23. Lightner LK, Ewert A, Corredor A, Sabogal E. A parasitologic survey for Mansonella ozzardi in the Comisaría del Vaupés, Colombia. Am J Trop Med Hyg. **1980**; 29(1):42–45.
- 24. Kozek WJ, D'Alessandro A, Silva J, Navarette SN. Filariasis in Colombia: prevalence of mansonellosis in the teenage and adult population of the Colombian bank of the Amazon, Comisaria del Amazonas. Am J Trop Med Hyg. **1982**; 31(6):1131–1136.
- 25. Tidwell MA, Tidwell MA. Development of Mansonella ozzardi in Simulium amazonicum, S. argentiscutum, and Culicoides insinuatus from Amazonas, Colombia. Am J Trop Med Hyg. American Society of Tropical Medicine and Hygiene; **1982**; 31(6):1137–1141.
- Calvopina M, Chiluisa-Guacho C, Toapanta A, Fonseca D, Villacres I. High Prevalence of Mansonella ozzardi Infection in the Amazon Region, Ecuador. Emerg Infect Dis. 2019; 25(11):2081–2083.
- 27. Jiménez M, González LM, Carranza C, et al. Detection and discrimination of Loa loa, Mansonella perstans and Wuchereria bancrofti by PCR-RFLP and nested-PCR of ribosomal DNA ITS1 region. Exp Parasitol. **2011**; 127(1):282–286.
- 28. Tang T-HT, López-Vélez R, Lanza M, Shelley AJ, Rubio JM, Luz SLB. Nested PCR to detect and distinguish the sympatric filarial species Onchocerca volvulus, Mansonella ozzardi and Mansonella perstans in the Amazon Region. Mem Inst Oswaldo Cruz. **2010**; 105(6):823–828.
- 29. Fischer P, Büttner DW, Bamuhiiga J, Williams SA. Detection of the filarial parasite Mansonella streptocerca in skin biopsies by a nested polymerase chain reaction-based assay. Am J Trop Med Hyg. **1998**; 58(6):816–820.
- 30. Poole CB, Sinha A, Ettwiller L, et al. In Silico Identification of Novel Biomarkers and Development of New Rapid Diagnostic Tests for the Filarial Parasites Mansonella perstans and Mansonella ozzardi. Sci Rep. **2019**; 9(1):10275.
- 31. Zinser EW, McTier TL, Kernell NS, Woods DJ. Cryogenic preservation of Dirofilaria immitis microfilariae, reactivation and completion of the life-cycle in the mosquito and vertebrate hosts. Parasit Vectors. **2021**; 14(1):367.
- 32. Wheeler NJ, Gallo KJ, Rehborg EJG, Ryan KT, Chan JD, Zamanian M. wrmXpress: A modular package for high-throughput image analysis of parasitic and free-living worms. PLoS Negl Trop Dis. **2022**; 16(11):e0010937.
- 33. Crainey JL, Marín MA, Silva TRR da, et al. Mansonella ozzardi mitogenome and pseudogene characterisation provides new perspectives on filarial parasite systematics and

- CO-1 barcoding. Sci Rep. **2018**; 8(1):6158.
- Sinha A, Li Z, Poole CB, et al. Multiple origins of nematode-Wolbachia symbiosis in supergroup F and convergent loss of bacterioferritin in filarial Wolbachia [Internet]. bioRxiv. 2022 [cited 2023 May 7]. p. 2021.03.23.436630. Available from: https://www.biorxiv.org/content/biorxiv/early/2022/04/27/2021.03.23.436630
- 35. Langmead B, Salzberg SL. Fast gapped-read alignment with Bowtie 2. Nat Methods. **2012**; 9(4):357–359.
- 36. Danecek P, Bonfield JK, Liddle J, et al. Twelve years of SAMtools and BCFtools. Gigascience [Internet]. **2021**; 10(2). Available from: http://dx.doi.org/10.1093/gigascience/giab008
- 37. Jin J-J, Yu W-B, Yang J-B, et al. GetOrganelle: a fast and versatile toolkit for accurate de novo assembly of organelle genomes. Genome Biol. **2020**; 21(1):241.
- 38. Chung M, Aluvathingal J, Bromley RE, et al. Complete Mitochondrial Genome Sequence of Mansonella perstans. Microbiol Resour Announc [Internet]. **2020**; 9(30). Available from: http://dx.doi.org/10.1128/MRA.00490-20
- 39. Yoon S-H, Ha S-M, Lim J, Kwon S, Chun J. A large-scale evaluation of algorithms to calculate average nucleotide identity. Antonie Van Leeuwenhoek. **2017**; 110(10):1281–1286.
- 40. Nakamura T, Yamada KD, Tomii K, Katoh K. Parallelization of MAFFT for large-scale multiple sequence alignments. Bioinformatics. **2018**; 34(14):2490–2492.
- 41. Trifinopoulos J, Nguyen L-T, Haeseler A von, Minh BQ. W-IQ-TREE: a fast online phylogenetic tool for maximum likelihood analysis. Nucleic Acids Res. **2016**; 44(W1):W232–5.
- 42. Kalyaanamoorthy S, Minh BQ, Wong TKF, Haeseler A von, Jermiin LS. ModelFinder: fast model selection for accurate phylogenetic estimates. Nat Methods. **2017**; 14(6):587–589.
- 43. Hoang DT, Chernomor O, Haeseler A von, Minh BQ, Vinh LS. UFBoot2: Improving the Ultrafast Bootstrap Approximation. Mol Biol Evol. **2018**; 35(2):518–522.
- 44. Letunic I, Bork P. Interactive Tree Of Life (iTOL) v5: an online tool for phylogenetic tree display and annotation. Nucleic Acids Res. **2021**; 49(W1):W293–W296.
- 45. Crawley MJ. The R Book. John Wiley & Sons; 2012.
- 46. Mazerolle MJ. AICcmodavg: Model selection and multimodel inference based on (Q)AIC(c) [Internet]. 2023. Available from: https://cran.r-project.org/package=AICcmodavg
- 47. Burnham KP, Anderson DR. Model Selection and Inference: A Practical Information-Theoretic Approach. Springer New York; 1998.
- 48. Fox J, Weisberg S. An R Companion to Applied Regression. SAGE Publications; 2018.
- 49. Mischlinger J, Manego RZ, Mombo-Ngoma G, et al. Diagnostic performance of capillary and venous blood samples in the detection of Loa loa and Mansonella perstans

- microfilaraemia using light microscopy. PLoS Negl Trop Dis. 2021; 15(8):e0009623.
- 50. Shelley AJ. A preliminary survey of the prevalence of Mansonella ozzardi in some rural communities on the river Purus, state of Amazonas, Brazil. Ann Trop Med Parasitol. **1975**; 69(3):407–412.
- 51. Abrahim CMM, Py-Daniel V, Luz SLB, Fraiji NA, Stefani MMA. Detection of Mansonella ozzardi among blood donors from highly endemic interior cities of Amazonas state, northern Brazil. Transfusion . **2019**; 59(3):1044–1051.
- 52. Medeiros JF, Almeida TAP, Silva LBT, et al. A field trial of a PCR-based Mansonella ozzardi diagnosis assay detects high-levels of submicroscopic M. ozzardi infections in both venous blood samples and FTA card dried blood spots. Parasit Vectors. **2015**; 8:280.
- 53. Medeiros JF, Fontes G, Nascimento VL do, et al. Sensitivity of diagnostic methods for Mansonella ozzardi microfilariae detection in the Brazilian Amazon Region. Mem Inst Oswaldo Cruz. **2018**; 113(3):173–177.
- 54. Lima NF, Veggiani Aybar CA, Dantur Juri MJ, Ferreira MU. Mansonella ozzardi: a neglected New World filarial nematode. Pathog Glob Health. **2016**; 110(3):97–107.
- 55. Amambo GN, Innocentia N, Abong RA, et al. Application of loop mediated isothermal amplification (LAMP) assays for the detection of Onchocerca volvulus, Loa loa and Mansonella perstans in humans and vectors. Frontiers in Tropical Diseases [Internet]. **2023**; 3. Available from: https://www.frontiersin.org/articles/10.3389/fitd.2022.1016176
- 56. Ta-Tang T-H, Berzosa P, Rubio JM, et al. Evaluation of LAMP for the diagnosis of Loa loa infection in dried blood spots compared to PCR-based assays and microscopy. Mem Inst Oswaldo Cruz. **2022**; 116:e210210.
- 57. Poole CB, Li Z, Alhassan A, et al. Colorimetric tests for diagnosis of filarial infection and vector surveillance using non-instrumented nucleic acid loop-mediated isothermal amplification (NINA-LAMP). PLoS One. **2017**; 12(2):e0169011.
- 58. Avendaño C, Patarroyo MA. Loop-Mediated Isothermal Amplification as Point-of-Care Diagnosis for Neglected Parasitic Infections. Int J Mol Sci [Internet]. **2020**; 21(21). Available from: http://dx.doi.org/10.3390/ijms21217981
- 59. Njouendou AJ, Kien CA, Esum ME, et al. In vitro maintenance of Mansonella perstans microfilariae and its relevance for drug screening. Exp Parasitol. **2019**; 206:107769.
- 60. Fischer P, Tukesiga E, Büttner DW. Long-term suppression of Mansonella streptocerca microfilariae after treatment with ivermectin. J Infect Dis. **1999**; 180(4):1403–1405.
- 61. Metenou S, Babu S, Nutman TB. Impact of filarial infections on coincident intracellular pathogens: Mycobacterium tuberculosis and Plasmodium falciparum. Curr Opin HIV AIDS. **2012**; 7(3):231–238.

Figures

Figure 1 A) Map of the study region in the Amazonas Department of Colombia depicting the capital city of Leticia and the Puerto Nariño municipality where samples were collected across three surveys. The study region is adjacent to the Amazon River at the borders of Colombia, Brazil, and Peru. **B)** Schematic of sampling efforts and endpoints for blood samples acquired from adult volunteers. Blood smears and preparations of cryopreserved samples were conducted in the field. Whole blood was obtained in EDTA tubes and transferred on ice to a laboratory in Leticia. Aliquots of whole blood and plasma were prepared from samples and used for downstream serology, molecular diagnostics, and genomic analyses. Questionnaires were filled out at the time of sampling.

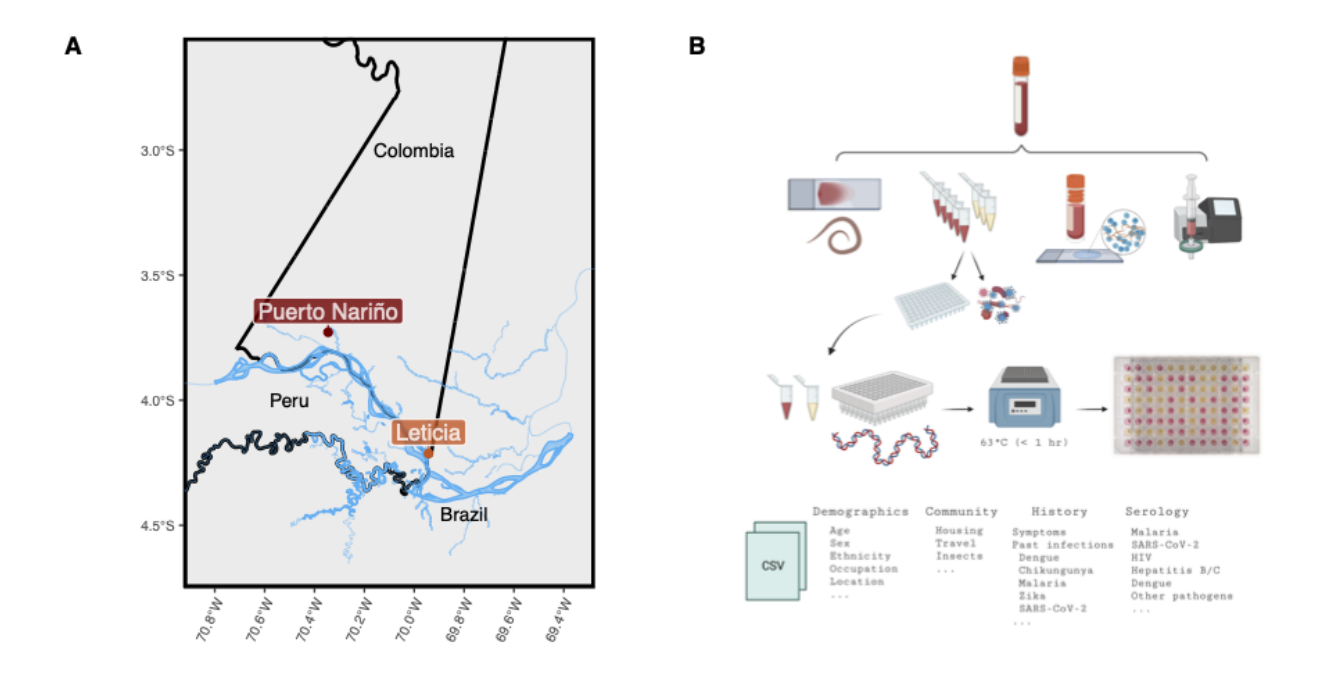


Figure 2 A) Diagnostic results derived from survey one blood samples (1-117) for in-field microscopy smears (M), LAMP using DNA extracted from whole blood (L_b), and LAMP using matched DNA extracted from plasma (L_p). **B)** Diagnostic results derived from surveys two and three (samples 118-244) for in-field microscopy smears (M), LAMP using DNA extracted from whole blood (L_b), and LAMP using matched DNA extracted from plasma (L_p). **C)** Quantitative microscopy counts (qM) derived from surveys two and three blood samples (118-244). **D)** Quantitative microscopy counts of microfilariae stratified by L_b and L_p results and coloured by microscopy smear results. (NN = negative L_b and negative L_p , IN= inconclusive L_b and negative L_p , PN = positive L_b and negative L_p , and positive L_p , NP = negative L_b and positive L_p). Grey = negative for *M. ozzardi*; White = no result (A-C). LAMP assay data are specific to *M. ozzardi*.

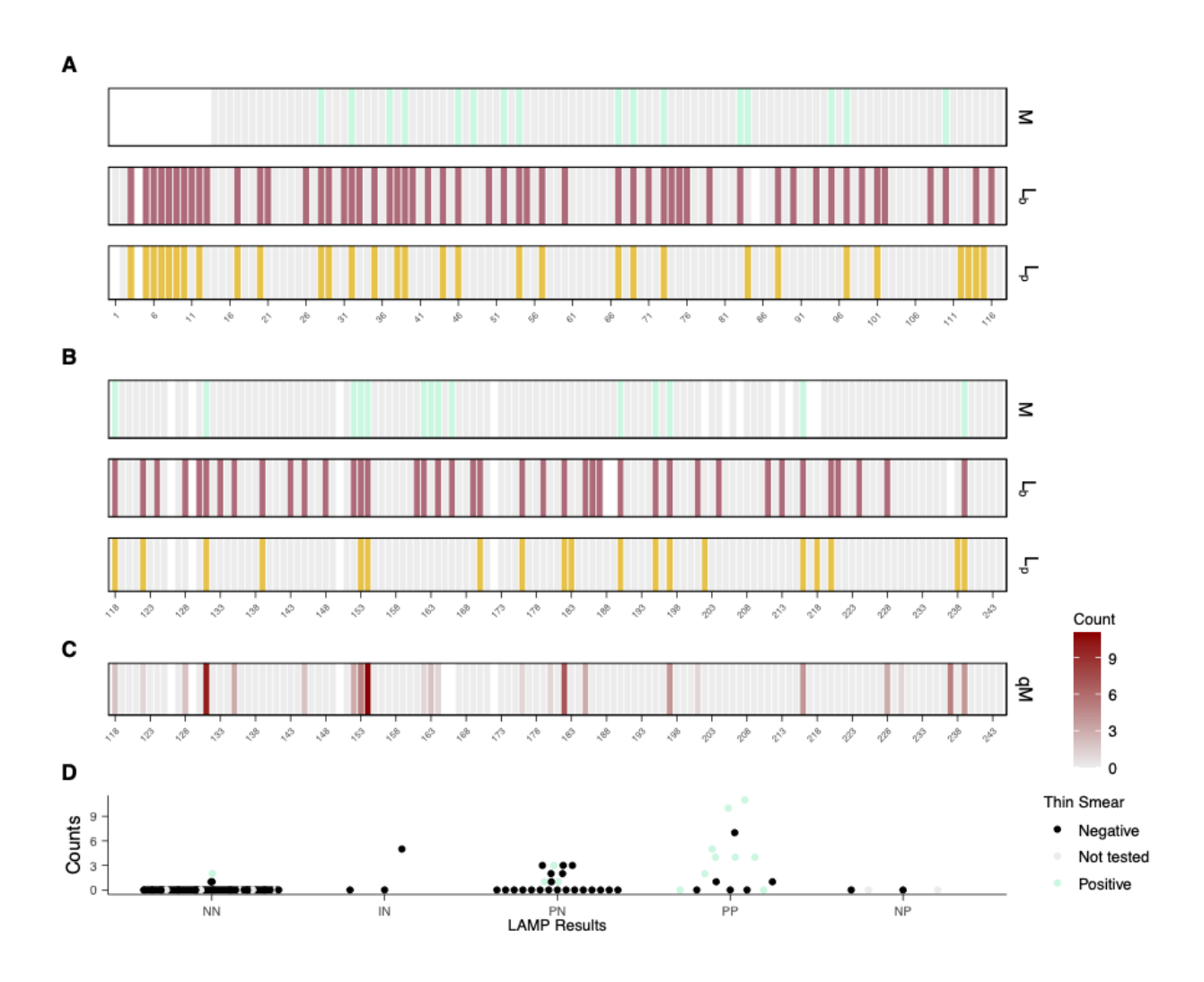


Table 1. Summary and comparison of *M. ozzardi* diagnostic results for the entire study population.

	Microscopy Smear / LAMP-Plasma Positive	Microscopy Smear / LAMP-Plasma Negative	No Result	Total
LAMP- Blood Positive	27 / 42	57 / 52	10 / 0	94
LAMP- Blood Negative	3/8	129 / 132	9/1	141
	30 / 50	186 / 184	19/1	235

Figure 3 A) A map of the study region in the Amazonas Department of Colombia depicting the community where individual participants reside. Point size reflects the number of samples collected and color represents the prevalence of *M. ozzardi* infection for each community. **B**) *M. ozzardi* prevalence as determined by whole blood LAMP assay stratified by sex and age (95% CI) (left) and histogram of *M. ozzardi* prevalence distribution by age (right). F = female, M = male **C**) *M. ozzardi* infection status and reported symptoms and serological test results for survey two and three individuals (n = 120). Orange = positive, present; Grey = negative, not-present; white indicates missing data. **D**) Donut plots reflecting relative fractions of *M. ozzardi* L_b positive and L_b negative individuals who self-reported symptoms and lab confirmed serological test results.

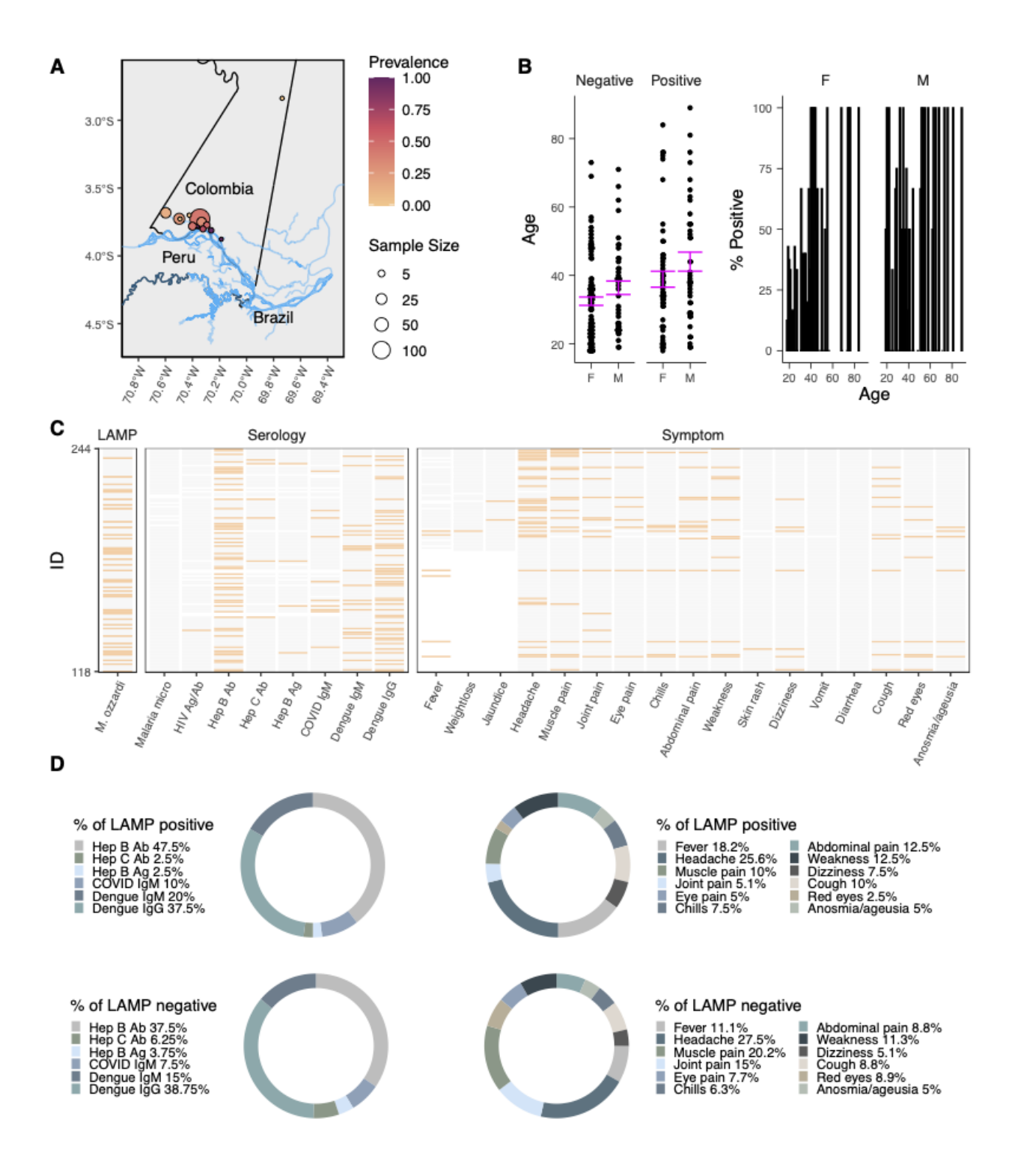


Table 2. Summary of Demographic and diagnostic data. Data includes a subset of the total study population where all summarized demographic information was provided on the questionnaire. (Age in years).

	Young Adult 18 - 32	Adult 33 - 54	Mature Adult 55 - 89	Total
Individuals	101	104	29	234
Sex (Female / Male)	69 / 32	68 / 36	12 / 17	149 / 85
M. ozzardi (Lb / Lp / Microscopy)	31 / 16 / 9	42 / 24 / 16	20 / 10 / 5	93 / 50 / 30

	Primary	High School	Technical	University	Other	Not Reported		
Education	59	81	52	16	2	24		
	Bora	Cocama	Senu	Ticuna	Tokami	Multiethnic	Not Reported	
Ethnicity	1	5	1	151	1	3	72	
	Lomas Lindas	12 De Octubre	San Francisco	Villa Andrea	Puerto Narino	San Pedro De Tipisca	Other	Not Reported
Location	11	25	9	15	136	21	14	3

Figure 4 Maximum-likelihood tree based on whole-mitogenome alignments of various *M. ozzardi* and *M. perstans* isolates. Abbreviation Moz and Mpe and indicate *M. ozzardi* and *M. perstans* respectively. The GenBank accessions are indicated in parenthesis next to isolate names, followed by the country of origin in the second parenthesis. Blue colors mark the isolates sequenced in this study. The DNA substitution model HKY+F+I was found to be the best fit according to Bayesian Information Criteria in ModelFinder. Values of ultrafast bootstrap support calculated with 1000 replicates is shown for branches with value higher than 80.

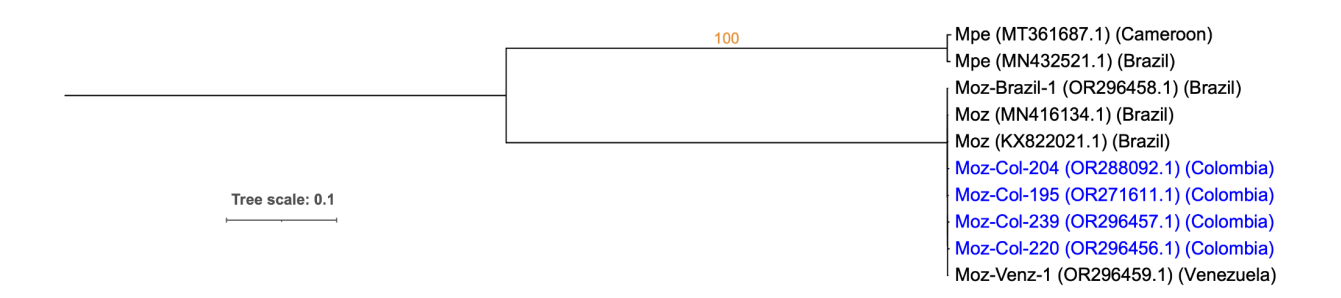
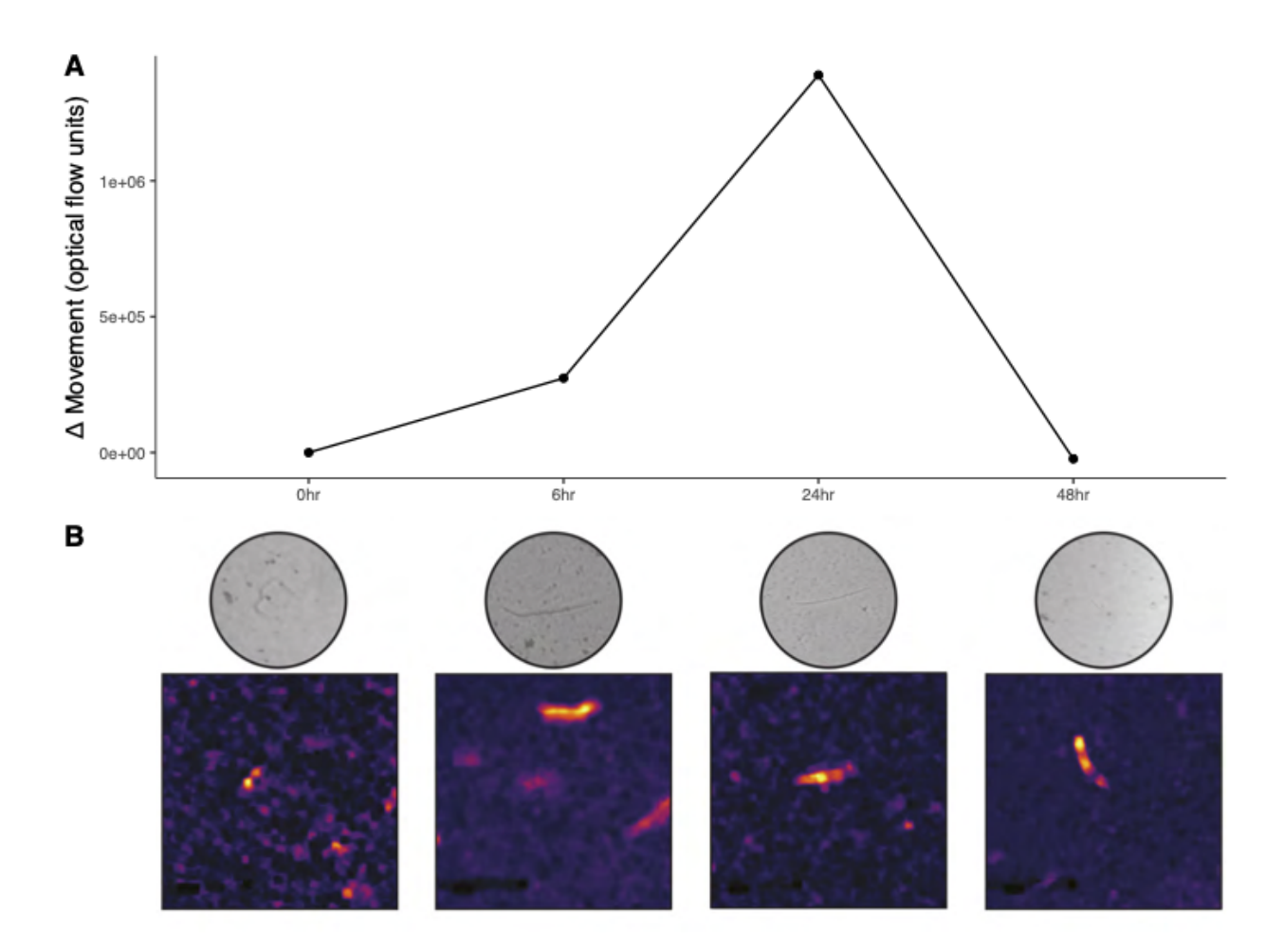


Figure 5 A) Motility of cryo-preserved *M. ozzardi* microfilariae over 48 hours as measured by an optical flow algorithm. **B)** Brightfield images and optical flowmaps of videos used for motility analysis of thawed cryopreserved *Mansonella* samples aligned with the timepoints in (A). Brighter regions of the flowmaps reflect areas where more parasite movement was detected.



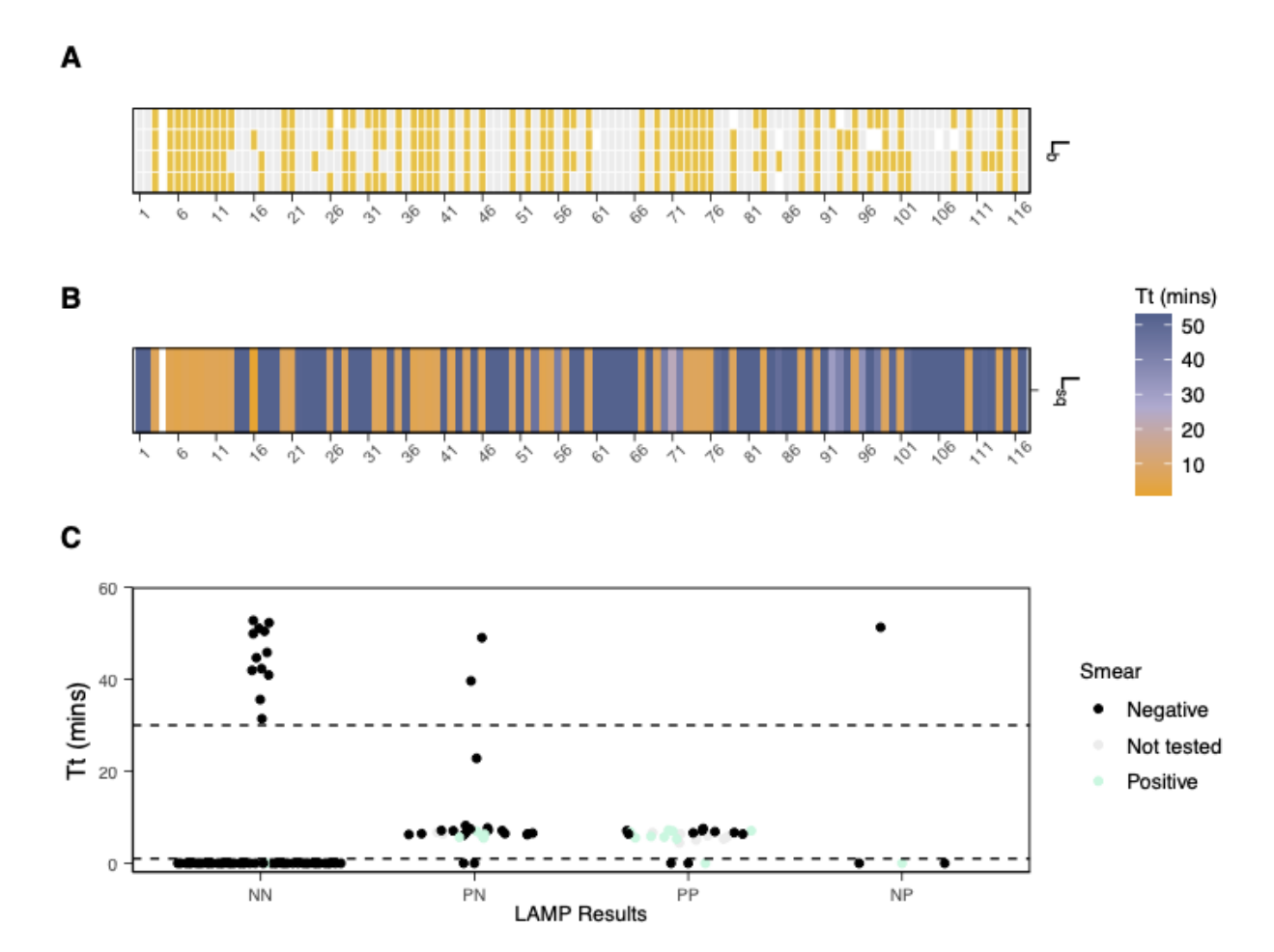
Supplementary Material

Supplementary Table 1. Model selection for prevalence of *M. ozzardi* across demographic variables. Variables include age, sex, education, ethnicity, and location. Global = focal model, m8 = winning model.

Table 1: Model selection table on Prevalence of infection

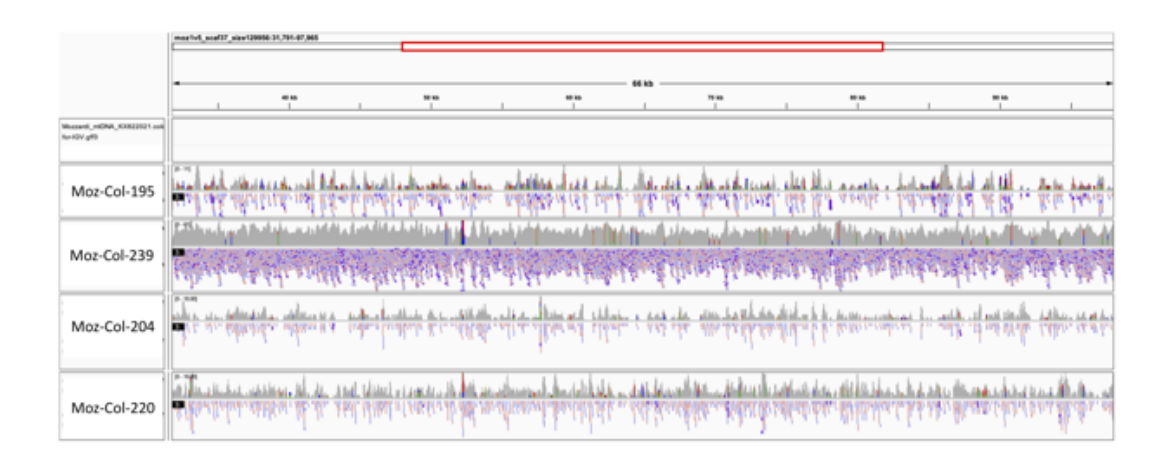
Model	K	AIC	Delta AIC	AIC weight	Log-Likelihood
m8	14	145.41	0.00	0.54	-58.71
m7	15	147.60	2.19	0.18	-58.80
m2	16	149.02	3.61	0.09	-58.51
m11	18	149.43	4.01	0.07	-56.71
m5	19	150.33	4.92	0.05	-56.17
m9	13	151.55	6.13	0.02	-62.77
m6	10	151.72	6.30	0.02	-65.86
m4	20	153.38	7.79	0.01	-56.69
m10	14	154.25	8.83	0.01	-63.12
m1	21	154.30	8.89	0.01	-56.15
m3	15	154.49	9.09	0.01	-62.25
global	23	155.58	10.17	0.00	-54.79

Supplementary Figure 1 A) Diagnostic results derived from survey one blood samples (1-117) for four replicates of LAMP using DNA extracted from whole blood samples (L_b) across two laboratories. Grey = negative for *M. ozzardi*. White = no result. **B)** Diagnostic results derived from survey one whole blood samples (1-117) for semi-quantitative LAMP (Tt). ND = not detected **C)** Semi-quantitative LAMP Tt counts (minutes) stratified by L_b and L_p results and colored by thin smear results. Dashed lines indicate Tt cuttoffs (> 1, <30 minutes = positive sq_LAMP). (NN = negative L_b and negative L_p , PN = positive L_b and negative L_p , PP = positive L_b and positive L_p , NP = negative L_b and positive L_p). LAMP assay data are specific to *M. ozzardi*.

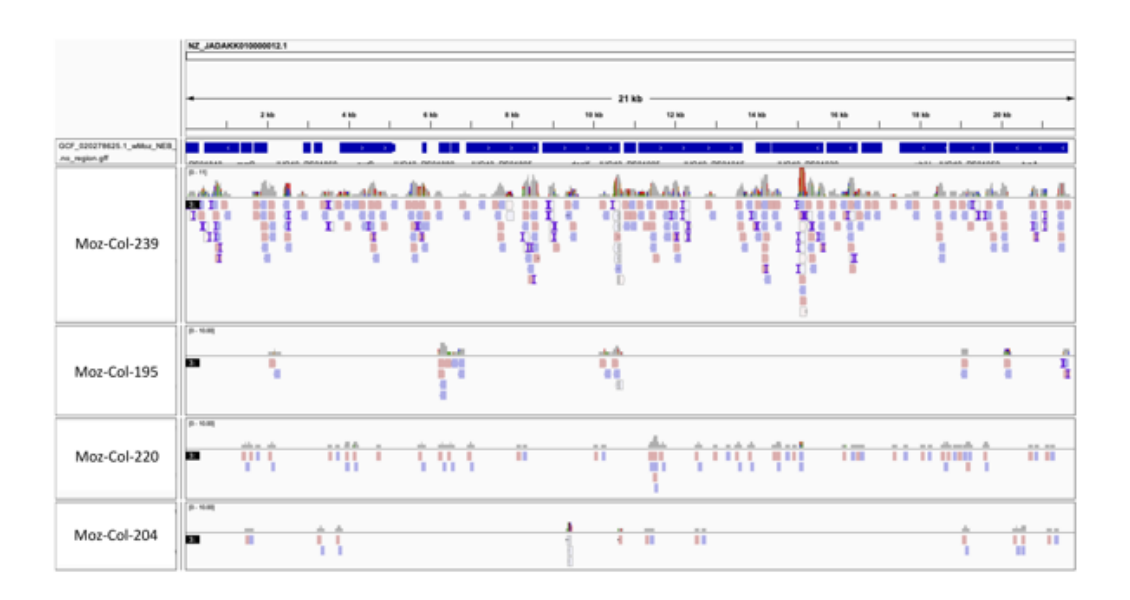


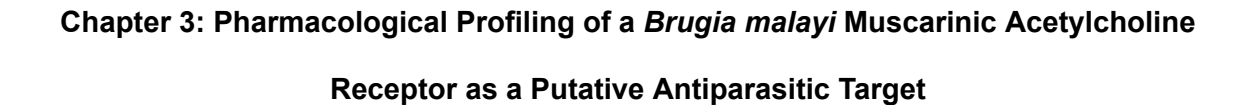
Supplementary Figure 2 A) Sequencing read coverage from different *M. ozzardi* isolates on the reference nuclear contigs from Moz-Venz-1 genome assembly. **B)** Sequencing read coverage from different *M. ozzardi* isolates on the *Wolbachia w*Moz reference genome assembly.

Α



В





Gallo KJ, Wheeler NJ, Elmi AM, Airs PM, Zamanian M. Pharmacological Profiling of a *Brugia* malayi Muscarinic Acetylcholine Receptor as a Putative Antiparasitic Target.

Antimicrob Agents Chemother. 2023; :e0118822. DOI: 10.1128/aac.01188-22

Abstract

The diversification of anthelmintic targets and mechanisms of action will help ensure the sustainable control of nematode infections in response to the growing threat of drug resistance. G protein-coupled receptors (GPCRs) are established drug targets in human medicine but remain unexploited as anthelmintic substrates despite their important roles in nematode neuromuscular and physiological processes. Bottlenecks in exploring the druggability of parasitic nematode GPCRs include a limited helminth genetic toolkit and difficulties establishing functional heterologous expression. In an effort to address some of these challenges, we profile the function and pharmacology of muscarinic acetylcholine receptors in the human parasite Brugia malayi, an etiological agent of human lymphatic filariasis. While acetylcholine-gated ion channels are intensely studied as targets of existing anthelmintics, comparatively little is known about metabotropic receptor contributions to parasite cholinergic signaling. Using multivariate phenotypic assays in microfilariae and adults, we show that nicotinic and muscarinic compounds disparately affect parasite fitness traits. We identify a putative G protein-linked acetylcholine receptor (Bma-GAR-3) that is highly expressed across intra-mammalian life stages and adapt spatial RNA in situ hybridization to map receptor transcripts to critical parasite tissues. Tissue-specific expression of Bma-gar-3 in Caenorhabditis elegans (body wall muscle, sensory neurons, and pharynx) enabled receptor deorphanization and pharmacological profiling in a nematode physiological context. Lastly, we developed an image-based feeding assay as a reporter of pharyngeal activity to facilitate GPCR screening in parasitized strains. We expect that these receptor characterization approaches and improved knowledge of GARs as putative drug targets will further advance the study of GPCR biology across medically important nematodes.

Introduction

Parasitic nematodes cause infectious diseases of poverty endemic to underdeveloped and exploited countries, accounting for the loss of over 8 million disability-adjusted life years [1]. Current control mechanisms for helminth infections rely on mass drug administration (MDA) with a limited arsenal of drugs. Lymphatic filariasis (LF) is a neglected tropical disease caused by mosquito-transmitted nematodes (*Wuchereria bancrofti, Brugia malayi,* and *Brugia timori*) that migrate to and develop in human lymphatics [2]. An estimated 50 million people currently have LF with at least 36 million people suffering from chronic debilitating and highly stigmatizing conditions such as elephantiasis and hydrocele [3–6]. Anthelmintics used for LF treatment are suboptimal; they do not kill adult stage parasites and are contraindicated in regions co-endemic for closely related parasites. Further, the threat of anthelmintic resistance [7–13] underscores a recognized need for new drugs to treat vector and soil-transmitted nematode infections in human and animal populations.

Current anthelmintics were primarily discovered using animal or whole-organism screening approaches [14,15] and no new anthelmintics have been approved for human use in decades. Target-based approaches may provide an alternative route to screening validated molecular targets at much higher throughput [15–17], but bottlenecks derive from limited knowledge of basic parasite biology, a dearth of actionable targets, and difficulties in establishing reliable heterologous platforms for target expression and screening [16,18]. While ligand-gated ion channels (LGICs) receive warranted attention as the primary targets of existing anthelmintics, there is a need to diversify and pursue other druggable proteins critical to the physiology and survival of parasitic nematodes [9,19–22].

G protein-coupled receptors (GPCRs) are highly druggable and are the targets of over one-third of all FDA approved drugs in human medicine [23]. Despite their recognition as lucrative targets [24–29], helminth GPCRs have yet to be effectively exploited as anthelmintic

substrates. Studies of GPCRs and their ligands in free-living nematodes show that this receptor family is involved in a range of important physiological processes [30–34]. Biogenic amines and neuropeptides elicit phenotypes of interest in free-living [30,31,35,36] and parasitic nematodes [26,37–39], many of which are likely mediated by metabotropic receptors. However, there is little data on the localization and function of parasitic nematode GPCRs, and pharmacological data is scant partly owing to difficulties in establishing reliable heterologous expression in single-cell systems [18,40,41]. Methods to characterize GPCRs in less tractable parasite species will better enable the prioritization of new receptor leads with host-divergent pharmacological profiles that can be selectively targeted.

Acetylcholine (ACh) and its receptor targets are essential for growth, development, and neuromuscular function in the clade V model nematode *Caenorhabditis elegans* [42,43]. The contribution of nicotinic acetylcholine receptors (nAChRs) to cholinergic signaling is underscored by the successful development of nicotinic channel agonists as antiparasitics [44–50], but much less is known about the druggability of muscarinic acetylcholine receptors (mAChRs) associated with slower but more sustained synaptic and extrasynaptic transmission. The *C. elegans* genome encodes three known G protein-linked acetylcholine receptors (GARs) [51–54] that are widely expressed in the nervous system and muscle tissues [53,55] and are involved in the regulation of feeding, mating, egg laying, and locomotion [32,52,56–58]. While some of the GAR functions in *C. elegans* are likely conserved in parasitic nematodes, very little is known about GAR biology in filariae and other clade III parasites. GAR-1 from the gastrointestinal nematode *Ascaris suum* displays atypical pharmacologic responses [25,59] and muscarinic compounds affect motility in adult stage *B. malayi* [60], justifying closer examination of the GAR receptor subfamily.

Here, we focus our efforts on the characterization of a phylum-conserved muscarinic acetylcholine receptor in *B. malayi* (*Bma-gar-3*). We examine the effects of muscarinic compounds on microfilariae and adult *Brugia* using multivariate phenotyping approaches, and

determine temporal and spatial gene expression patterns for *Bma-gar-3*. Building on previous work [35,61–64], we exploit the physiological context of *C. elegans* as a versatile heterologous platform for the study and characterization of parasite GPCRs as anthelmintic targets. We establish functional expression of *Bma-GAR-3* in *C. elegans* and tissue-specific phenotypic endpoints in parasitized strains that allow for deorphanization and pharmacologic characterization. Lastly, we validate a high-throughput assay that enables screening of *Bma-GAR-3* expressed in the *C. elegans* pharynx. These approaches circumvent some of the challenges associated with the study of GPCRs in difficult helminth systems, and are likely extensible to many other parasitic nematodes and receptors.

Results and Discussion

Brugia malayi GAR-3 is highly expressed across intra-mammalian life cycle stages and may mediate whole-organism effects of muscarinic compounds

Homology-based searches of annotated *C. elegans* G protein-linked acetylcholine receptors (GARs) were used to identify closely related biogenic amine receptors across six parasitic nematode species. Phylogenetic analysis of putative GARs reveals *B. malayi* possesses one-to-one orthologs of *C. elegans* GAR-2 and GAR-3 but not GAR-1 (**Figure 1A**). The clade IIIb nematode *A. suum* possesses a GAR-1 ortholog, but GAR-1 could not be identified in the *B. malayi* clade IIIc sublineag. Although GAR-3 clusters closest to human mAChRs [65], nematode GARs are significantly diverged from their mammalian host orthologs and likely exhibit distinct pharmacological profiles that may allow for selective targeting [25,53,66]. In order to determine temporal patterns of *B. malayi gar-2 and gar-3* gene expression, we performed qPCR across intra-mammalian life cycle stages (microfilariae (mf), L3, adult male, and adult female). *Bma-gar-3* is constitutively expressed across all life cycle stages and is much more highly

expressed than *Bma-gar-2* (**Figure 1B**), suggesting potentially outsized physiological roles throughout development.

To explore the gross effects of cholinergic compounds on parasite health, we optimized a number of phenotypic readouts in *Brugia* adults and microfilariae [67]. Parasites were incubated in muscarinic and nicotinic compounds and the stage-specific effects of these chemical perturbations on worm motility, viability, and fecundity were measured using a customized imaging platform [68]. Male and female *Brugia* adults were exposed to 10 μM and 100 μM of acetylcholine (ACh), atropine (ATR), arecholine (ARE), carbachol (CAR), oxotremorine-M (OXO), nicotine (NIC), and levamisole (LEV). ACh leads to a slow increase in baseline movement after prolonged exposure (24 and 48 hours), attributable to inefficient penetration of thecuticle [69] (**Figure 1C**). Treatment with nicotinic compounds (NIC and LEV) leads to an immediate drop in female and male (10 μM and 100 μM) worm motility followed by quick recovery, mediated by fast responding nAChRs [70].

Treatment with compounds associated with muscarinic activity (ATR, ARE, CAR, OXO) elicit a range of subtle-to-large effects on motility. ATR and ARE immediately decrease motility in male and female worms (100 μM) and CAR decreases motility in male worms (10 μM and 100 μM), in agreement with previous work [60]. *Cel*-GAR-2 is unaffected by the muscarinic agonists ARE and OXO or the antagonist ATR [53,65], suggesting that effects driven by these compounds are mediated by *Bma*-GAR-3. Given the promiscuity of some muscarinic compounds, it is possible that some of these effects are partly mediated by nicotinic receptors or that acute effects are dominated by ionotropic as opposed to metabotropic signaling. Fecundity was not significantly altered by any of the treatments except for 10 μM LEV at 24 hrs, a nicotinic compound that stimulates egg-laying in *C. elegans* [71] (**Figure 1D**).

Dose responses were carried out in mf stage parasites over three time points (0, 24, and 48 hours) to measure the effects of cholinergic compounds on motility and cell death. NIC and LEV both cause immediate inhibition of mf motility at high (>10⁻⁴ M) and low (>10⁻⁷ M)

concentrations, respectively (**Figure 1E**). OXO, a GAR-3 selective muscarinic compound, significantly decreases motility at high concentrations (>10⁻² M) in the 24-48 hour time frame. Morphologies of mf at 48 hours varied among treatments suggesting effects not fully captured by motility. LEV, NIC, and OXO treatment causes worms to become flaccid much like heat-killed (HK) control worms while ACh-treated worms maintain the posture of untreated controls. Some cell death was noticeable for all treatments except acetylcholine at high concentrations (>1 mM) at 48 hours (**Figure 1F**). While OXO-mediated effects suggest that perturbation of *Bma*-GAR-3 may elicit phenotypes of interest, the slower neuromodulatory action of this general receptor class may require assays sensitized to other subtle but important phenotypes in the host context [72,73]. More insight into tissue-specific expression patterns of this highly-expressed receptor would allow for better prediction of its physiological roles.

<u>Bma-gar-3 transcripts are widely expressed across critical tissues in adult stage</u> parasites

While GARs have been localized to specific cells and tissues using genetic tools in the tractable *C. elegans* system, the fine spatial distribution of these receptors is unknown in filarial or other parasitic nematodes. Building on an RNA tomography protocol [74], we developed a strategy to map *Bma-gar-3* transcripts across the adult female head and mid-section at 8 µm resolution while preserving spatial information (https://doi.org/10.6084/m9.figshare.20757481.v1). Individual sections were sequentially captured from the anterior tip (216 sections) of a single adult female *B. malayi* worm and RNAscope was used to localize *Bma-gar-3* transcripts within sections, allowing for reconstruction of expression patterns down the anterior-posterior axis of the head region (**Figure 2A**). *Bma-gar-3* is widely expressed across several tissue types including the body wall muscle and neurons, with near ubiquitous expression in digestive and reproductive tissues (**Figure 2B-D**). The expression of *Bma-gar-3* across these important

tissues overlaps with the expression pattern of *C. elegans gar-3* (body wall muscle, pharyngeal muscle, cord and other neurons) [75–78], suggesting some conservation of pleiotropic receptor function across clades.

Heterologous expression and deorphanization of *Bma*-GAR-3 in *C. elegans*

We sought to establish heterologous assays to characterize the pharmacology of *B. malayi* GPCRs through functional expression in discrete *C. elegans* tissues. Pharmacological profiling of parasite GPCRs in this heterologous system requires that the receptors are properly folded and exported to the membrane, that they signal through endogenous G proteins, and that their activation in response to exogenous ligands can be measured through convenient phenotypic endpoints. Building on previous work leveraging *C. elegans* as a heterologous expression platform for the expression of human GPCRs [79,80] and anthelmintic targets [35,61–63], we first established transgenic lines expressing *Bma*-GAR-3 in the *C. elegans* ASH sensory amphid neuron and the body wall muscle. These parasitized strains were used to develop and optimize tissue-specific assays to measure receptor activation.

To limit background signaling, transgenic lines were created in a *Cel*-GAR-3 knockout (*gar-3(gk305)*) genetic background. We employed simple plate-based assays to verify proper cell surface expression of *B. malayi* GAR-3 and to deorphanize the receptor by confirming activation by the putative ligand ACh. Activation of the *C. elegans* ASH neuron by noxious stimuli results in a well-characterized avoidance response whereby worms reverse their movement. We hypothesized that the successful activation of parasite GPCRs expressed in this neuron should lead to increased reversal frequency. We adapted an aversion assay [81,82] that involved placing individual worms in the center of a compound ring and monitoring for reversals in movement in response to test compounds (**Figure 3A**). Worms expressing *Bma*-GAR-3 in the ASH neuron (*sra-6p::Bma-gar-3*) exhibited strong aversion responses to ACh (100 mM) and the selective muscarinic agonist oxotremorine-M (100 mM) (**Figure 3B**). OXO has been shown to

specifically activate *C. elegans* GAR-3, but not *Cel*-GAR-1 or *Cel*-GAR-2 [51,53,66]. Neither the wild-type (N2) or knock-out (*gar-3(gk305)*) strains demonstrated aversion to ACh or OXO but all strains maintained consistent responses to negative (water) and positive (4 M fructose) controls.

We then assayed the effects of a cholinesterase inhibitor (aldicarb) on worms expressing *Bma*-GAR-3 in the body wall muscle (*myo-3p::Bma-gar-3*), predicting that the build up of ACh at the receptor synapse would lead to flaccid paralysis of this parasitized *C. elegans* strain. We adapted a protocol [83] that involved transferring worms onto plates with 1 mM aldicarb, restricting their movement with copper rings, and monitoring responses to touch stimuli over a 120 minute period. *myo-3p::Bma-gar-3* worms are hypersensitive to aldicarb-induced paralysis compared to wild-type and knock-out strains (Figure 3C-D). Combined, these results show that *Bma*-GAR-3 can be functionally expressed in both sensory neurons and body wall muscle, and that this receptor is activated by acetylcholine and oxotremorine-M.

Establishing pharyngeal endpoints for profiling Bma-GAR-3 pharmacology

In order to improve the pharmacologic profiling of parasite GPCRs in this heterologous system, we optimized more quantitative assays to measure receptor activation in response to exogenous drugs. Any eventual anthelmintic screen of parasite receptors expressed in this model system will require quantitative and scalable phenotypic readouts of receptor activity. We generated a strain of *C. elegans* expressing *Bma*-GAR-3 in the pharyngeal muscle (*myo-2p::Bma-gar-3*), hypothesizing that expression and activation of parasite acetylcholine receptors in the pharynx and the body wall would alter baseline and drug-induced pharyngeal pumping activity. Pharyngeal pumping activity can be directly measured by observing terminal bulb inversions [56,75,84] or using electropharyngeogram (EPG) recordings [85,86]. Each pump is highly regulated [57,87] by muscarinic receptors working in tandem with nAChRs [57,75,88].

To optimize assays that rely on pharyngeal function as a quantitative measure of direct or indirect parasite receptor activity, we investigated the effects of pumping stimuli across worm

developmental stages on our ability to resolve drug responses in parasitized strains. We first examined how different pharyngeal pumping stimuli would affect our ability to measure drug-induced changes in both larvae and adults. While OP50 and serotonin (5HT) are commonly used to elevate baseline pumping frequency [85,89–93] for assay sensitization, it is important that these stimuli do not mask drug effects and allow for the reliable capture of both inhibitory and stimulatory responses to drug exposure. We tested combinations of OP50, 5HT, and a known GAR-3-dependent inhibitor of pharyngeal pumping (arecoline) [75] to assess our ability to capture effects in both directions in L1 and young adult animals.

L1 assays carried out on OP50 plates confirmed that this food stimulant does not saturate pumping responses or mask expected drug effects. The inhibitory effect of arecoline can be measured in strains expressing either *C. elegans* GAR-3 (N2) or *B. malayi* GAR-3 (*myo-2p::Bma-gar-3*) in the pharynx (**Figure 4A**). A dynamic range of pump frequencies is observable using OP50 and we conclude from these data that L1 assays should be carried out in the presence of OP50 and without 5HT. OP50 leads to a non-saturating increase in L1 baseline pharyngeal pumping that allows us to measure both drug-induced stimulation and inhibition of pump frequency. In contrast, adult stage assays carried out in the presence of OP50 saturated baseline pharyngeal pumping frequency. The addition of 5HT leads to no further increase in pumping rate and the inhibitory effects of ARE are largely masked in these conditions (**Figure 4A**). Assays carried out in the absence of OP50 allow for the robust detection of both 5HT stimulation and arecoline inhibition. We conclude from these data that adult assays should be carried out in the absence of OP50 and with drugs in combination with 5HT to allow for the largest dynamic range of stimulation and inhibition.

We next used these optimized L1 and adult stage assays (**Figure 4B**) to confirm the action of the selective *Cel*-GAR-3 agonist oxotremorine-M. OXO increases pumping frequency in L1 (~ 41%) and adult (~26%) stage N2 worms (**Figure 4C-D**). Knock-out of native *gar-3* leads to a loss of OXO responsiveness, which is near completely rescued by expression of *Bma-gar-3*

in the pharynx but not the body wall muscle. We next profiled the responses of parasitized strains to muscarinic and nicotinic compounds with less receptor specificity. In L1 stage worms, expression of *Bma-gar-3* in the pharynx restores the wild-type response profile (**Figure 4E**). In adult stage worms, expression of *Bma-gar-3* in the body wall leads to hyperstimulation of pumping in response to CAR, while expression of *Bma-gar-3* in both the pharynx and body wall leads to a decreased inhibitory response to ATR compared with either wild-type or *gar-3(gk305)* strains (**Figure 4F**).

Although it is known that pharyngeal pumping can be modulated by cholinergic signaling in both tissue types, the precise mechanism by which the body wall and pharynx communicate is unclear [86,94,95]. Interpretations of how pharyngeal pumping is modulated by direct versus indirect pharmacological action at our receptor of interest can be confounded by the promiscuous binding of cholinergic compounds to a range of muscarinic and nicotinic receptors expressed across relevant tissues and perhaps differentially expressed across stages. Despite these complications, it is reasonable to expect that compounds with high specificity for GAR-3 can be identified by comparing responses across gar-3(gk305) and gar-3(gk305); myo-2p::Bma-gar-3 strains.

<u>Electropharyngeal measurements of Bma-GAR-3 activity in parasitized strains</u>

Electrophysiological recordings from the pharynx can provide more detailed information about pharyngeal function in response to drug. Using established protocols [85], we sought to use electropharyngeogram (EPG) recordings to investigate other pharyngeal phenotypes modulated by *Bma*-GAR-3 expression in the body wall and pharynx of young adult *C. elegans*. We recorded individual worms for two minutes after a 20 minute drug incubation period, mirroring the visual counting assay (**Figure 5A**). The use of 5HT in combination with test drugs was necessary to capture the inhibitory effects of ARE and to recapitulate trends from visual counting data (**Figure 5B**).

We next used EPG recordings to test whether the effects of cholinergics on electrophysiological features could be linked to Bma-GAR-3 activity in parasitized strains. We found that EPG-derived pump frequency did not correlate well with visual counting data. Most notably, OXO did not exhibit a pattern of differential response and rescue in gar-3(gk305) and gar-3(gk305);myo-2p::Bma-gar-3, respectively (Figure 5C). General discrepancies between visual counts and EPG-derived pump frequency are likely due to the disconnect between terminal bulb movement and action potentials, supported by the fact that C. elegans GAR-3 regulates both membrane potential and excitation-contraction coupling through a yet defined signaling pathway [75]. While EPG-derived pump frequency was not a reporter of Bma-GAR-3 activation in this assay, other electrophysiologic features show patterns consistent with Bma-GAR-3 phenotypic rescue (Figure 5D). Specifically, expression of Bma-gar-3 in the pharynx rescues the OXO-induced increase in peak amplitude that is lost in the *gar-3(gk305)* background (Figure 5E). EPG recordings provide a rich set of features (Sup Figure 1) that can reveal the activation of parasite receptors in response to exogenous drug. While these electrophysiological assays provide deeper insight into electric and chemical signaling dynamics, they do not enable high-throughput screening of parasitized strains to identify drugs that act on receptors of interest.

Establishing a high throughput image-based feeding assay for screening of parasitized strains

We developed a high-throughput imaging assay to measure pharyngeal pumping as a reporter of receptor activity in parasitized animals. Fluorescence uptake in the form of beads, bacteria, and dye has been used to measure feeding behaviors in *C. elegans*, whereby drug modulation of pumping rates can be expected to impact the amount of intestinal fluorescence. Many of these assays are low in throughput [96–99] or require a large particle sorter [100–103], or

luminometer [84]necessitating the development of a high-throughput and high-content imaging endpoint that allows for the measurement of intestinal fluorescence and transgenic markers.

We optimized parameters for a microtiter plate assay that measures intestinal accumulation of fluorescent dye as a correlate of pharyngeal activity. L1 synchronized worms were aliquoted into 96-well plates and grown to adults over 48 hours in the presence of HB101. Worms are then treated with a test compound for 20 minutes followed by a 20 minute BODIPY 558/568 (red) incubation. We tested two concentrations of BODIPY to help minimize background fluorescence and ensure that dye was not a limiting reagent. We tested the inclusion of 5HT and HB101 as feeding stimulants for the duration of the drug exposure, as well as the inclusion of HB101 in the BODIPY incubation period. Assays using at least 90 ng/mL BODIPY (2x) generated the best conditions to detect both pharyngeal stimulation (5HT and HB101) and inhibition (NIC) (**Figure 6A**). The inclusion of HB101 in the dye incubation period was not necessary to detect these differences (**Figure 6A**).

To validate this protocol as a means to screen parasite receptors at higher throughput, we compared the effects of cholinergic compounds in *gar-3(gk305)* and *gar-3(gk305)*; *myo-2p::Bma-gar-3* animals. We treated worms with cholinergic compounds followed by BODIPY incubation. An image processing pipeline was established to identify transgene (+) worms via pharyngeal GFP expression. OXO causes an increase in dye uptake in wild-type worms compared to non-treated controls (~ 17%, p = 9.4e-07), consistent with increased pumping frequency observed in visual counting assays. OXO decreases dye uptake in the *gar-3(gk305)* background, which is rescued by expression of *Bma-gar-3* in the pharynx (**Figure 6B**). These results reaffirm that OXO has selective effects on *Bma-*GAR-3 in the pharynx and provides proof of principle for this high content imaging approach for pharmacological profiling of transgenically expressed parasite GPCRs.

Conclusion

Parasite G protein-coupled receptors remain unexploited as anthelmintic targets despite their involvement in critical nematode neuromuscular and physiological processes. One significant bottleneck in exploring the pharmacology of parasite GPCRs results from difficulties in consistently establishing heterologous expression in single-cell systems. Yeast and mammalian cell culture systems have paved the way for deorphanization of helminth GPCRs [18,25,104], but not all receptors express or behave properly in cell types derived from distant phylogenetic lineages. The combinations of accessory proteins, molecular chaperones, G proteins, and membrane determinants required for the successful folding, cell-surface expression, and signaling of parasite receptors in surrogate systems have not been comprehensively identified. To avoid some of these complications, we explored a range of assays for parasite GPCR expression and profiling in the model nematode *C. elegans*.

We identified a *B. malayi* muscarinic GPCR (*Bma-gar-3*) that is highly expressed throughout the intra-mammalian life stages and developed a spatial RNAscope protocol to map receptor transcripts in multiple tissue types in the adult stage. Multivariate phenotypic assays of cholinergic effects on microfilariae and adult parasites reveal differential effects of nicotinic and muscarinic agents. We show that muscarinic compounds affect motility in both adult and mf stage parasites, some of which are likely to be mediated by GAR-3. We predict that sampling a broader array of muscarinic compounds will likely reveal other overt and subtle but important phenotypes that are relevant to potential anthelmintic mechanisms of action.

Building upon previous work [35,61–64], we expressed *Bma-gar-3* in the *C. elegans* body wall muscle, pharynx, and sensory neurons. Different phenotypic endpoints were optimized to measure receptor activity across these parasitized strains. Simple plate-based assays allowed for the deorphanization of *Bma*-GAR-3 expressed in the body wall and sensory neurons. We focused primarily on pharyngeal expression, given amenability to a range of visual,

electrophysiological, and imaging assays. While visual observations of pharyngeal pumping and electropharyngeogram recordings provided different measurements of *Bma*-GAR-3 perturbation, these assays are ultimately low in throughput. To enable more facile and higher throughput screening of pharynx-expressed receptors, we deployed a microtiter plate imaging assay that measures the accumulation of lipophilic dye as a reporter of pharyngeal pumping. We show that this feeding assay can be used to detect activation of *Bma*-GAR-3 within the pharynx.

The suitability of these approaches for a given parasite GPCR will depend on the complement of related receptors and endogenous ligands that signal in targeted tissues. We show that transgenic strains can be created in various genetic knockout backgrounds to help mitigate some of these concerns. While expression in scalable single-cell systems will remain an important objective for high-throughput screening (HTS) against GPCR targets, functional parasite receptor assays in a more native nematode cell and physiological environment can provide important baseline pharmacological data and transgenic whole-organism assays can conceivably be adapted for high-throughput screening and anthelmintic discovery.

Methods

Protocol and data availability

All primary data (phylogenetic, qPCR, phenotypic) and pipelines for statistical analysis and data visualization are available at https://github.com/zamanianlab/Bm-GAR-ms.

Parasites and chemical reagents

B. malayi and *B. pahangi* adults extracted from the *Meriones unguiculatus* infection system (NIH/NIAID Filariasis Research Reagent Resource Center) [105] were maintained in daily changes of RPMI 1640 with L-glutamine (Sigma-Aldrich) supplemented with FBS (10% v/v, Fisher Scientific) and penicillin-streptomycin (0.1 mg/mL, Gibco) at 37°C with 5% CO₂ unless

otherwise specified. *Brugia* microfilariae isolated from the same system were maintained in RPMI 1640 with L-glutamine (Sigma-Aldrich) supplemented and penicillin-streptomycin (0.1 mg/mL, Gibco) at 37°C with 5% CO₂ unless otherwise specified.

Chemicals used in assays include serotonin (Fisher Scientific cat#AAB2126306), arecoline (Fisher Scientific cat# AC250130050), atropine (Santa Cruz Biotechnology cat# sc-252392), nicotine (Santa Cruz Biotechnology cat# sc-482740), levamisole (VWR cat #TCL0231-1G), carbachol (Santa Cruz Biotechnology cat# sc-202092), acetylcholine (Fisher Scientific cat# AC159170050), oxotremorine-M (Santa Cruz Biotechnology cat# sc-203656), aldicarb (Santa Cruz Biotechnology cat# sc-254939).

Phylogenetics

Putative parasite GARs were identified using a reciprocal BLASTp [106] approach using known *C. elegans* GARs. This initial list of GARs was expanded with homology-based searches against the *C. elegans* predicted proteome and a broader list of *C. elegans* [107] biogenic amine receptors was used to carry out blastp searches against the predicted proteomes of *B. malayi* [108], Ancylostoma caninum [109], Ascaris suum [110], Haemonchus contortus [111], Strongyloides ratti [112], and Trichuris muris [113] (WormBase ParaSite v16 [114]). Filtered hits (percent identity > 30%, E-value < 10⁻⁴, and percent coverage > 40%) that survived a reciprocal blastp search against *C. elegans* were retained. This list was combined with human muscarinic receptors for phylogenetic inference and annotation. Receptors were aligned with MAFFT [115], trimmed with trimAl [116], and phylogenetic trees were inferred with IQ-TREE [117]. Bootstrap values from 1,000 replicates were drawn as nodal support onto the maximum-likelihood tree. Trees were visualized and annotated with ggtree [118].

Adult parasite assays

Multivariate phenotyping of adult parasites was performed as described [67,119]. After receipt from the FR3, adult male and female *B. pahangi* parasites were manually sorted into 24-well plates filled with 750 μL of complete media (RPMI 1640 + 10% FBS + pen/strep) per well. Parasites were incubated overnight, after which individual parasites were transferred to new plates with 750 μL incomplete media. 100X compound stocks were made fresh daily in H₂O. Plates were recorded for 15 sec, compound was added, and plates were immediately recorded again. Recordings were taken 1 hr post-treatment and 24 hr post-treatment, prior to transferring parasites to a new pre-loaded drug plate. Final recordings were taken 48 hr post-treatment. Three biological replicates from separate batches of parasite infection cohorts were assayed with four worms per treatment. Videos were analyzed with the optical flow (motility) module of wrmXpress [68].

Conditioned media from female worms from the initial overnight incubation in complete media and 24/48 hr treatment plates were transferred to 1.5 mL tubes and centrifuged for 5 min at 10,000 *x g* to pellet progeny. 500 µL of the supernatant was removed, and the remainder was stored at 4°C for >48 hr. To quantify progeny, 50 µL aliquots were transferred to wells of a 96-well plate (Greiner), and each well was imaged with transmitted light at 2X with an ImageXpress Nano (Molecular Devices). Images of progeny were segmented as previously described [67], and segmented pixels were counted to infer output of progeny using a previously generated model [67].

Microfilariae assays

B. malayi microfilariae motility and cell toxicity assays were performed as described [67,120]. Briefly, mf are purified using a PD-10 Desalting Column (VWR, cat# 95017-001) into culture media and titered to a concentration of 10 mf/μL. 100 μL containing 1,000 mf were added to

each well of a 96-well plate. Heat killed controls were incubating for 1 hr at 60°C before being added to wells. Serial dilutions of 100 mM stock of each drug was made fresh in water. Plates were imaged immediately after treatment (0 hr) and 24 and 48 hr after treatment. At least two replicates with high technical replication were run for motility assays. CellTox (Promega cat# G8742) staining was performed at 48 hr following the kit protocol with half the recommended concentration of CellTox. Wells were imaged using an ImageXpress Nano (Molecular Devices). Three replicate dose-response plates were assayed using CellTox assays. Videos were analyzed with the motility and segmentation modules of wrmXpress [68] and output data was analyzed using the R statistical software.

qPCR

Parasites were flash frozen in liquid N₂ in 1.5 mL tubes and stored at -80°C in TRIzol LS (Thermo Scientific cat# 10296028) in batches of 500,000 (mf), 300-500 (L3), or 3 (adults). Three independent samples originating from different batches of animal infections were collected for each stage (mf, L3, adult male, and adult female). Freeze-thawed samples were homogenized by compact bead mill (TissueLyser LT, Invitrogen) and RNA was extracted using the Zymo Direct-zol RNA Miniprep kit (cat# R2050). RNA integrity and concentration were assessed via NanoDrop, and cDNA was generated with the SuperScript III kit (ThermoFisher cat# 18080051) using equal amounts of oligo(dT) and random hexamer primers for first-strand synthesis. qPCR primers for *Bma-gar-2* (F: 5'-TAATACGACTCACTATAGGGCGACGTACTTCCTCCGATGT-3', R: 5'-TAATACGACTCACTATAGGGCCGCTCATCGTATTCCATTT-3') and *Bma-gar-3* (F: 5'-TTTTGGCCACCATGGATTATT-3', R: 5'-TGTATAACGCAACGGTCAGG-3') were designed with Primer3 [121] and optimized to quantify expression levels from cDNA. GAPDH primers [122] were used as a control. 20 μL qPCR reactions were carried out using 2x PowerUp SYBR Green Master Mix (Fisher Scientific cat# A25776), 800 nM primers, and 10 ng of cDNA as input. Reactions were run in triplicate on a StepOnePlus real-time PCR system with the following

program: 2 min for 50°C, 95°C for 5 min, 40 cycles of: 95°C for 15 sec, 55°C for 15 sec, and 72°C for 1 min. C_T values were calculated with the system's automatic threshold.

RNAscope in situ hybridization

Adult *B. malayi* females were cultured overnight and separated in 10 cm petri dishes, dipped in 70% ethanol, and spatially embedded in 1% bacto-agar. Blocks of bacto-agar were dehydrated for 5 minutes in 25%, 50%, 70% ethanol sequentially and stored in 100% ethanol overnight. The bacto-agar embedded tissue was processed into a paraffin block and agar was trimmed from the anterior tip of the agar block before embedding for cross-sections. Blocks were sectioned at 8 µm and sections were arranged sequentially on slides, keeping all sections.

Hybridization probes used for RNAscope (ACD Bio) include DapB (dihydrodipicolinate reductase, *Bacillus subtilis*) as a negative control and two highly-expressed *B. malayi* genes as positive controls: *Bma-Bm4733* (*B. malayi* β-tubulin targeting 2-1031 of XM_001896580.2 (20ZZ)) and *Bma-cdc-42* (*B. malayi* putative GTP-binding protein targeting 2-550 of XM_001899971.1 (11ZZ)). Our *Bma-*GAR-3 target probe targets 400-1501 of XM_043081323.1 (20ZZ). The standard RNAscope™ 2.5 HD Assay-RED kit (ACD Bio) protocol was followed with an adjusted length of 8 min for retrieval using a steamer and 45 min for amp 5. Imaging was done in bright field with 40x-Nikon Plan Apo on a Nikon Eclipse80i. Presence of red punctate staining, indicating target gene expression, was quantified by manual annotation by two independent observers. Annotation and alignment were carried out with Fiji [123] using TrakEM2 [124].

Cloning and transgenegic C. elegans strains

The open-reading frame (ORF) for the longest predicted isoform of *Bma-gar-3* (isoform a, WormBase ParaSite version 17) was selected for study based on manual assessment and

alignment with homologous GARs. This isoform is supported by long-read RNA sequencing data [125] that extends the model upstream of the 5' end of isoform b. The ORF was synthesized (GenScript) and cloned into pPD133.48, L4663 (a gift from Andrew Fire, Addgene plasmid #1665) using BamHI/KpnI sites to create pMZ0005 (*myo3p::Bma-gar-3::unc-54-3'UTR*). pMZ0012 (*sra-6p::Bma-gar-3::unc-54-3'UTR*) was created by subcloning *Bma-gar-3* into *sra-6p::ChR2*YFP* (a gift from Shawn Lockery [126]) using BamHI/EcoRI sites. pMZ0018 (*myo-2p::Bma-gar-3::unc-54-3'UTR*) was created by amplifying *myo-2p* from pPD96.48, L2531 (a gift from Andrew Fire, Addgene plasmid #1607) with 5' Xbal and 3' BamHI sites and using this amplicon to replace *myo-3p* in pMZ0012.

Genotypes generated and used in this study include: ZAM7 (*gar-3(gk305*) V, *maz7Ex*[*sra-6p::Bma-gar-3::unc-54* 3'UTR; *sra-6p::GCaMP3*; *unc-122p::GFP*]), ZAM10 (*gar-3(gk305*) V, *maz10Ex*[*myo-3p::Bma-gar-3::unc-54* 3'UTR; *myo-2p::GFP*]), and ZAM11 (*gar-3(gk305*) V, *maz11Ex*[*myo-2p::Bma-gar-3::unc-54* 3'UTR; *myo-2p::GFP*]) were created as described [127] by injecting pMZ0012 (75 ng/μL), pMZ0005 (30 ng/μL), and pMZ0018 (30 ng/μL) into *gar-3(gk305)*, respectively, along with fluorescent markers (*unc-122p::GFP* or *myo-2p::GFP*) and empty vector (pPD95.75) to create a final concentration of 100 ng/μL. ZAM19 ([*myo-2p::GFP*]) and ZAM20 (*gar-3(gk305)*) V [*myo-2p::GFP*]) were created by injecting 10 ng/μL of a fluorescent marker (*myo-2p::GFP*) and empty vector (pPD95.75) to create a final concentration of 100 ng/μL. VC657(*gar-3(gk305)* V) was sourced from the *C. elegans* Gene Knockout Consortium [128]. Lines were maintained at 20°C on NGM plates seeded with *E. coli* strain OP50 and routinely picked to fresh plates at the L4 stage.

Ring aversion assay

Bleach synchronized adult worms were rinsed three times in M9 and pipetted onto unseeded 6 cm plates. To assemble the assay plate, a copper ring (PlumbMaster cat# 17668) was soaked in a test compound with fast green dye as a visual marker and placed in the center of the plate. 1

μL of 1:1000 diluted diacetyl (attractant) was combined with 1 μL fast green and added outside of the ring. Plates were used immediately after assembly. The copper ring was removed after 1 minute to allow soaking of the test compound into the agar. Individual worms were picked without bacteria to the center of the compound ring on assay plates and monitored for reversals in response to test compounds. Three biological replicates from three independent bleaches were run using four worms per treatment per strain. Observations were made until either the worm crossed the compound ring or six attempts to cross the compound ring occurred without the worm crossing. Water was used as a negative control and 4 M D-fructose was used as a positive control.

Aldicarb paralysis assay

1 mM aldicarb plates were made by diluting 100 mM aldicarb (in 70% ethanol) in NGM. Plates were stored at 4°C and used within 30 days. Thirty L4s from each strain were picked to OP50 seeded NGM plates and cultured at 20°C overnight until they reached the young adult stage. Aldicarb plates were acclimated to room temperature on the morning of the assay. Four copper rings (PlumbMaster cat# 17668) were dipped in 70% ethanol and briefly flamed before placement onto a single aldicarb plate to form quadrants. 10 µL of OP50 from overnight liquid culture was spotted into the center of each of the copper rings and allowed to dry for 30 min. A minimum of 10 worms per strain were picked to the center of a quadrant, allowing the testing of four strains per plate. Four biological replicates were carried out across strains. After 30 min and every 10 min thereafter, each worm was tapped 3 times on the head and tail, paralyzed worms were removed, and remaining worms were tallied. This process continued until the 2 hr mark.

Visual pharyngeal pumping assay

For L1 stage assays, gravid worms were bleached and embryos were hatched on unseeded 10 cm NGM plates overnight (2,000 embryos per plate). L1s were washed from plates into 1.5 mL tubes and treated with drug for 20 min. 500 µL of the treated worm mixture was then transferred to an unseeded 10 cm NGM plate and allowed to dry for 5 min. Individual transgene (+) worms were then picked to seeded 6 cm NGM assay plates and given 10 min to acclimate. Adult assays required minor modifications of the L1 protocol. Young adults were developed on seeded 10 cm NGM plates, drug-treated worms were transferred to 10 cm plates with no drying period, and transgene (+) worms were picked to unseeded 6 cm NGM assay plates. For optimization and cholinergic assays, an average of 8 worms were visually phenotyped for each strain-condition combination. Pumps were measured by the motion of the terminal bulb grinder over a 30 sec (L1s) or 10 sec (adults) interval using a Zeiss Axio Vert.A1 at 10x with DIC optics.

Electropharyngeogram recordings

Electropharyngeograms (EPGs) were recorded with the ScreenChip system (InVivo Biosystems). Briefly, worms were bleach synchronized and embryos were hatched and developed on seeded 10 cm NGM plates. Young adult worms were washed 3 times with M9 in 1.5 mL tubes. Worms were treated for 20 min before loading them into the ScreenChip40 microfluidic chamber. Each worm was vacuumed into the channel, acclimated for 30 sec, and recorded for 2 min using the NemaAcquire 2.1 software. Worms from three biological replicates representing independent bleaches were assayed for optimization (minimum of 15 worms per condition), and one replicate was assayed for the cholinergic panel (minimum of 5 worms per condition). Analysis was done using NemaAnalysis 0.2 with default settings found under customize analysis. Filtering of data was done by modifying "parameters left" for signal to noise

ratio (SNR), E and R highpass cutoffs, and minimum absolute threshold followed by visually ensuring all pumps were identified and background noise was ignored.

Image-based feeding assay

Bleach synchronized larval stage worms (L1) were aliquoted into 96-well plates at a titer of 50 L1 per well along with E. coli HB101 bacterial food (2.5 mg/mL final concentration). Worms were incubated for 48 hr at 20°C, shaking at 180 RPM until reaching adult stage [129]. For the initial screen, adult stage worms were drug treated for 20 min followed by addition of 180 ng/mL BODIPY 558/568 (Thermo Scientific cat#D3835) combined with HB101 and again incubated for 20 min. For optimization assays, 45 ng/mL (1x) or 90 ng/mL (2x) BODIPY 558/568 combined with M9 or HB101 was added to the plate with the same incubation time. Plates were washed 3 times with M9 and paralyzed with 50 mM sodium azide. Images of worms in transmitted light, GFP, and TxRed were taken on an ImageXpress Nano (Molecular Devices) at 2x. Images were analyzed with the feeding module of wrmXpress, which incorporates a custom CellProfiler model using the Worm Toolbox plugin [130,131]. Segmented worms were computationally straightened and GFP and TxRed were quantified. Transgenic worms were identified using a robust cutoff of GFP quantification such that only worms expressing Bma-gar-3 were analyzed (Sup Figure 2 A-B). Non-worm objects and contaminating fluorescence were further filtered with size thresholds and outlier pruning (TxRed FLU z-score > 3). Total fluorescent dye uptake for GFP(+) worms was quantified using the StdIntensity parameter.

Acknowledgements

The authors thank the University of Wisconsin Translational Research Initiatives in Pathology laboratory (TRIP), supported by the UW Department of Pathology and Laboratory Medicine, UWCCC (P30 CA014520) and the Office of The Director- NIH (S10 OD023526) for use of its

facilities and services. Some strains were provided by the CGC, which is funded by NIH Office of Research Infrastructure Programs (P40 OD010440). *Brugia* life cycle stages were obtained through the NIH/NIAID Filarial Research Reagent Resource Center (FR3), morphological voucher specimens are stored at the Harold W. Manter Museum at University of Nebraska, accession numbers P2021-2032. Image processing was performed using the compute resources and assistance of the UW-Madison Center For High Throughput Computing (CHTC) in the Department of Computer Sciences. The CHTC is supported by UW-Madison, the Advanced Computing Initiative, the Wisconsin Alumni Research Foundation, the Wisconsin Institutes for Discovery, and the National Science Foundation, and is an active member of the OSG Consortium, which is supported by the National Science Foundation and the U.S. Department of Energy's Office of Science. The authors would also like to thank the members of the Zamanian laboratory for critical comments on the manuscript. **Author contributions**: Study design: Gallo KJ, Zamanian M. Execution: Gallo KJ, Wheeler NJ, Elmi AM. Analysis and interpretation: Gallo KJ, Wheeler NJ, Airs PM, Zamanian M. Writing and proofing: Gallo KJ, Wheeler NJ, Elmi AM, Airs PM, Zamanian M.

Funding

This work was supported by National Institutes of Health NIAID grant R01 AI151171 to MZ. KJG was supported by a UW-SciMed GRS Fellowship (scimedgrs.wisc.edu) and NIH Parasitology and Vector Biology Training grant T32 AI007414 (NIH.gov). NJW was supported by NIH Ruth Kirschstein NRSA fellowship F32 AI152347 (NIH.gov).

References

- Hotez PJ, Alvarado M, Basáñez M-G, et al. The global burden of disease study 2010: interpretation and implications for the neglected tropical diseases. PLoS Negl Trop Dis. 2014; 8(7):e2865.
- 2. Roberts L, Schmidt GD, Janovy J Jr. Foundations of Parasitology. McGraw-Hill Education; 2009.
- 3. Ton TGN, Mackenzie C, Molyneux DH. The burden of mental health in lymphatic filariasis. Infect Dis Poverty. **2015**; 4:34.
- 4. Weiss MG. Stigma and the social burden of neglected tropical diseases. PLoS Negl Trop Dis. **2008**; 2(5):e237.
- 5. World Health Organization. Guideline: Alternative Mass Drug Administration Regimens to Eliminate Lymphatic Filariasis. Geneva: World Health Organization; 2018.
- Local Burden of Disease 2019 Neglected Tropical Diseases Collaborators. The global distribution of lymphatic filariasis, 2000-18: a geospatial analysis. Lancet Glob Health. 2020; 8(9):e1186–e1194.
- 7. International Helminth Genomes Consortium. Comparative genomics of the major parasitic worms. Nat Genet. **2019**; 51(1):163–174.
- 8. Geary TG, Woo K, McCarthy JS, et al. Unresolved issues in anthelmintic pharmacology for helminthiases of humans. Int J Parasitol. **2010**; 40(1):1–13.
- 9. Abongwa M, Martin RJ, Robertson AP. A BRIEF REVIEW ON THE MODE OF ACTION OF ANTINEMATODAL DRUGS. Acta Vet . **2017**; 67(2):137–152.
- 10. Campbell WC. Efficacy of the avermectins against filarial parasites: a short review. Vet Res Commun. Springer; **1982**; 5(3):251–262.
- 11. Wolstenholme AJ, Evans CC, Jimenez PD, Moorhead AR. The emergence of macrocyclic lactone resistance in the canine heartworm, Dirofilaria immitis. Parasitology. **2015**; 142(10):1249–1259.
- 12. Ismail M, Botros S, Metwally A, et al. Resistance to praziquantel: direct evidence from Schistosoma mansoni isolated from Egyptian villagers. Am J Trop Med Hyg. **1999**; 60(6):932–935.
- 13. Osei-Atweneboana MY, Awadzi K, Attah SK, Boakye DA, Gyapong JO, Prichard RK. Phenotypic evidence of emerging ivermectin resistance in Onchocerca volvulus. PLoS Negl Trop Dis. **2011**; 5(3):e998.
- 14. Laing R, Gillan V, Devaney E. Ivermectin Old Drug, New Tricks? Trends Parasitol. **2017**; 33(6):463–472.
- 15. Geary TG. Mechanism-based screening strategies for anthelmintic discovery. Parasitic Helminths. Weinheim, Germany: Wiley-VCH Verlag GmbH & Co. KGaA; 2012. p. 121–134.

- 16. Nixon SA, Welz C, Woods DJ, Costa-Junior L, Zamanian M, Martin RJ. Where are all the anthelmintics? Challenges and opportunities on the path to new anthelmintics. Int J Parasitol Drugs Drug Resist. **2020**; 14:8–16.
- 17. Zamanian M, Chan JD. High-content approaches to anthelmintic drug screening. Trends Parasitol. **2021**; 37(9):780–789.
- 18. Kubiak TM, Larsen MJ, Bowman JW, Geary TG, Lowery DE. FMRFamide-like peptides encoded on the flp-18 precursor gene activate two isoforms of the orphan Caenorhabditis elegans G-protein-coupled receptor Y58G8A. 4 heterologously expressed in mammalian cells. Pept Sci. Wiley Online Library; **2008**; 90(3):339–348.
- 19. Clare JJ. Targeting ion channels for drug discovery. Discov Med. 2010; 9(46):253–260.
- 20. Wolstenholme AJ. Ion channels and receptor as targets for the control of parasitic nematodes. Int J Parasitol Drugs Drug Resist. Elsevier; **2011**; 1(1):2–13.
- 21. Geary TG. Are new anthelmintics needed to eliminate human helminthiases? Curr Opin Infect Dis. **2012**; 25(6):709–717.
- 22. Geary TG, Sakanari JA, Caffrey CR. Anthelmintic drug discovery: into the future. J Parasitol. **2015**; 101(2):125–133.
- 23. Hauser AS, Attwood MM, Rask-Andersen M, Schiöth HB, Gloriam DE. Trends in GPCR drug discovery: new agents, targets and indications. Nat Rev Drug Discov. **2017**; 16(12):829–842.
- 24. Mani T, Bourguinat C, Prichard RK. G-protein-coupled receptor genes of Dirofilaria immitis. Mol Biochem Parasitol. **2018**; 222:6–13.
- 25. Kimber MJ, Sayegh L, El-Shehabi F, et al. Identification of an Ascaris G protein-coupled acetylcholine receptor with atypical muscarinic pharmacology. Int J Parasitol. **2009**; 39(11):1215–1222.
- 26. Greenwood K, Williams T, Geary T. Nematode neuropeptide receptors and their development as anthelmintic screens. Parasitology. **2005**; 131 Suppl:S169–77.
- 27. Atkinson LE, McCoy CJ, Crooks BA, et al. Phylum-Spanning Neuropeptide GPCR Identification and Prioritization: Shaping Drug Target Discovery Pipelines for Nematode Parasite Control. Front Endocrinol . **2021**; 12:718363.
- 28. Campos TDL, Young ND, Korhonen PK, et al. Identification of G protein-coupled receptors in Schistosoma haematobium and S. mansoni by comparative genomics. Parasit Vectors. **2014**; 7:242.
- 29. Hamdan FF, Abramovitz M, Mousa A, Xie J, Durocher Y, Ribeiro P. A novel Schistosoma mansoni G protein-coupled receptor is responsive to histamine. Mol Biochem Parasitol. **2002**; 119(1):75–86.
- 30. Komuniecki RW, Hobson RJ, Rex EB, Hapiak VM, Komuniecki PR. Biogenic amine receptors in parasitic nematodes: what can be learned from Caenorhabditis elegans? Mol Biochem Parasitol. **2004**; 137(1):1–11.

- 31. Hobson RJ, Hapiak VM, Xiao H, Buehrer KL, Komuniecki PR, Komuniecki RW. SER-7, a Caenorhabditis elegans 5-HT7-like receptor, is essential for the 5-HT stimulation of pharyngeal pumping and egg laying. Genetics. **2006**; 172(1):159–169.
- 32. Keating CD, Kriek N, Daniels M, et al. Whole-genome analysis of 60 G protein-coupled receptors in Caenorhabditis elegans by gene knockout with RNAi. Curr Biol. **2003**; 13(19):1715–1720.
- 33. Geary TG, Kubiak TM. Neuropeptide G-protein-coupled receptors, their cognate ligands and behavior in Caenorhabditis elegans. Trends Pharmacol Sci. **2005**; 26(2):56–58.
- 34. Bargmann Cl. Chemosensation in C. elegans. WormBook. 2006; :1-29.
- 35. Law W, Wuescher LM, Ortega A, Hapiak VM, Komuniecki PR, Komuniecki R. Heterologous Expression in Remodeled C. elegans: A Platform for Monoaminergic Agonist Identification and Anthelmintic Screening. PLoS Pathog. **2015**; 11(4):e1004794.
- 36. Frooninckx L, Van Rompay L, Temmerman L, et al. Neuropeptide GPCRs in C. elegans. Front Endocrinol . **2012**; 3:167.
- 37. Brownlee DJ, Holden-Dye L, Fairweather I, Walker RJ. The action of serotonin and the nematode neuropeptide KSAYMRFamide on the pharyngeal muscle of the parasitic nematode, Ascaris suum. Parasitology. **1995**; 111 (Pt 3):379–384.
- 38. Maule AG, Geary TG, Bowman JW, et al. Inhibitory effects of nematode FMRFamide-related peptides (FaRPs) on muscle strips fromAscaris suum. Invert Neurosci. **1995**; 1(3):255–265.
- 39. Geary TG, Klein RD, Vanover L, Bowman JW, Thompson DP. The nervous systems of helminths as targets for drugs. J Parasitol. **1992**; 78(2):215–230.
- 40. McCusker EC, Bane SE, O'Malley MA, Robinson AS. Heterologous GPCR expression: a bottleneck to obtaining crystal structures. Biotechnol Prog. **2007**; 23(3):540–547.
- 41. Tate CG, Grisshammer R. Heterologous expression of G-protein-coupled receptors. Trends Biotechnol. **1996**; 14(11):426–430.
- 42. Rand JB. Acetylcholine. WormBook; 2007.
- 43. Treinin M, Jin Y. Cholinergic transmission in C. elegans: Functions, diversity, and maturation of ACh-activated ion channels. J Neurochem. **2021**; 158(6):1274–1291.
- 44. Evans AM, Martin RJ. Activation and cooperative multi-ion block of single nicotinic-acetylcholine channel currents of Ascaris muscle by the tetrahydropyrimidine anthelmintic, morantel. Br J Pharmacol. **1996**; 118(5):1127–1140.
- 45. Robertson SJ, Martin RJ. Levamisole-activated single-channel currents from muscle of the nematode parasite Ascaris suum. Br J Pharmacol. **1993**; 108(1):170–178.
- 46. Aceves J, Erlij D, Martínez-Marañón R. The mechanism of the paralysing action of tetramisole on Ascaris somatic muscle. Br J Pharmacol. **1970**; 38(3):602–607.
- 47. Aubry ML, Cowell P, Davey MJ, Shevde S. Aspects of the pharmacology of a new

- anthelmintic: pyrantel. Br J Pharmacol. 1970; 38(2):332–344.
- 48. Kaminsky R, Ducray P, Jung M, et al. A new class of anthelmintics effective against drug-resistant nematodes. Nature. **2008**; 452(7184):176–180.
- 49. Hu Y, Xiao S-H, Aroian RV. The new anthelmintic tribendimidine is an L-type (levamisole and pyrantel) nicotinic acetylcholine receptor agonist. PLoS Negl Trop Dis. **2009**; 3(8):e499.
- 50. Martin RJ. Neuromuscular transmission in nematode parasites and antinematodal drug action. Pharmacol Ther. **1993**; 58(1):13–50.
- 51. Hwang JM, Chang DJ, Kim US, et al. Cloning and functional characterization of a Caenorhabditis elegans muscarinic acetylcholine receptor. Receptors Channels. **1999**; 6(6):415–424.
- 52. Park YS, Lee YS, Cho NJ, Kaang BK. Alternative splicing of gar-1, a Caenorhabditis elegans G-protein-linked acetylcholine receptor gene. Biochem Biophys Res Commun. **2000**; 268(2):354–358.
- 53. Lee YS, Park YS, Nam S, et al. Characterization of GAR-2, a novel G protein-linked acetylcholine receptor from Caenorhabditis elegans. J Neurochem. **2000**; 75(5):1800–1809.
- 54. Park Y-S, Kim S, Shin Y, Choi B, Cho NJ. Alternative splicing of the muscarinic acetylcholine receptor GAR-3 in Caenorhabditis elegans. Biochem Biophys Res Commun. **2003**; 308(4):961–965.
- 55. Yemini E, Lin A, Nejatbakhsh A, et al. NeuroPAL: A Multicolor Atlas for Whole-Brain Neuronal Identification in C. elegans. Cell. **2021**; 184(1):272–288.e11.
- 56. Kozlova AA, Lotfi M, Okkema PG. Crosstalk with the GAR-3 Receptor Contributes to Feeding Defects in Caenorhabditis eleganseat-2 Mutants. Genetics [Internet]. **2019**; . Available from: http://dx.doi.org/10.1534/genetics.119.302053
- 57. Avery L, You Y-J. C. elegans feeding. WormBook. 2012; :1-23.
- 58. Acetylcholine [Internet]. [cited 2020 Oct 14]. Available from: http://www.wormbook.org/chapters/www_acetylcholine/acetylcholine.html
- 59. Colquhoun L, Holden-Dye L, Walker RJ. The pharmacology of cholinoceptors on the somatic muscle cells of the parasitic nematode Ascaris suum. J Exp Biol. **1991**; 158:509–530.
- 60. Hillman GR, Ewert A, Westerfield L, Grim SO. Effects of selected cholinergic and anticholinergic drugs on Brugia malayi (Nematoda). Comp Biochem Physiol C. **1983**; 74(2):299–301.
- 61. Kwa MS, Veenstra JG, Van Dijk M, Roos MH. Beta-tubulin genes from the parasitic nematode Haemonchus contortus modulate drug resistance in Caenorhabditis elegans. J Mol Biol. **1995**; 246(4):500–510.
- 62. Cook A, Aptel N, Portillo V, et al. Caenorhabditis elegans ivermectin receptors regulate locomotor behaviour and are functional orthologues of Haemonchus contortus receptors. Mol Biochem Parasitol. **2006**; 147(1):118–125.

- 63. Glendinning SK, Buckingham SD, Sattelle DB, Wonnacott S, Wolstenholme AJ. Glutamate-gated chloride channels of Haemonchus contortus restore drug sensitivity to ivermectin resistant Caenorhabditis elegans. PLoS One. **2011**; 6(7):e22390.
- 64. Wheeler NJ, Heimark ZW, Airs PM, Mann A, Bartholomay LC, Zamanian M. Genetic and functional diversification of chemosensory pathway receptors in mosquito-borne filarial nematodes. PLoS Biol. Public Library of Science; **2020**; 18(6):e3000723.
- 65. Suh SJ, Park YS, Lee YS, Cho TJ, Kaang BK, Cho NJ. Three functional isoforms of GAR-2, a Caenorhabditis elegans G-protein-linked acetylcholine receptor, are produced by alternative splicing. Biochem Biophys Res Commun. **2001**; 288(5):1238–1243.
- 66. Lee YS, Park YS, Chang DJ, et al. Cloning and expression of a G protein-linked acetylcholine receptor from Caenorhabditis elegans. J Neurochem. **1999**; 72(1):58–65.
- 67. Wheeler NJ, Ryan KT, Gallo KJ, et al. Multivariate chemogenomic screening prioritizes new macrofilaricidal leads [Internet]. bioRxiv. 2022 [cited 2022 Jul 27]. p. 2022.07.25.501423. Available from: https://www.biorxiv.org/content/10.1101/2022.07.25.501423v1
- 68. Wheeler NJ, Garncarz EJ, Gallo KJ, Chan JD, Zamanian M. wrmXpress: A modular package for high-throughput image analysis of parasitic and free-living worms [Internet]. bioRxiv. 2022 [cited 2022 May 20]. p. 2022.05.18.492482. Available from: https://www.biorxiv.org/content/10.1101/2022.05.18.492482v1
- 69. Christ D, Goebel M, Saz HJ. Actions of acetylcholine and GABA on spontaneous contractions of the filariid, Dipetalonema viteae. Br J Pharmacol. **1990**; 101(4):971–977.
- 70. Kashyap SS, Verma S, McHugh M, et al. Anthelmintic resistance and homeostatic plasticity (Brugia malayi). Sci Rep. **2021**; 11(1):14499.
- 71. Kim J, Poole DS, Waggoner LE, et al. Genes affecting the activity of nicotinic receptors involved in Caenorhabditis elegans egg-laying behavior. Genetics. **2001**; 157(4):1599–1610.
- 72. Spensley M, Del Borrello S, Pajkic D, Fraser AG. Acute Effects of Drugs on Caenorhabditis elegans Movement Reveal Complex Responses and Plasticity. G3 . **2018**; 8(9):2941–2952.
- 73. Tissenbaum HA, Hawdon J, Perregaux M, Hotez P, Guarente L, Ruvkun G. A common muscarinic pathway for diapause recovery in the distantly related nematode species Caenorhabditis elegans and Ancylostoma caninum. Proc Natl Acad Sci U S A. **2000**; 97(1):460–465.
- 74. Airs PM, Vaccaro K, Gallo KJ, et al. Spatial transcriptomics reveals antiparasitic targets associated with essential behaviors in the human parasite Brugia malayi [Internet]. bioRxiv. 2021 [cited 2021 Aug 27]. p. 2021.08.24.456436. Available from: https://www.biorxiv.org/content/10.1101/2021.08.24.456436v1
- 75. Steger KA, Avery L. The GAR-3 muscarinic receptor cooperates with calcium signals to regulate muscle contraction in the Caenorhabditis elegans pharynx. Genetics. **2004**; 167(2):633–643.
- 76. Liu Y, LeBoeuf B, Garcia LR. G alpha(q)-coupled muscarinic acetylcholine receptors

- enhance nicotinic acetylcholine receptor signaling in Caenorhabditis elegans mating behavior. J Neurosci. **2007**; 27(6):1411–1421.
- 77. Chan JP, Staab TA, Wang H, Mazzasette C, Butte Z, Sieburth D. Extrasynaptic muscarinic acetylcholine receptors on neuronal cell bodies regulate presynaptic function in Caenorhabditis elegans. J Neurosci. **2013**; 33(35):14146–14159.
- 78. Hendricks M, Ha H, Maffey N, Zhang Y. Compartmentalized calcium dynamics in a C. elegans interneuron encode head movement. Nature. **2012**; 487(7405):99–103.
- 79. Teng MS, Shadbolt P, Fraser AG, Jansen G, McCafferty J. Control of feeding behavior in *C. elegans* by human G protein-coupled receptors permits screening for agonist-expressing bacteria. Proc Natl Acad Sci U S A. **2008**; 105(39):14826–14831.
- 80. Teng MS, Dekkers MPJ, Ng BL, et al. Expression of mammalian GPCRs in C. elegans generates novel behavioural responses to human ligands. BMC Biol. **2006**; 4:22.
- 81. Ward S. Chemotaxis by the nematode Caenorhabditis elegans: identification of attractants and analysis of the response by use of mutants. Proc Natl Acad Sci U S A. **1973**; 70(3):817–821.
- 82. Calahorro F, Alejandre E, Ruiz-Rubio M. Osmotic avoidance in Caenorhabditis elegans: synaptic function of two genes, orthologues of human NRXN1 and NLGN1, as candidates for autism. J Vis Exp [Internet]. **2009**; (34). Available from: http://dx.doi.org/10.3791/1616
- 83. Oh KH, Kim H. Aldicarb-induced Paralysis Assay to Determine Defects in Synaptic Transmission in Caenorhabditis elegans. Bio Protoc [Internet]. **2017**; 7(14). Available from: http://dx.doi.org/10.21769/BioProtoc.2400
- 84. Rodríguez-Palero MJ, López-Díaz A, Marsac R, Gomes J-E, Olmedo M, Artal-Sanz M. An automated method for the analysis of food intake behaviour in Caenorhabditis elegans. Sci Rep. **2018**; 8(1):3633.
- 85. Weeks JC, Robinson KJ, Lockery SR, Roberts WM. Anthelmintic drug actions in resistant and susceptible C. elegans revealed by electrophysiological recordings in a multichannel microfluidic device. Int J Parasitol Drugs Drug Resist. **2018**; 8(3):607–628.
- 86. Calahorro F, Keefe F, Dillon J, Holden-Dye L, O'Connor V. Neuroligin tuning of pharyngeal pumping reveals extrapharyngeal modulation of feeding in Caenorhabditis elegans. J Exp Biol [Internet]. **2019**; 222(Pt 3). Available from: http://dx.doi.org/10.1242/jeb.189423
- 87. Avery L. The genetics of feeding in Caenorhabditis elegans. Genetics. **1993**; 133(4):897–917.
- 88. Raizen DM, Lee RY, Avery L. Interacting genes required for pharyngeal excitation by motor neuron MC in Caenorhabditis elegans. Genetics. **1995**; 141(4):1365–1382.
- 89. Song B-M, Avery L. Serotonin activates overall feeding by activating two separate neural pathways in Caenorhabditis elegans. J Neurosci. **2012**; 32(6):1920–1931.
- 90. Raizen DM, Avery L. Electrical activity and behavior in the pharynx of Caenorhabditis elegans. Neuron. **1994**; 12(3):483–495.

- 91. Avery L, Horvitz HR. Effects of starvation and neuroactive drugs on feeding in Caenorhabditis elegans. J Exp Zool. **1990**; 253(3):263–270.
- 92. Horvitz HR, Brenner S, Hodgkin J, Herman RK. A uniform genetic nomenclature for the nematode Caenorhabditis elegans. Mol Gen Genet. **1979**; 175(2):129–133.
- 93. Croll NA, Smith JM. Integrated behaviour in the feeding phase of Caenorhabditis elegans (Nematoda). J Zool . Wiley; **1978**; 184(4):507–517.
- 94. Takahashi M, Takagi S. Optical silencing of body wall muscles induces pumping inhibition in Caenorhabditis elegans. PLoS Genet. **2017**; 13(12):e1007134.
- 95. G. Izquierdo P, Calahorro F, Thisainathan T, et al. Cholinergic signalling at the body wall neuromuscular junction distally inhibits feeding behaviour in C. elegans. J Biol Chem. **2021**; :101466.
- 96. Kiyama Y, Miyahara K, Ohshima Y. Active uptake of artificial particles in the nematode Caenorhabditis elegans. J Exp Biol. **2012**; 215(Pt 7):1178–1183.
- 97. Ding SS, Romenskyy M, Sarkisyan KS, Brown AEX. Measuring Caenorhabditis elegans Spatial Foraging and Food Intake Using Bioluminescent Bacteria. Genetics. **2020**; 214(3):577–587.
- 98. Raizen D, Song B-M, Trojanowski N, You Y-J. Methods for measuring pharyngeal behaviors. WormBook. **2012**; :1–13.
- 99. You Y-J, Kim J, Raizen DM, Avery L. Insulin, cGMP, and TGF-beta signals regulate food intake and quiescence in C. elegans: a model for satiety. Cell Metab. **2008**; 7(3):249–257.
- 100. Nika L, Gibson T, Konkus R, Karp X. Fluorescent Beads Are a Versatile Tool for Staging Caenorhabditis elegans in Different Life Histories. G3 . **2016**; 6(7):1923–1933.
- 101. Boyd WA, McBride SJ, Freedman JH. Effects of genetic mutations and chemical exposures on Caenorhabditis elegans feeding: evaluation of a novel, high-throughput screening assay. PLoS One. **2007**; 2(12):e1259.
- 102. Andersen EC, Shimko TC, Crissman JR, et al. A Powerful New Quantitative Genetics Platform, Combining Caenorhabditis elegans High-Throughput Fitness Assays with a Large Collection of Recombinant Strains. G3 . **2015**; 5(5):911–920.
- 103. Zamanian M, Cook DE, Zdraljevic S, et al. Discovery of genomic intervals that underlie nematode responses to benzimidazoles. PLoS Negl Trop Dis. **2018**; 12(3):e0006368.
- 104. Ribeiro P, Gupta V, El-Sakkary N. Biogenic amines and the control of neuromuscular signaling in schistosomes. Invert Neurosci. **2012**; 12(1):13–28.
- 105. Michalski ML, Griffiths KG, Williams SA, Kaplan RM, Moorhead AR. The NIH-NIAID Filariasis Research Reagent Resource Center. PLoS Negl Trop Dis. **2011**; 5(11):e1261.
- 106. Altschul SF, Gish W, Miller W, Myers EW, Lipman DJ. Basic local alignment search tool. J Mol Biol. **1990**; 215(3):403–410.
- 107. C. elegans Sequencing Consortium. Genome sequence of the nematode C. elegans: a

- platform for investigating biology. Science. 1998; 282(5396):2012–2018.
- 108. Ghedin E, Wang S, Spiro D, et al. Draft genome of the filarial nematode parasite Brugia malayi. Science. science.sciencemag.org; **2007**; 317(5845):1756–1760.
- 109. Abubucker S, Martin J, Yin Y, et al. The canine hookworm genome: analysis and classification of Ancylostoma caninum survey sequences. Mol Biochem Parasitol. **2008**; 157(2):187–192.
- 110. Jex AR, Liu S, Li B, et al. Ascaris suum draft genome. Nature. **2011**; 479(7374):529–533.
- 111. Laing R, Kikuchi T, Martinelli A, et al. The genome and transcriptome of Haemonchus contortus, a key model parasite for drug and vaccine discovery. Genome Biol. **2013**; 14(8):R88.
- 112. Hunt VL, Tsai IJ, Coghlan A, et al. The genomic basis of parasitism in the Strongyloides clade of nematodes. Nat Genet. **2016**; 48(3):299–307.
- 113. Foth BJ, Tsai IJ, Reid AJ, et al. Whipworm genome and dual-species transcriptome analyses provide molecular insights into an intimate host-parasite interaction. Nat Genet. **2014**; 46(7):693–700.
- 114. Howe KL, Bolt BJ, Shafie M, Kersey P, Berriman M. WormBase ParaSite a comprehensive resource for helminth genomics. Mol Biochem Parasitol. **2017**; 215:2–10.
- 115. Katoh K, Standley DM. MAFFT multiple sequence alignment software version 7: improvements in performance and usability. Mol Biol Evol. **2013**; 30(4):772–780.
- Capella-Gutiérrez S, Silla-Martínez JM, Gabaldón T. trimAl: a tool for automated alignment trimming in large-scale phylogenetic analyses. Bioinformatics. 2009; 25(15):1972–1973.
- 117. Minh BQ, Schmidt HA, Chernomor O, et al. IQ-TREE 2: New Models and Efficient Methods for Phylogenetic Inference in the Genomic Era. Mol Biol Evol. 2020; 37(5):1530–1534.
- 118. Yu G, Smith DK, Zhu H, Guan Y, Lam TT-Y. ggtree: an r package for visualization and annotation of phylogenetic trees with their covariates and other associated data. McInerny G, editor. Methods Ecol Evol. Wiley Online Library; **2017**; 8(1):28–36.
- 119. Wheeler NJ, Zamanian M, Ryan KT, Gallo KJ. Multivariate screening of Brugia spp. adults. **2022** [cited 2022 Aug 29]; . Available from: https://protocolexchange.researchsquare.com/article/pex-1918/v1
- 120. Wheeler NJ, Zamanian M, Ryan KT, Gallo KJ. Bivariate, high-content screening of Brugia malayi microfilariae. 2022 [cited 2022 Aug 29]; . Available from: https://protocolexchange.researchsquare.com/article/pex-1916/v1
- 121. Untergasser A, Cutcutache I, Koressaar T, et al. Primer3--new capabilities and interfaces. Nucleic Acids Res. **2012**; 40(15):e115.
- 122. Ballesteros C, Tritten L, O'Neill M, et al. The Effect of In Vitro Cultivation on the

- Transcriptome of Adult Brugia malayi. PLoS Negl Trop Dis. 2016; 10(1):e0004311.
- 123. Schindelin J, Arganda-Carreras I, Frise E, et al. Fiji: an open-source platform for biological-image analysis. Nat Methods. **2012**; 9(7):676–682.
- 124. Cardona A, Saalfeld S, Schindelin J, et al. TrakEM2 software for neural circuit reconstruction. PLoS One. **2012**; 7(6):e38011.
- 125. Wheeler NJ, Airs PM, Zamanian M. Long-read RNA sequencing of human and animal filarial parasites improves gene models and discovers operons. PLoS Negl Trop Dis. **2020**; 14(11):e0008869.
- 126. Lindsay TH, Thiele TR, Lockery SR. Optogenetic analysis of synaptic transmission in the central nervous system of the nematode Caenorhabditis elegans. Nat Commun. **2011**; 2:306.
- 127. Mello C, Fire A. DNA transformation. Methods Cell Biol. 1995; 48:451–482.
- 128. The C. elegans Deletion Mutant Consortium. Large-Scale Screening for Targeted Knockouts in the Caenorhabditis elegans Genome. G3 Genes|Genomes|Genetics. Oxford Academic; **2012**; 2(11):1415–1425.
- 129. Gallo K, Zamanian M. High-throughput image-based drug screening of Caenorhabditis elegans movement, development, and viability. **2022** [cited 2022 Nov 15]; . Available from: https://protocolexchange.researchsguare.com/article/pex-2018/v1
- 130. Wählby C, Kamentsky L, Liu ZH, et al. An image analysis toolbox for high-throughput C. elegans assays. Nat Methods. **2012**; 9(7):714–716.
- 131. McQuin C, Goodman A, Chernyshev V, et al. CellProfiler 3.0: Next-generation image processing for biology. PLoS Biol. **2018**; 16(7):e2005970.

Figures

Figure 1. B. malayi expresses two GARs and muscarinic compounds elicit neuromuscular effects in microfilariae and adult stage parasites. A) Phylogeny based on protein sequence alignment of characterized and putative nematode and human GARs. B. malayi expresses two GARs (Bma-GAR-2 and Bma-GAR-3), but lacks a GAR-1 homolog. Nodal values represent bootstrap support of 1,000 replicates. B) Gene expression of Bma-gar-2 and Bma-gar-3 across intra-mammalian life stages of B. malayi as assayed by quantitative reverse transcription PCR (qPCR) (control = B. malayi GAPDH). Bma-gar-3 is abundantly and constitutively expressed throughout the life cycle. C) Effects of cholinergic compounds on adult B. pahangi movement over 48 hours as measured by optical flow. Log₂ normalized movement compared to untreated controls using a t-tests (*p \leq 0.05; **p \leq 0.01, ***p \leq 0.001) (brown: 10 μM, cyan: 100 μM). **D)** Effects of cholinergic compounds on adult female *B. pahangi* fecundity as measured by microfilariae output. Percent change mf output from untreated controls by time point, t-tests (*p \leq 0.05; **p \leq 0.01, ***p \leq 0.001) (brown: 10 μ M, cyan: 100 μ M). **E)** Dose-response of cholinergic compounds on microfilariae motility over 48 hours. Images from mf motility plates taken at 48 hours showing diverse morphologies from cholinergic treatment at 10 mM. Log2 normalized movement compared to untreated controls using t-tests (*p ≤ 0.05; **p ≤ 0.01, ***p ≤ 0.001). **F)** Effects of cholinergic compounds on microfilariae cell health over 48 hours as measured by cell toxicity stain (CellTox fluorescence). Percent change in fluorescence from untreated controls, t-tests (*p \leq 0.05; **p \leq 0.01, ***p \leq 0.001).

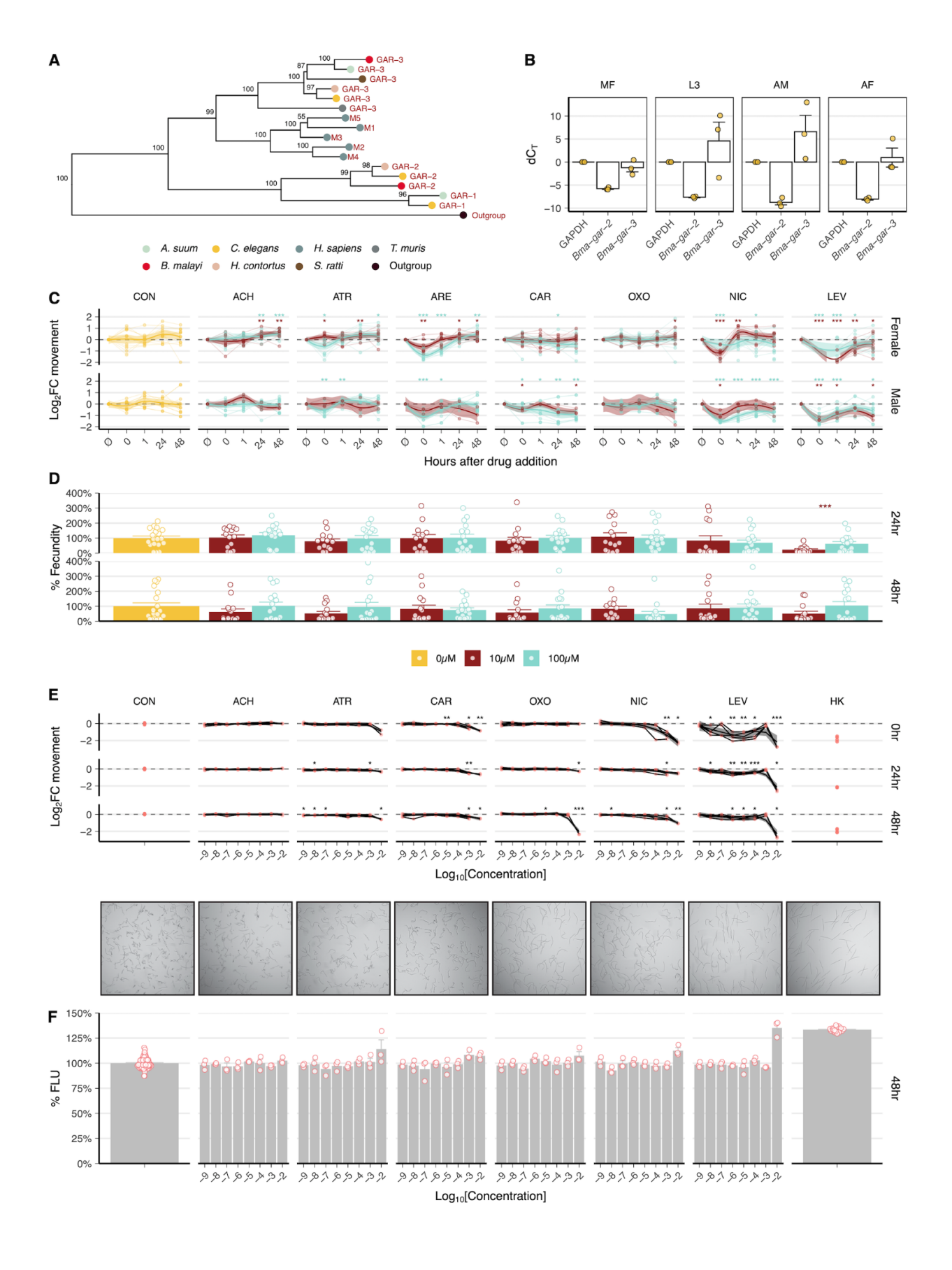


Figure 2. RNAscope spatial localization of *Bma-gar-3* in the *B. malayi* adult female head. **A)** Illustration of tissue distribution along the anterior-posterior axis and transverse illustrations at approximately (a') 400 μm, (b') 715 μm, (c') 1024 μm, and (d') 1400 μm, with a key of representative section locations shown in part C. **B)** RNAscope *Bma-gar-3* punctae counts per tissue per 8 μm section. **C)** Representative section images with key in part A, showing 3x zoom insets of punctate staining in the pharynx (iii), vulva (iv), uterus (v), esophageal-intestinal junction (vi), body wall muscle (vii), intestine (viii), and lateral cords (ix). Scale bar = 50 μm. Positive (*Bma-cdc-42* and *Bm4733*) and negative (bacterial *DapB*) controls for RNAscope validate RNA integrity, show that punctate staining is probe specific, and that nonspecific background staining is minimal. **D)** Proportion of sections containing *Bma-gar-3* punctae where tissue is present and defined. Colors in C and D represent counts performed by two independent researchers.

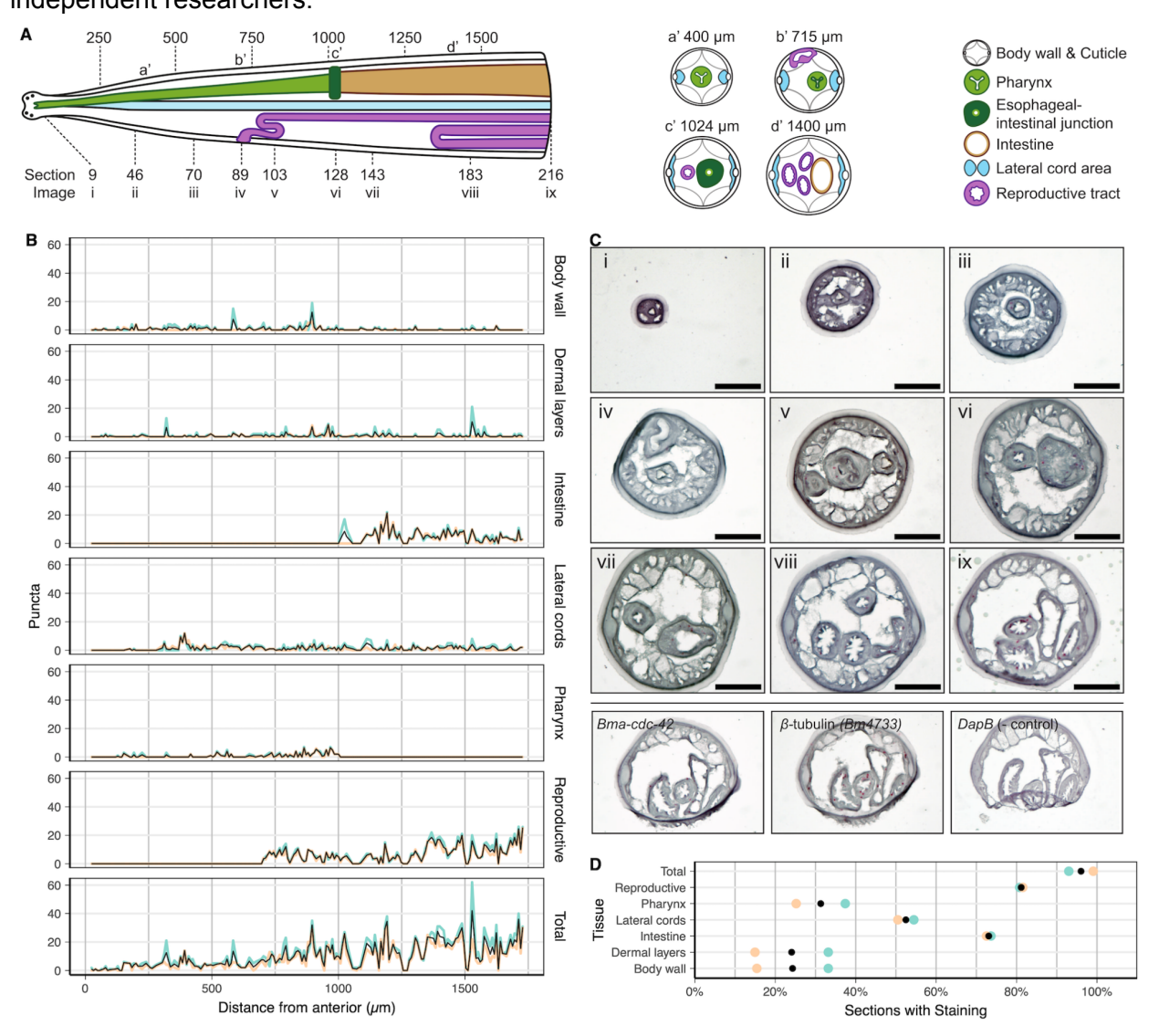


Figure 3. *Bma*-GAR-3 is activated by the selective muscarinic agonist oxotremorine-M and confers hypersensitivity to aldicarb induced paralysis

A) Schematic of plate-based aversion assay. Bleach-synchronized adult worms are monitored to capture reversal frequency in response to a test compound ring, in the presence of a known attractant (diacetyl). **B)** Acetylcholine and oxotremorine-M activate the ASH neuron of parasitized *C. elegans* expressing *Bma*-GAR-3 and elicits reversal behaviors. t-tests (*p \leq 0.05; **p \leq 0.01, ***p \leq 0.001) were used to identify differences in comparison to *gar-3(gk305)* (gray) and N2 (black). **C)** Schematic of aldicarb paralysis assay. Paralysis of young adult worms is monitored on agar plates containing test drug over a two hour period. **D)** Kaplan-Meier survival plot showing paralysis measured every 10 minutes. Knock-out of *Cel*-GAR-3 leads to resistance to aldicarb induced paralysis. *myo-3p::Bma-gar-3* worms paralyze more rapidly than wild-type N2 and *gar-3(gk305)* worms. Pairwise survival t-tests (*p \leq 0.05; **p \leq 0.01, ***p \leq 0.001).

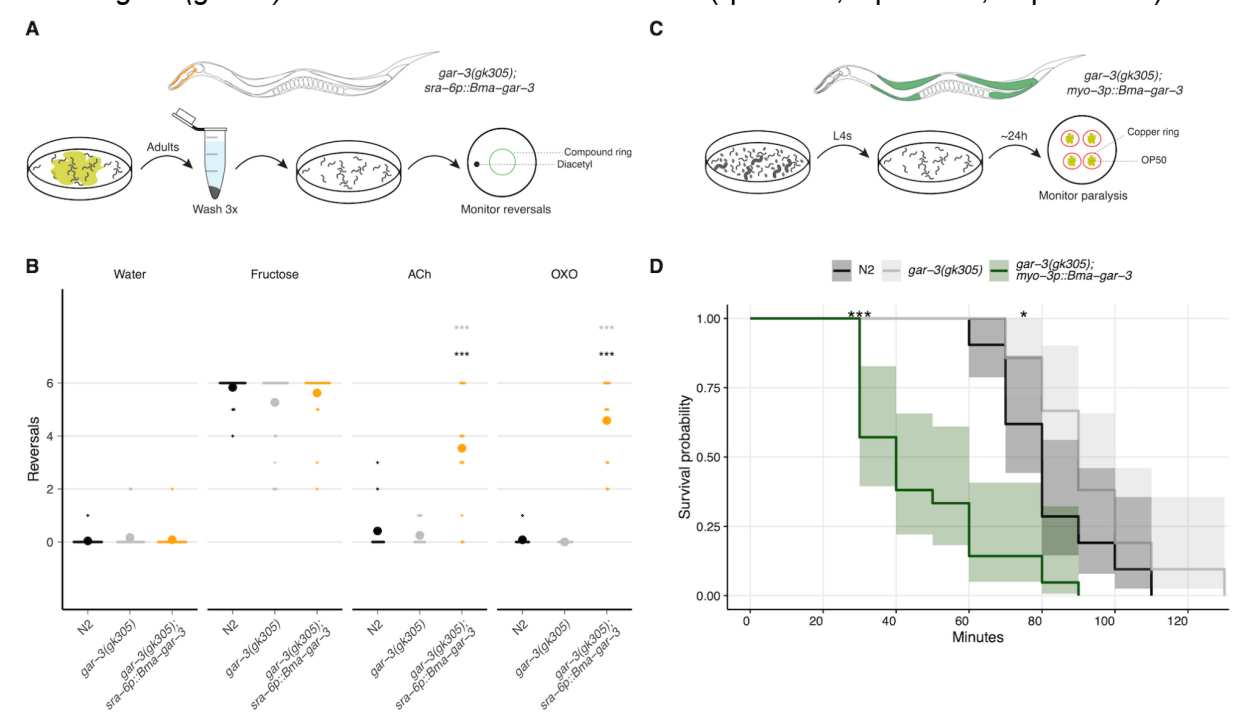


Figure 4. *Bma*-GAR-3 modulates pharyngeal pumping via expression in the *C. elegans* body wall and pharynx. A) Iteration across chemical (5HT) and food (OP50) pumping stimuli for optimization of visual pumping assay in L1 and adult stage *C. elegans*. (brown: comparisons to 5HT, black: comparisons to untreated). B) Schematic of the optimized visual pharyngeal pumping assay. Bleach synchronized worms are treated with drug for 20 minutes and pumps are counted on seeded (L1s) or unseeded (adults) 6 cm agar plates. Drug treatments are tested in combination with 5HT in the adult stage. C-D) Modulation of pharyngeal pumping by OXO in L1 and adult parasitized strains. L1 data are normalized to untreated controls while adult data are normalized to 5HT-stimulated controls. E-F) Effects of cholinergic compounds on stage specific pharyngeal pump frequency compared to untreated (L1) or 5HT-stimulated (adult) pump frequency. All statistics were calculated using t-tests (*p \leq 0.05; **p \leq 0.01, ***p \leq 0.001).

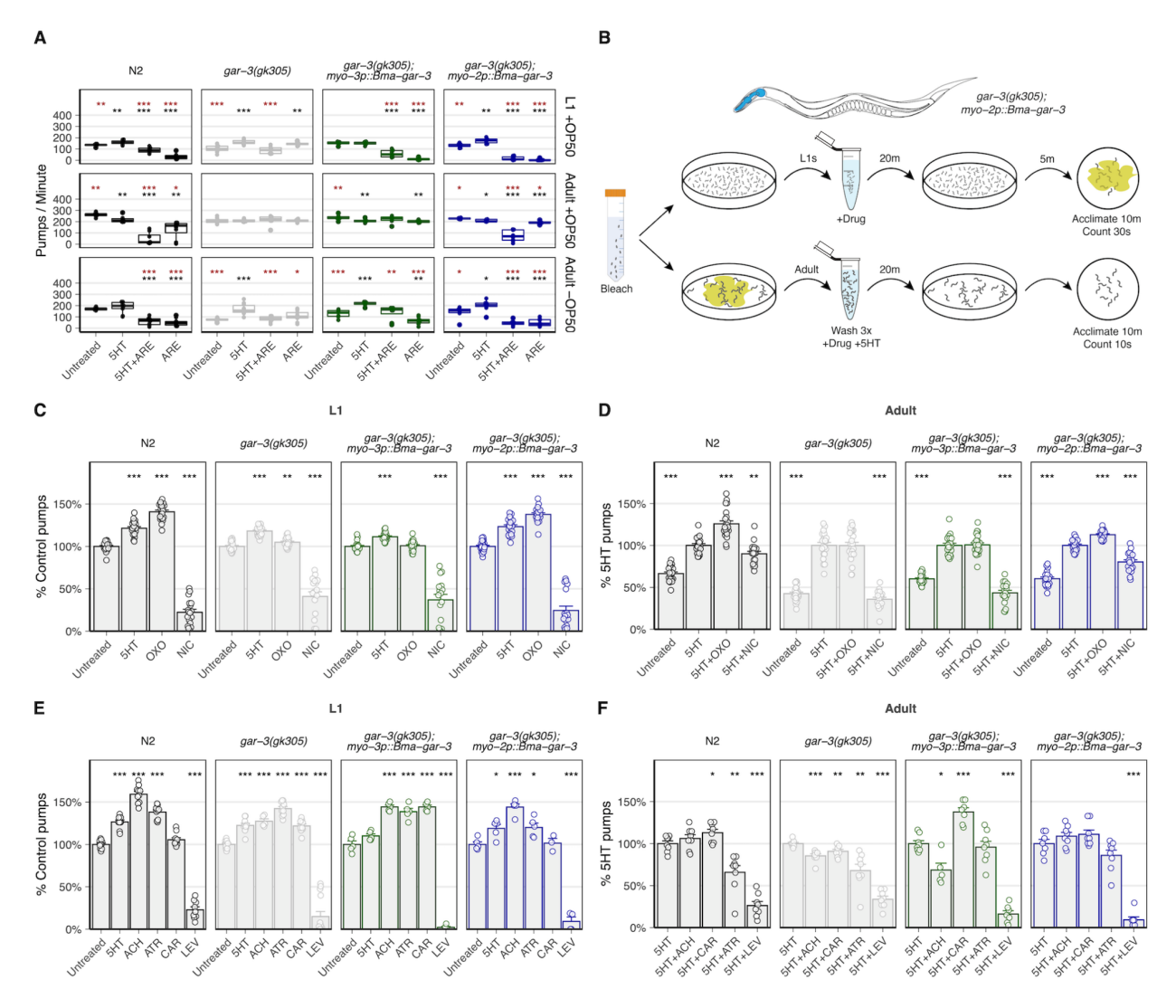


Figure 5. EPG recordings in parasitized strains provide alternative reporters of parasite receptor activity. A) Schematic of electropharyngeogram (EPG) assay. Adult worms are bleach synchronized, washed three times, treated with drugs for 20 minutes, and positioned into the microfluidics chip. Worms are recorded for two minutes. B) EPG recordings used to measure pharyngeal pump frequency show that 5HT in combination with drugs allows for the capture of inhibitory effects of ARE. (brown: comparisons to 5HT, black: comparisons to untreated). C) Cholinergic effects on pharyngeal pump frequency as measured by EPG do not align with visual pumping assay. D) Heatmap depicting scale-normalized electrophysiological features across all strain conditions. Clustering of these features identifies subsets that provide similar information. E) Bma-GAR-3 expressed in the pharynx increases the peak amplitude of OXO treated worms compared to gar-3(gk305) knockout, revealing receptor-specific modulation of this electrophysiological feature. All statistics were calculated using t-tests (*p \leq 0.05; **p \leq 0.01, ***p \leq 0.001).

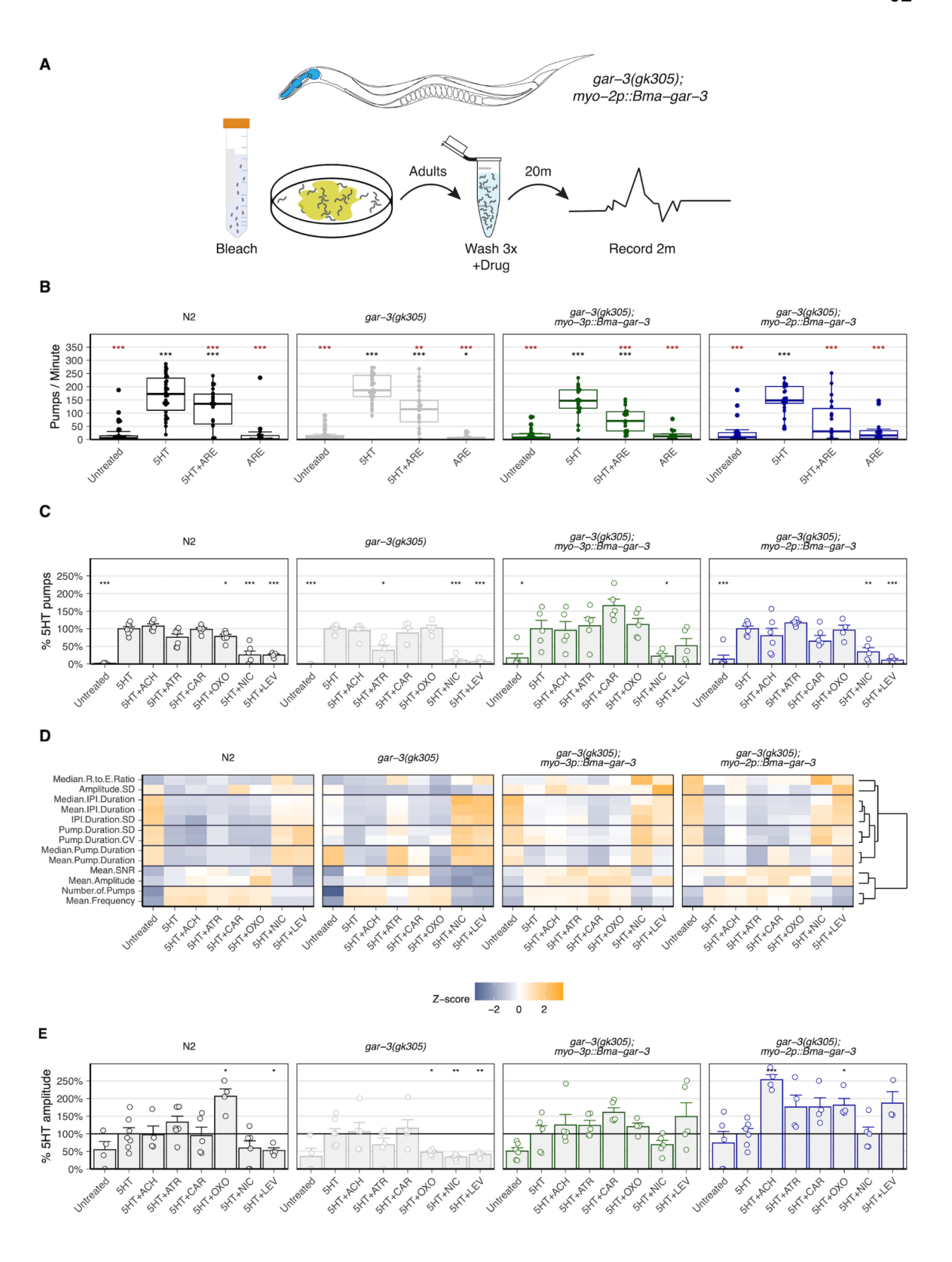
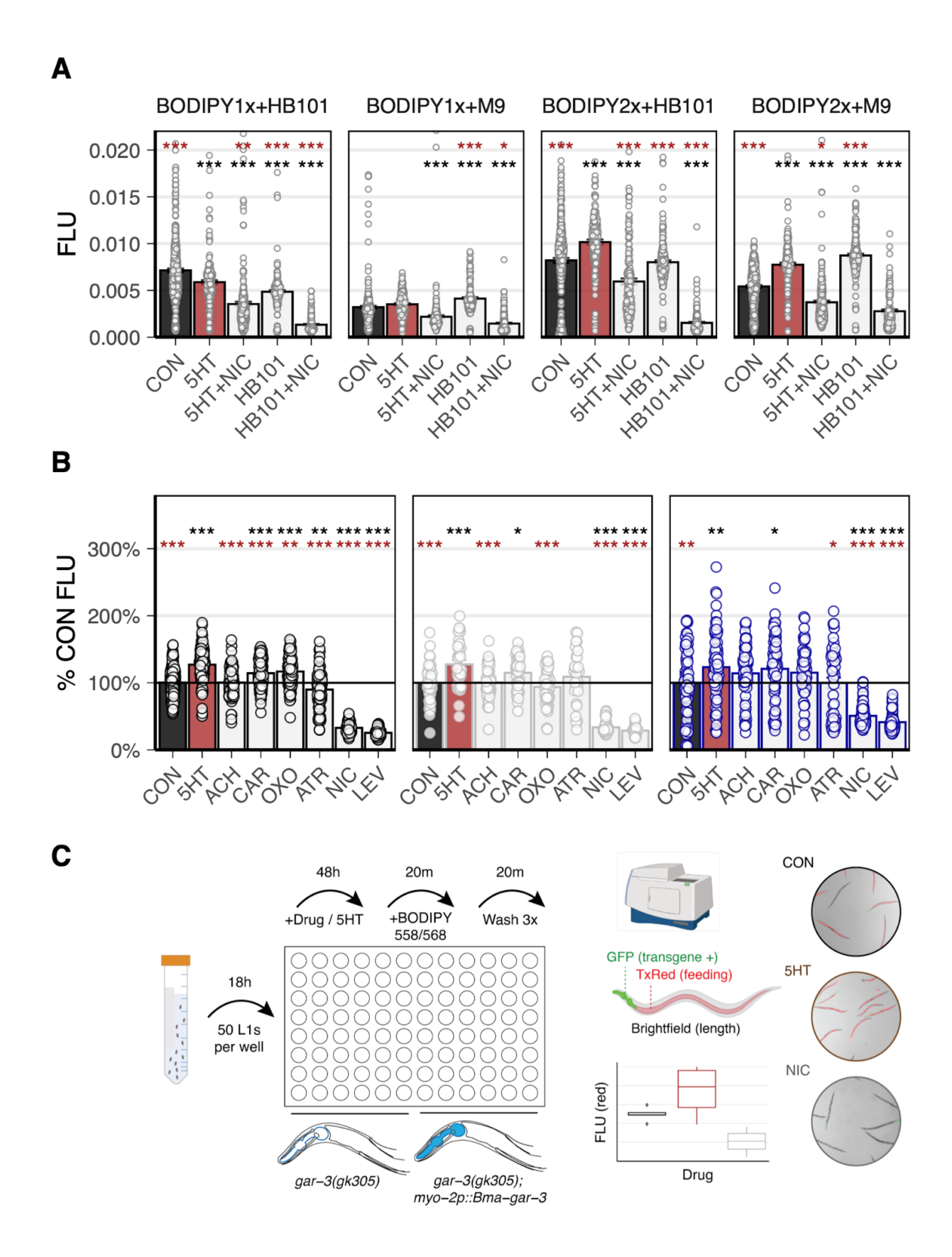


Figure 6. Development of an image-based feeding assay to enable high-throughput screening of parasitized strains.

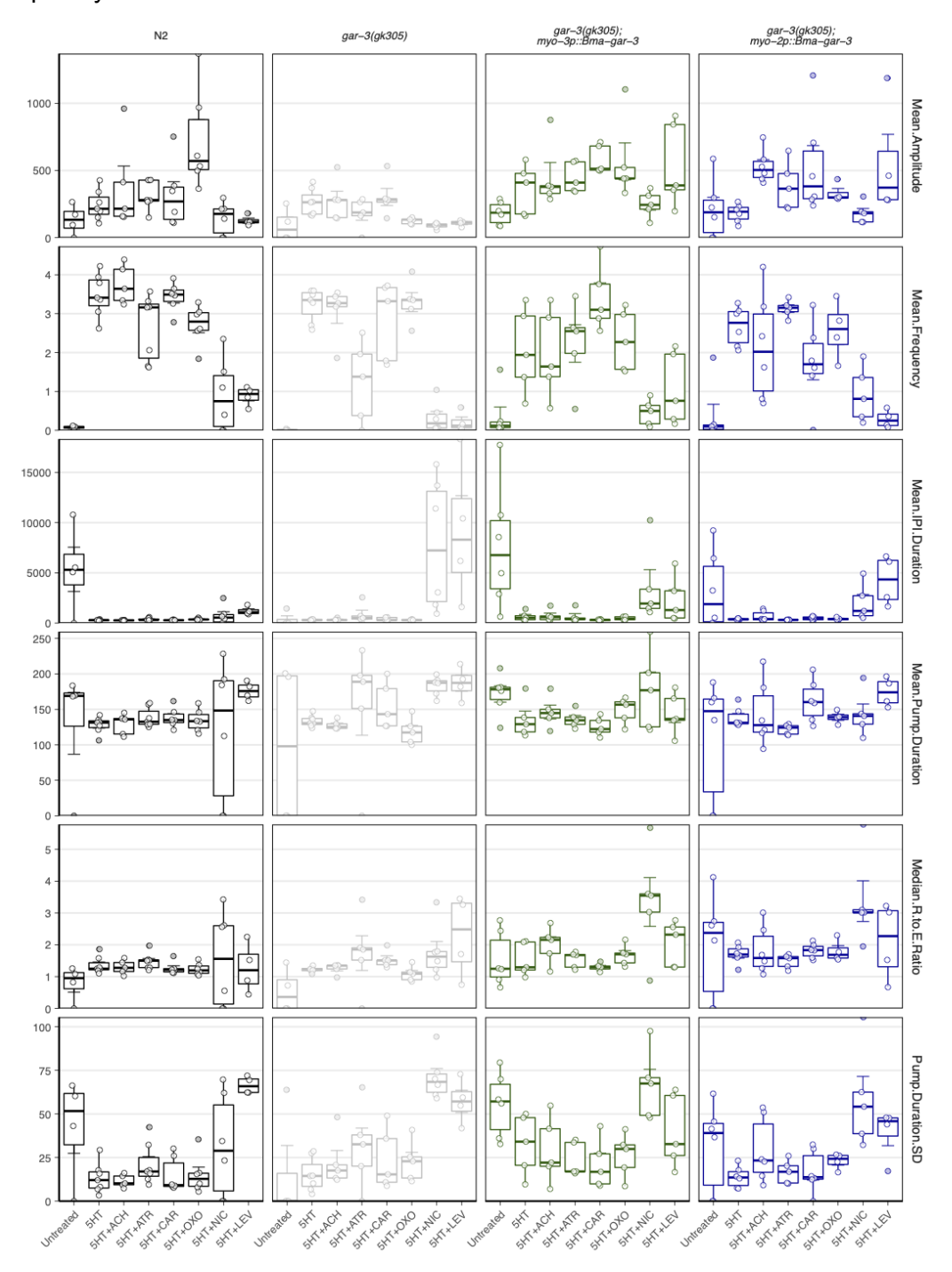
A) Testing lipophilic dye (BODIPY) concentration (1x: 45 ng/mL, 2x: 90 ng/mL) and the inclusion of HB101 for the development of a feeding assay. Treatment with 2x BODIPY in the absence of HB101 allowed the detection of both pharyngeal stimulation and inhibition as quantified by the accumulation of red intestinal fluorescence. (brown: comparisons to 5HT, black: comparisons to untreated). t-tests (*p \leq 0.05; **p \leq 0.01, ***p \leq 0.001). **B)** Feeding assay carried out using a panel of cholinergic treatments. *Bma*-GAR-3 expression in the pharynx partially rescues the wild-type OXO effect that is lost in the *gar-3(gk305)* background, as measured by fluorescent dye uptake. (brown: comparisons to 5HT, black: comparisons to untreated). t-tests (*p \leq 0.05; **p \leq 0.01, ***p \leq 0.001). **C)** Schematic of the dye feeding assay. Bleach synchronized L1 worms are grown in 96-well plates for 48 hours followed by 20 minute drug treatment. Worms are then fed >90 ng/mL BODIPY 558/568 for 20 minutes. Plates are washed three times and worms are paralyzed and straightened with 50 mM sodium azide before images are acquired using an high-content imaging system. Fluorescence is quantified using a wrmXpress [68] pipeline.



Supplemental Material

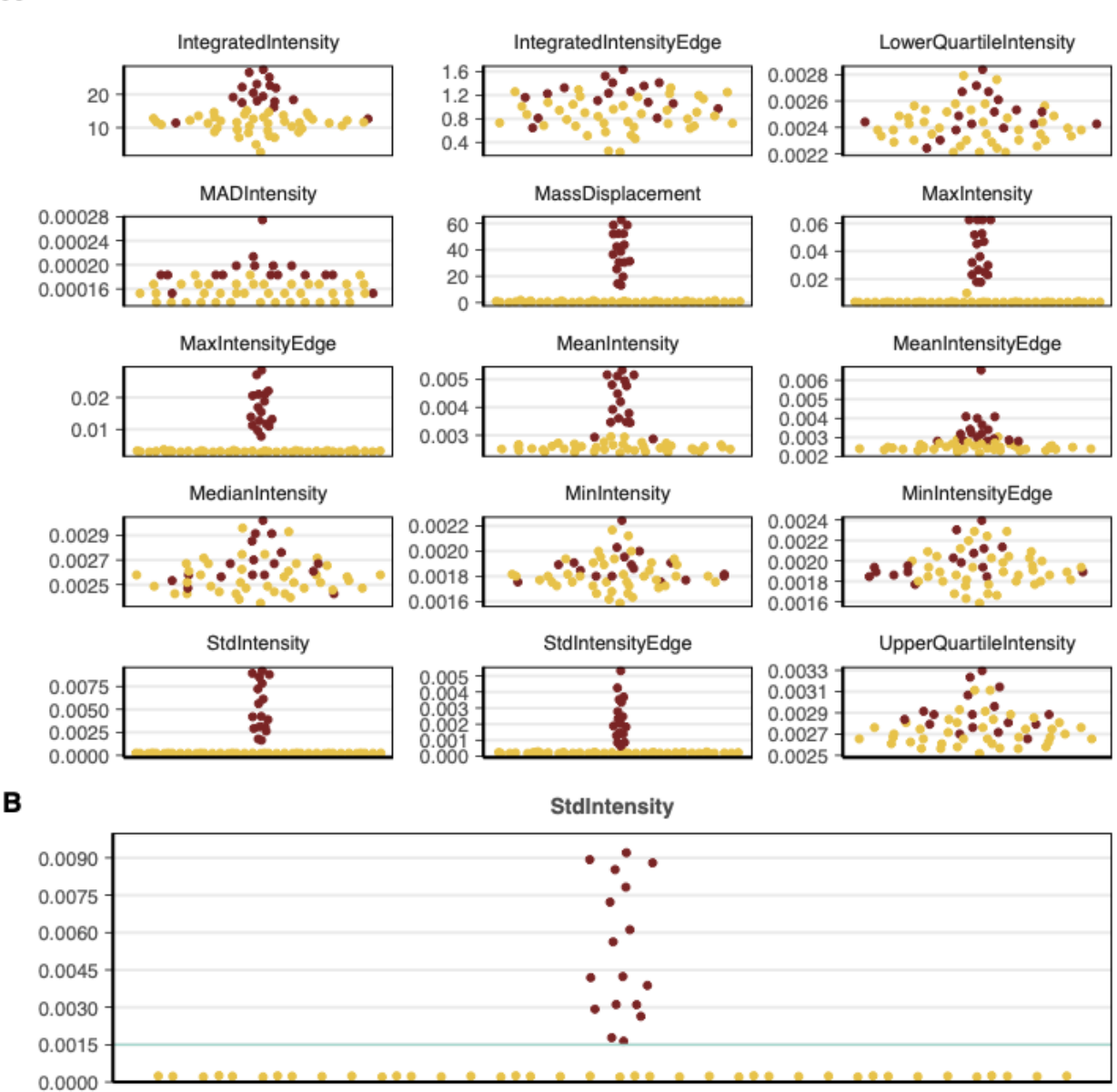
All supplemental data and pipelines for analysis and data visualization are available at https://github.com/zamanianlab/Bm-GAR-ms.

Supplemental Figure 1. Effects of cholinergic treatment on electrophysiological phenotypes measured using EPG recordings. Duration measures are reported in ms, amplitude = μ V, and frequency = Hz.



Supplemental Figure 2 A) Data was manually annotated by visually labeling worms in wrmXpress output images as GFP+ or GFP- (transgenic strain populations created with extrachromosomal arrays contain both GFP+ and GFP- populations indication expression of transgenes). Each GFP-related measure was plotted to determine a metric for filtering data for only GFP+ (transgene expressing) worms. B) StdIntensity, used to filter GFP+ worms from mixed populations, shows a clear separation between GFP+/- populations at a threshold of .0015.





Chapter 4: High throughput aminergic library screen prioritizes dopaminergic receptors for anthelmintic discovery

Abstract

Nearly one billion people worldwide are at risk for lymphatic filariasis (LF), a neglected tropical disease caused by mosquito-transmitted filarial parasites. Current mass drug administration regimes have successfully interrupted transmission and led to elimination in some countries, however, the drugs used do not cure or prevent reinfection and new drugs with diversified targets are needed to continue to combat this disease. Limited information is available on druggable targets in filarial parasites and biological and pharmacological profiles are needed for pursuing novel druggable targets in these filarial parasites. We pursue biogenic amine G protein-coupled receptor (BA-GPCRs) as anthelmintic drug targets and begin to establish pharmacologic profiles using multiplexed phenotypic readouts across both the model nematode C. elegans and the parasitic nematode Brugia malayi, an etiologic agent of LF. We report that dopamine and dopaminergic compounds negatively affect fitness phenotypes and we prioritize 12 dopaminergic compounds from a neurotransmitter library that have strong microfilarial and mixed adulticidal effects. Using homology-based searches, we identify BA-GPCRs and ion channel receptors that could be mediating the observed effects. We are in the process of genetic screens and heterologous expression assays to determine the receptor target of the dopaminergic compounds. These data will expand our understanding of helminth basic biology and provide valuable knowledge about BA-GPCRs as drug targets.

Introduction

Neglected tropical diseases (NTDs) are infectious diseases of poverty endemic to underdeveloped and exploited countries and account for 26 million disability-adjusted life years with nearly half of these caused by parasitic worm (helminth) infections [1]. Current treatment and control mechanisms for helminth infections almost entirely rely upon mass drug administration (MDA) with a limited arsenal of drugs. These drugs (anthelmintics) are inadequate and do not cure or prevent reinfection and reports of anthelmintic resistance have only emphasized the need for novel druggable targets (receptors, enzymes, transporters, structural proteins) and therapies [2,3].

Lymphatic filariasis (LF), a NTD, is caused by mosquito-transmitted filarial nematodes (Wuchereria bancrofti, Brugia malayi, and Brugia timori) with nearly one billion people are at risk of infection [4]. No new anthelmintics for LF have been brought to market in decades and with the growing threat of anthelmintic resistance for LF, new drugs are in dire need [5–8]. However, realization of new anthelmintics is hampered by the sparse information available on druggable targets in filarial parasites.

Current anthelmintics for LF treatment are poorly understood and their antiparasitic activities have all been discovered via *in vivo* experiments [9–11]. The field has recently moved toward more cost effective, *in vitro* target-based high throughput screening (HTS) but difficulties prioritizing targets due to lack of fundamental knowledge about druggable targets in filarial parasites has hindered our ability to achieve true target-based HTS [7,12,13]. To date, no novel drugs have been discovered from these approaches [7,12,13]. Ligand-gated ion channels (LGICs) have been the predominant focus of anthelmintic research as a result of historic success as an anthelmintic target and their critical physiological role in nematodes, but with little knowledge of LGICs expression patterns, gating mechanism, and combination of subunits, target-based HTS remains elusive [14–16]. Moreover, resistance to anthelmintics targeting

LGICs is well established in veterinary medicine and continues to threaten disease control [7]. Diversification of drug targets are needed to continue helminth control efforts.

G protein-coupled receptors (GPCRs) constitute the most abundant drug targets in human medicine but remain unexploited as drug targets for anthelmintics [17,18]. Moreover, biogenic amine GPCRs (BA-GPCRs) have been shown to be essential for many biological functions in the model nematode *Caenorhabditis elegans* including growth, development, and neuromuscular function [18–22]. Specifically, BA-GPCRs regulate many of the same biological functions as the LGICs targeted by current anthelmintics such as movement, embryogenesis and pharyngeal pumping in *C. elegans* and GPCRs are more amenable to HTS than LGICs [14,16,23–25]. Exogenous application of octopamine (OCT) and tyramine (TYRA) inhibit both pharyngeal pumping and egg laying while serotonin (SER) stimulates both of these processes [26–32]. Despite the critical role of BA-GPCRs in *C. elegans*, little attention has been given to the study of these receptors in parasitic nematodes. Based on our understanding of BA-GPCRs in *C. elegans*, it is likely that BA-GPCRs have an essential function in *B. malayi* biology and that dysregulation of these receptors will be detrimental to the worm.

The future success of helminth control requires the identification of diverse targets for novel antiparasitic therapies [33]. We need to explore a diversity of drug targets outside of ion channel receptors in order to mitigate potential anthelmintic resistance and continue effective control of helminth infections. Here, we begin to uncover the importance and pharmacology of BA-GPCRs in parasitic filarial nematodes, we measured multiple phenotypic outputs from both *C. elegans* and *Brugia* adults as well as microfilariae under perturbation of biogenic amines.

Results and Discussion

Multivariate phenotypic screen of exogenous biogenic amine neurotransmitters

We sought to measure whole-organism phenotypic effects of biogenic amines (serotonin, dopamine, histamine, octopamine, and tyramine) on *Brugia* adults and microfilariae as well as on *C. elegans*. Stage-specific effects of biogenic amines on worm motility, viability, and fecundity were measured using established protocols [34–37] and analyzed with wrmXpress, a customized image processing platform [38]. Dose responses were first carried out in mf stage *B. malayi* parasites at three timepoints (0 hr, 24 hr, 48 hr) followed by cell viability measures at the terminal timepoint. All compounds (SER, DOP, HIS, OCT, TYRA) had immediate effects leading to decreased motility at high concentrations (≥10-2 M) (**Fig 1 A**). Interestingly, at the 24 and 48 hr timepoints SER and DOP maintained hypomotility, while HIS and OCT displayed a hypermotile phenotype across all tested concentrations (≥10-9 M). Mf viability was not significantly affected by any of the biogenic amine compounds (**Fig 1 B**). Oxidation of dopamine in liquid culture can produce toxic reactive oxygen species [39] which can have confounding

Male and female *B. malayi* and *B. pahangi* adults were then exposed to 10 μM and 100 μM of each biogenic amine and motility was measured at five timepoints (0hr, 0.1 hr, 1hr, 24 hr, 48 hr). Additionally, adult female fecundity was measured at baseline (0 hr) and 48 hr timepoints. At 10 μM, all compounds except SER decreased 48 hr motility in male *B. pahangi* (**Fig 1 C**). 100 μM DOP decreased motility at 24 and 48 hr timepoints in both species of adult males but only had an effect in *B. pahangi* female worms at 48 hr. No strong motility effects were measured in *B. malayi* female worms even though 100 μM TYRA decreased motility in *B. pahangi* female worms. OCT and TYRA (100 μM) decreased mf output in *B. malayi* and *B. pahangi*, respectively (**Fig 1 D**). Given that nematodes possess biogenic amine responsive ion

effects on media color, image clarity, and worm health.

channels, it is possible that some of these effects may be mediated by ionotropic as opposed to metabotropic signaling.

We next screened *C. elegans* for development effects caused by exogenous application of biogenic amines. As expected, dose responses of biogenic amines on *C. elegans* development over 48 hr showed few significant growth effects (**Fig 1 E**). Comparative assays using this distantly related free-living nematodes can provide a path to identifying underlying targets that may be mediating phenotypic effect using genetic tools not readily available for *Brugia* parasites. Further, these screens and future genetic screens using *C. elegans* can provide insight on potential for pan-nematodal drug effects.

Poor cuticular permeation by some amine neurotransmitters [40,41] and the natural abundance of these biogenic amines within nematodes limits the utility of their exogenous application as a means of detecting whole-organism phenotypes or predicting specific receptors that mediate significant phenotypic effects.

Neurotransmitter compound library screen prioritizes dopaminergic compounds

We next sought to screen a neurotransmitter compound library with ligands known to target mammalian BA-GPCRs expecting an increased likelihood of hits against our nematode BA-GPCRs compared to unmodified exogenous application of biogenic amines. Added moieties are expected to increase the permeability of some compounds across the cuticle allowing for bioavailability and selective binding at receptors of interest. Using compounds with known activity against human receptor ortholog provides prospects of repurposing drugs as anthelmintics and the information about possible targets in *B. malayi* can be useful for

Using the Screen-Well Neurotransmitter library, we measured motility and viability of B. malayi mf at 10 μ M across all 661 compounds. In this primary screen we identified 47 compounds that were hits (z-scores > 1) at the terminal 48 hr timepoint (Fig 2 A). Overall, a

heterologous receptor expression and subsequent target-based screening approaches.

total of 59 hits (8.9% of the library) with three different hit type patterns were observed (**Fig 2 B**). Clustering of these hit patterns revealed 26 hits that decreased motility only at 48 hr or had motility effects and lead to cell death, 13 hits led to immediate motility decreases but recovered by 48 hr, and 20 hits were early on-set and had sustained motility effects but did not lead to cell death during the timeline of our assay (**Fig 2 C**). Phenotypes observed from all three of these clusters are of interest from an anthelmintic discovery point of view. Many current anthelmintic drugs lead to reversible or sustained paralysis while others, such as the benzimidazoles, can lead to worm death [7,42,43].

We conducted the same library screen in *C. elegans* measuring development over 48 hr and motility of adult worms at three timepoints (01 hr, 24 hr, 48 hr). This screen identified 93 hit compounds (z-scores > 1) that either inhibited development or motility at the 48 hr timepoint (Fig 2 D). Interestingly, only 16 of the 81 development hits overlapped with the 80 motility hits (total hits = 145, ~22% of the library) (Fig 2 E). Clustering of these hit compounds identified three motility patterns ranging from recovery to sustained motility inhibition. To narrow our hit list to compounds we would further pursue, we identified the class of neurotransmitter and associated mammalian receptor. Dopaminergic compounds were the most represented (Fig 2 F-G) accounting for 20 hits in the mf screen and 21 hits in the *C. elegans* screen with varying hit patterns. A total of 18 hits overlapped between the mf and *C. elegans* screens, 6 of which were dopaminergic compounds.

Identification of biogenic amine receptors in Brugia malayi

In order to begin to investigate possible targets driving the observed phenotypes of dopaminergic compounds and inform our genetic screens, homology-based searches of annotated *C. elegans* BA-GPCRs were used to identify closely related biogenic amine receptors across seven parasitic nematode species. Phylogenetic analysis of putative BA-GPCRs reveals *B. malayi* possesses one-to-one orthologs of eleven *C. elegans* BA-GPCRs (**fig 3 A**). Notably *B.*

malayi possesses three putative dopamine receptors, dop-1, dop-2, and dop-5. Further homology-based searches for orthologs of *C. elegans* biogenic amine ligand-gated ion channels (BA-LGIC) revealed five putative BA-LGICs in *B. malayi* (**Fig 3 B**). Both *lgc-53* and *Bm12502* (likely *lgc-51*) are putative dopamine responsive receptors. While mammals lack BA-LGICs, there is some close clustering of the human BA-GPCRs with *Brugia* receptors. However, nematode receptors are significantly diverged from their mammalian host orthologs and likely exhibit distinct pharmacological profiles that may allow for selective targeting.

Dose responses of dopaminergic hits on microfilariae and adult phenotypic effects

Dose response for the twelve prioritized dopaminergic hit compounds from the initial

Screen-Well Neurotransmitter library screen were assayed against *B. malayi* mf and motility was measured at three timepoints (0 hr, 24 hr, 48 hr). All compounds recapitulate previous motility results except for L-741,626 which did not show any change in motility (**Fig 4 A**). Since the primary screen only had one replicate for each compound, we expected to reveal some false-positive hits with higher replication. Of the 11 compounds with motility effects in the dose response, five were slow acting and six had immediate motility effects. Slower action of anthelmintic hit compounds could be beneficial in treatment regimes to mitigate adverse reaction to antigens or commensal *Wolbachia* released by dead and dying worms [44,45]. ED50 values fell between 1 μM and 10 μM at all timepoints.

To assess if these prioritized compounds had any phenotypic effects on adult *B. malayi* in vitro, we exposed adult male and female worms to 1 µM of each compound and measured motility and female fecundity over 48 hr. Adult motility effects were mostly transient in both sexes (**Fig 4 B**). For example, Apomorphine, a dopamine agonist, significantly decreased motility in adult female worms at early timepoints and in males at 24 and 48 hr timepoints. The reduction in mf output from adult female worms did not significantly differ from the controls (**Fig 4 C**).

Despite lack of strong adulticidal effects *in vitro* biogenic amine receptors may still pose as actionable targets for novel anthelmintics. In fact, there are no motility or mortality phenotypes associated with application of ivermectin, a frontline anthelmintic, directly to parasites in culture [6,10,46]. Target-based screens and reverse genetic approaches can provide a path to further understanding the importance of biogenic amines and their receptors for nematode biology.

Conclusion and Future directions

Reverse genetic screens in C. elegans

In order to begin to identify receptor targets that may be mediating the observed phenotypes from the Screen-Well Neurotransmitter library screen, we will create CRISPR knockout strains of *C. elegans* where each stain lacks one biogenic amine GPCR. We created a premature stop codon near the 5' region of each gene with the insertion of a ssODN that includes the restriction site *Nhel*. Co-CRISPR with *dpy-10* will be used to screen for edited progeny. Screening for edited progeny will involve initial injections into young adult gonad arms followed by recovery on individual 6 cm seeded NGM plates. Worms that have laid progeny overnight will be moved to a new 6 cm plate. The F1 progeny will be examined for the non-dumpy, roller phenotype and segregated to individual 6 cm NGM plates to lay a brood. After F1s have laid the F2 progeny, we will single-worm genotype the F1s for the short range mutation by PCR amplifying the gene target region and subjecting the PCR product to the *NhellI* restriction digest. Edited progeny will produce two or three bands (depending on homo- or heterozygosity) and unedited progeny will have a single band. We will select F2 progeny from plates where the F1 was edited and genotype the F2s to isolate a homozygous line. These individual strains will be used for counter screens of compounds of interest.

Insight into receptors driving the phenotypes observed in wild type worms can be gained if worms lacking the functional receptor (BA-GPCR or BA-LGIC) are resistant to drug induced motility or development effects. The utility in directly screening *C. elegans* has had mixed utility for anthelmintic discovery but the tractable genetics and molecular tools have enabled target identification and exploration of anthelmintic compounds [32,34,47–52].

<u>Functional expression of dopaminergic GPCRs in mammalian cell lines</u>

We have designed a heterologous expression scheme with the objective of expressing B. malayi dopamine GPCRs in Chinese hamster ovary cells (CHO) and HEK293 T-REx cells in order to pharmacology profile Brugia BA-GPCRs. We will clone our dopamine receptors of interest into a transducible expression vector as well as into pcDNA vector allowing for both inducible and transient expression. We will establish receptor expression in cell lines with a promiscuous G-alpha subunit ($G_{15}\alpha$). Upon activation of the receptor, increased cytosolic calcium can be measured using the Fluo-4 DirectTM Calcium Assay Kit (Invitrogen).

Conclusion

Nearly half of all morbidities caused by neglected tropical diseases are a result of parasitic worm (helminth) infections. Mass drug administration (MDA) of anthelmintics has been implemented to control these infections but current anthelmintics are suboptimal and drug resistance threatens our ability to continue to manage disease transmission. Furthermore, development of new anthelmintics is inhibited by our lack of knowledge on putative drug targets in helminths. This gap in knowledge is exacerbated by lack of fundamental information on the basic biology of helminths. These gaps in knowledge have not only hindered our ability to prioritize drug targets responsible for critical biological processes in helminths but have also impaired our ability to understand the current mode of action for the anthelmintics used in MDA.

Despite significant investment, *in vitro* HTA have not produced any anthelmintic compounds with adulticidal effects. While screening compounds with known mammalian targets can be useful for deducing potential nematode targets, nematode orthologs may not have the same evolutionarily conserved binding pockets or other regions needed for compound interactions. In order to mitigate these complexities and to begin to address some gaps in knowledge in *Brugia malayi*, we used established methods to perturb druggable targets and began to establish pharmacological profiles for BA-GPCRs, a lucrative set of drug targets. Using a library of 661 neurotransmitters we identified 59 bioactive compounds with a large proportion (20/59) of these hits targeting dopamine receptors and pathways. We identified eleven BA-GPCRs and five putative BA-LGICs in *B. malayi* using homology-based searches that may be mediating observed phenotypic effects of these hit compounds. Dose-responses and adult screens of dopaminergic compounds revealed that the action of these compounds lead to both fast and slow acting phenotypic effects likely through a mix of ionotropic and metabotropic receptors.

We will continue to comprehensively characterize these putative drug targets native function, expression, and pharmacology via reverse genetic screens and heterologous expression platforms in order to expand our understanding of basic helminth biology and pursue novel drug targets. Deorphanize and pharmacological screens of *B. malayi* BA-GPCRs in heterologous cell lines is in progress. Additional work proposed here incldues developing a spatiotemporal expression profile of BA-GPCRs and *in silico* compound docking using AlphaFold2. Completion of this research will generate valuable knowledge on BA-GPCRs as drug targets, expand our understanding of helminth basic biology, and validate methods for novel anthelmintic target discovery.

Methods

Protocol and data availability

All primary data and pipelines for statistical analysis and data visualization will be available on github.

Parasites

B. malayi and *B. pahangi* adults extracted from the *Meriones unguiculatus* infection system (NIH/NIAID Filariasis Research Reagent Resource Center) [53] were maintained in daily changes of RPMI 1640 with L-glutamine (Sigma-Aldrich) supplemented with FBS (10% v/v, Fisher Scientific) and penicillin-streptomycin (0.1 mg/mL, Gibco) at 37°C with 5% CO₂ unless otherwise specified. *Brugia* microfilariae isolated from the same system were maintained in RPMI 1640 with L-glutamine (Sigma-Aldrich) supplemented and penicillin-streptomycin (0.1 mg/mL, Gibco) at 37°C with 5% CO₂ unless otherwise specified.

compound Library

For the SCREEN-WELL® Neurotransmitter library (10 plate set) (further referred to as Screenwell compound library), assay-ready plates (ARPs) were generated at the UW-Madison Small Molecule Screening Facility with a Labcyte Echo 650 (Beckman Coulter) liquid handler by spotting each compound onto 96-well assay plates (Greiner Bio-One), which were sealed with adhesive foil and stored at -80 °C until the time of the assay.

Microfilariae assays

B. malayi microfilariae motility and cell toxicity assays were performed as described [36,37]. Briefly, mf are purified using a PD-10 Desalting Column (VWR, cat# 95017-001) into culture

media and titered to a concentration of 10 mf/µL. 100 µL containing 1,000 mf were added to each well of a 96-well plate. Heat killed controls were incubating for 1 hr at 60°C before being added to wells. For primary screens, serial dilutions of 100 mM stock of each drug was made fresh in water. Plates were imaged immediately after treatment (0 hr) and 24 and 48 hr after treatment. Two biological replicates across six 96-well plates were run for motility assays. Each plate contained two replicates per condition with high technical replication per well. Plates were imaged 1, 24 and 48 hr after treatment. CellTox (Promega cat# G8742) staining was performed on six technical replicates at 48 hr following the kit protocol with half the recommended concentration of CellTox. Wells were imaged using an ImageXpress Nano (Molecular Devices). Videos were analyzed with the motility and segmentation modules of wrmXpress [54] and output data was analyzed using the R statistical software.

For Screenwell compound library assays, mf were added directly to assay ready plates with a final concentration of 10 μ M or to dose response plates with three replicates of dose-responses per compound. All downstream processing and analyses were performed the same as the primary screen.

Adult parasite assays

Multivariate phenotyping of adult parasites was performed as described [37,55]. For primary screens, after receipt from the FR3, adult male and female *B. pahangi* parasites were manually sorted into 24-well plates filled with 750 μL of complete media (RPMI 1640 + FBS + pen/strep) per well. Parasites were incubated overnight, after which individual parasites transferred to new plates with 675 μL incomplete media (RPMI 1640 + pen/strep). Plates were recorded for 15 sec, 75 μL of compound was added for final concentrations of 10 μM or 100 μM, and plates were immediately recorded again. Recordings were taken 1 hr post-treatment, 24 hr post-treatment, and 48 hr post-treatment. Three biological replicates from separate batches of parasite infection cohorts were assayed with four worms per treatment. Conditioned media from adult female from

the initial overnight incubation in complete media and the combined 24+48 hr treatment plate were transferred to 1.5 mL tubes and centrifuged for 5 min at 10,000 *x g* to pellet progeny. 500 µL of the supernatant was removed and the remainder was stored at 4°C for >48 hr. To quantify progeny, 50 µL aliquots were transferred to wells of a 96-well plate (Greiner), and each well was imaged with transmitted light at 2X with an ImageXpress Nano (Molecular Devices). Images of progeny were segmented as previously described [37], and segmented pixels were counted to infer output of progeny using a previously generated model [37]. Videos were analyzed with the optical flow (motility) module of wrmXpress [54] and output data was analyzed using the R statistical software.

For the 1 μ M Screenwell compound library assays, worms from the same batch of parasite infection cohort were assayed with four worms per treatment. Methods and timepoints were the same as for the primary screen with a few alterations. Worms were cultured in incomplete media for the entirety of the assays. Conditioned media from the initial overnight incubation in incomplete media and the combined 24+48 hr treatment plate were transferred to 1.5 mL tubes and centrifuged for 5 min at 10,000 x g for both male and female worms. 500 μ L of the supernatant was removed and filtered (0.45 μ m) for protein excretion analysis, and the remainder of the female media was stored at 4°C for >48 hr for fecundity analysis. All downstream processing and analyses were performed the same as the primary screen.

C. elegans development and motility

Bleach synchronized larval stage worms (L1) were aliquoted into 96-well drug plates (primary screens and motility library screen) or ARPs for Screenwell compound library development assays (10 µM final concentration) at a titer of 50 L1 per well along with *E. coli* HB101 bacterial food (2.5 mg/mL final concentration). Worms were incubated for 48 hr at 20°C, shaking at 180 RPM until reaching adult stage [35]. Plates were washed with M9 and paralyzed with 50 mM sodium azide. Four technical replicates were assayed with 50 worms per replicate per condition.

For adult motility Screenwell compound library screens, adult worms were transferred from original 96-well plates to ARPs. Images of worms in transmitted light and GFP were taken on an ImageXpress Nano (Molecular Devices) at 2x. Images were analyzed with the worm size module of wrmXpress [54], which incorporates a custom CellProfiler model using the Worm Toolbox plugin [56,57]. Segmented worms were computationally straightened and output data was analyzed using the R statistical software.

Phylogenetics

Putative parasite biogenic amine GPCRs and LGIC were identified using a reciprocal BLASTp [58] approach using known *C. elegans* receptors. This initial list of receptors was expanded with homology-based searches against the *C. elegans* predicted proteome and a broader list of *C. elegans* [59] biogenic amine receptors was used to carry out blastp searches against the predicted proteomes of *B. malayi* [60], *Ancylostoma caninum* [61], *Ascaris suum* [62], *Haemonchus contortus* [63], *Strongyloides ratti* [64], and *Trichuris muris* [65] (WormBase ParaSite v18 [66] Filtered hits (percent identity > 30%, E-value < 10⁻⁴, and percent coverage > 40%) that survived a reciprocal blastp search against *C. elegans* were retained. This GPCR list was combined with human biogenic amine receptors for phylogenetic inference and annotation. Receptors were aligned with MAFFT [67], trimmed with trimAl [68], and phylogenetic trees were inferred with IQ-TREE [69]. Bootstrap values from 1,000 replicates were drawn as nodal support onto the maximum-likelihood tree. Trees were visualized and annotated with ggtree [70].

C. elegans Co-CRISPR

Detailed methods for crRNA and ssODNs design [71–75] and working protocol are included in the supplementary materials (**Supplementary file 1**). Cas9 protein was obtained from IDT (Alt-R S.p. Cas9 Nuclease V3, 100 µg) and stored at -80°C until use.

Acknowledgements

Brugia worms in different life cycle stages were obtained through the NIH/NIAID

Filarial Research Reagent Resource Center (FR3); morphological voucher specimens are stored at the Harold W. Manter Museum at the University of Nebraska under accession numbers P2021 and P2032. Image processing was performed using the computer resources and assistance of the UW-Madison Center For High Throughput Computing (CHTC) in the Department of Computer Sciences. The CHTC is supported by UW-Madison, the Advanced Computing Initiative, the Wisconsin Alumni Research Foundation, the Wisconsin Institutes for Discovery, and the National Science Foundation, and is an active member of the OSG Consortium, which is supported by the National Science Foundation and the U.S. Department of Energy'sOffice of Science [76]. We also thank the members of the Zamanian laboratory for critical comments on the manuscript, as well as Gene Ananiev and staff at the UWCCC Small Molecule Screening Facility for assistance with compound library storage and preparation. Author contributions: Study design: Gallo KJ, Zamanian M. Execution: Gallo KJ, Henthorn CR. Analysis and interpretation: Gallo KJ, Henthorn CR, Zamanian M. Writing and proofing: Gallo KJ, Henthorn CR, Zamanian M.

Funding

This work was supported by National Institutes of Health NIAID grant R01 AI151171 to MZ. KJD was supported by a UW-SciMed GRS Fellowship (scimedgrs.wisc.edu) and NIH Parasitology and Vector Biology Training grant T32 AI007414 (NIH.gov).

References

1. Hotez PJ, Alvarado M, Basáñez M-G, et al. The global burden of disease study 2010: interpretation and implications for the neglected tropical diseases. PLoS Negl Trop Dis. **2014**; 8(7):e2865.

- 2. Ismail M, Botros S, Metwally A, et al. Resistance to praziquantel: direct evidence from Schistosoma mansoni isolated from Egyptian villagers. Am J Trop Med Hyg. **1999**; 60(6):932–935.
- Osei-Atweneboana MY, Awadzi K, Attah SK, Boakye DA, Gyapong JO, Prichard RK. Phenotypic evidence of emerging ivermectin resistance in Onchocerca volvulus. PLoS Negl Trop Dis. 2011; 5(3):e998.
- 4. Kalyanasundaram R, Khatri V, Chauhan N. Advances in Vaccine Development for Human Lymphatic Filariasis. Trends Parasitol. **2020**; 36(2):195–205.
- 5. International Helminth Genomes Consortium. Comparative genomics of the major parasitic worms. Nat Genet. **2019**; 51(1):163–174.
- 6. Geary TG, Woo K, McCarthy JS, et al. Unresolved issues in anthelmintic pharmacology for helminthiases of humans. Int J Parasitol. **2010**; 40(1):1–13.
- 7. Abongwa M, Martin RJ, Robertson AP. A BRIEF REVIEW ON THE MODE OF ACTION OF ANTINEMATODAL DRUGS. Acta Vet . **2017**; 67(2):137–152.
- 8. Campbell WC. Efficacy of the avermectins against filarial parasites: a short review. Vet Res Commun. Springer; **1982**; 5(3):251–262.
- Martin RJ, Robertson AP, Bjorn H. Target sites of anthelmintics. Parasitology. 1997; 114 Suppl:S111–24.
- 10. Laing R, Gillan V, Devaney E. Ivermectin Old Drug, New Tricks? Trends Parasitol. **2017**; 33(6):463–472.
- 11. Geary TG. Mechanism-based screening strategies for anthelmintic discovery. Parasitic Helminths. Weinheim, Germany: Wiley-VCH Verlag GmbH & Co. KGaA; 2012. p. 121–134.
- 12. Nixon SA, Welz C, Woods DJ, Costa-Junior L, Zamanian M, Martin RJ. Where are all the anthelmintics? Challenges and opportunities on the path to new anthelmintics. Int J Parasitol Drugs Drug Resist. **2020**; 14:8–16.
- 13. Zamanian M, Chan JD. High-content approaches to anthelmintic drug screening. Trends Parasitol. **2021**; 37(9):780–789.
- 14. Clare JJ. Targeting ion channels for drug discovery. Discov Med. 2010: 9(46):253–260.
- 15. Wolstenholme AJ. Ion channels and receptor as targets for the control of parasitic nematodes. Int J Parasitol Drugs Drug Resist. Elsevier; **2011**; 1(1):2–13.
- 16. Yu H-B, Li M, Wang W-P, Wang X-L. High throughput screening technologies for ion channels. Acta Pharmacol Sin. **2016**; 37(1):34–43.
- 17. Hauser AS, Attwood MM, Rask-Andersen M, Schiöth HB, Gloriam DE. Trends in GPCR drug discovery: new agents, targets and indications. Nat Rev Drug Discov. **2017**; 16(12):829–842.
- 18. Mani T, Bourguinat C, Prichard RK. G-protein-coupled receptor genes of Dirofilaria immitis. Mol Biochem Parasitol. **2018**; 222:6–13.

- Kozlova AA, Lotfi M, Okkema PG. Crosstalk with the GAR-3 Receptor Contributes to Feeding Defects in Caenorhabditis eleganseat-2 Mutants. Genetics [Internet]. 2019;
 Available from: http://dx.doi.org/10.1534/genetics.119.302053
- 20. Greenberg RM. Ion channels and drug transporters as targets for anthelmintics. Curr Clin Microbiol Rep. **2014**; 1(3-4):51–60.
- 21. Avery L, You Y-J. C. elegans feeding. WormBook. 2012; :1-23.
- 22. Park YS, Lee YS, Cho NJ, Kaang BK. Alternative splicing of gar-1, a Caenorhabditis elegans G-protein-linked acetylcholine receptor gene. Biochem Biophys Res Commun. **2000**; 268(2):354–358.
- 23. Komuniecki RW, Hobson RJ, Rex EB, Hapiak VM, Komuniecki PR. Biogenic amine receptors in parasitic nematodes: what can be learned from Caenorhabditis elegans? Mol Biochem Parasitol. **2004**; 137(1):1–11.
- 24. Hobson RJ, Hapiak VM, Xiao H, Buehrer KL, Komuniecki PR, Komuniecki RW. SER-7, a Caenorhabditis elegans 5-HT7-like receptor, is essential for the 5-HT stimulation of pharyngeal pumping and egg laying. Genetics. **2006**; 172(1):159–169.
- Law W, Wuescher LM, Ortega A, Hapiak VM, Komuniecki PR, Komuniecki R. Heterologous Expression in Remodeled C. elegans: A Platform for Monoaminergic Agonist Identification and Anthelmintic Screening. PLoS Pathog. 2015; 11(4):e1004794.
- 26. Horvitz HR, Chalfie M, Trent C, Sulston JE, Evans PD. Serotonin and octopamine in the nematode Caenorhabditis elegans. Science. **1982**; 216(4549):1012–1014.
- 27. Ségalat L, Elkes DA, Kaplan JM. Modulation of serotonin-controlled behaviors by Go in Caenorhabditis elegans. Science. **1995**; 267(5204):1648–1651.
- 28. Weinshenker D, Garriga G, Thomas JH. Genetic and pharmacological analysis of neurotransmitters controlling egg laying in C. elegans. J Neurosci. **1995**; 15(10):6975–6985.
- 29. Tsalik EL, Niacaris T, Wenick AS, Pau K, Avery L, Hobert O. LIM homeobox gene-dependent expression of biogenic amine receptors in restricted regions of the C. elegans nervous system. Dev Biol. **2003**; 263(1):81–102.
- 30. Sawin ER, Ranganathan R, Horvitz HR. C. elegans locomotory rate is modulated by the environment through a dopaminergic pathway and by experience through a serotonergic pathway. Neuron. **2000**; 26(3):619–631.
- 31. Alkema MJ, Hunter-Ensor M, Ringstad N, Horvitz HR. Tyramine Functions independently of octopamine in the Caenorhabditis elegans nervous system. Neuron. **2005**; 46(2):247–260.
- 32. Gallo KJ, Wheeler NJ, Elmi AM, Airs PM, Zamanian M. Pharmacological Profiling of a Brugia malayi Muscarinic Acetylcholine Receptor as a Putative Antiparasitic Target. Antimicrob Agents Chemother. **2023**; :e0118822.
- 33. Greenwood K, Williams T, Geary T. Nematode neuropeptide receptors and their development as anthelmintic screens. Parasitology. **2005**; 131 Suppl:S169–77.

- 34. Wheeler NJ, Ryan KT, Gallo KJ, et al. Multivariate chemogenomic screening prioritizes new macrofilaricidal leads [Internet]. bioRxiv. 2022 [cited 2022 Jul 27]. p. 2022.07.25.501423. Available from: https://www.biorxiv.org/content/10.1101/2022.07.25.501423v1
- 35. Gallo K, Zamanian M. High-throughput image-based drug screening of Caenorhabditis elegans movement, development, and viability. **2022** [cited 2022 Nov 15]; . Available from: https://protocolexchange.researchsquare.com/article/pex-2018/v1
- 36. Wheeler NJ, Zamanian M, Ryan KT, Gallo KJ. Bivariate, high-content screening of Brugia malayi microfilariae. **2022** [cited 2022 Aug 29]; . Available from: https://protocolexchange.researchsquare.com/article/pex-1916/v1
- 37. Wheeler NJ, Ryan KT, Gallo KJ, et al. Multivariate chemogenomic screening prioritizes new macrofilaricidal leads. Commun Biol. **2023**; 6(1):44.
- 38. Wheeler NJ, Garncarz EJ, Gallo KJ, Chan JD, Zamanian M. wrmXpress: A modular package for high-throughput image analysis of parasitic and free-living worms [Internet]. bioRxiv. 2022 [cited 2022 May 20]. p. 2022.05.18.492482. Available from: https://www.biorxiv.org/content/10.1101/2022.05.18.492482v1
- 39. Umek N, Geršak B, Vintar N, Šoštarič M, Mavri J. Dopamine Autoxidation Is Controlled by Acidic pH. Front Mol Neurosci. **2018**; 11:467.
- 40. Christ D, Goebel M, Saz HJ. Actions of acetylcholine and GABA on spontaneous contractions of the filariid, Dipetalonema viteae. Br J Pharmacol. **1990**; 101(4):971–977.
- 41. Postila PA, Vattulainen I, Róg T. Selective effect of cell membrane on synaptic neurotransmission. Sci Rep. **2016**; 6:19345.
- 42. Kashyap SS, Verma S, McHugh M, et al. Anthelmintic resistance and homeostatic plasticity (Brugia malayi). Sci Rep. **2021**; 11(1):14499.
- 43. Verma S, Kashyap SS, Robertson AP, Martin RJ. Diethylcarbamazine activates TRP channels including TRP-2 in filaria, Brugia malayi. Commun Biol. **2020**; 3(1):398.
- 44. Cross HF, Haarbrink M, Egerton G, Yazdanbakhsh M, Taylor MJ. Severe reactions to filarial chemotherapy and release of Wolbachia endosymbionts into blood. Lancet. **2001**; 358(9296):1873–1875.
- 45. Taylor MJ, Hoerauf A, Bockarie M. Lymphatic filariasis and onchocerciasis. Lancet. **2010**; 376(9747):1175–1185.
- 46. Blair LS, Williams E, Ewanciw DV. Efficacy of ivermectin against third-stage Dirofilaria immitis larvae in ferrets and dogs. Res Vet Sci. **1982**; 33(3):386–387.
- 47. Burns AR, Luciani GM, Musso G, et al. Caenorhabditis elegans is a useful model for anthelmintic discovery. Nat Commun. **2015**; 6:7485.
- 48. Holden-Dye L, Walker RJ. Anthelmintic drugs and nematicides: studies in Caenorhabditis elegans. WormBook. **2014**; :1–29.
- 49. Elfawal MA, Savinov SN, Aroian RV. Drug Screening for Discovery of Broad-spectrum Agents for Soil-transmitted Nematodes. Sci Rep. **2019**; 9(1):12347.

- 50. Dent JA, Smith MM, Vassilatis DK, Avery L. The genetics of ivermectin resistance in Caenorhabditis elegans. Proc Natl Acad Sci U S A. **2000**; 97(6):2674–2679.
- 51. Driscoll M, Dean E, Reilly E, Bergholz E, Chalfie M. Genetic and molecular analysis of a Caenorhabditis elegans beta-tubulin that conveys benzimidazole sensitivity. J Cell Biol. **1989**; 109(6 Pt 1):2993–3003.
- 52. Boulin T, Gielen M, Richmond JE, Williams DC, Paoletti P, Bessereau J-L. Eight genes are required for functional reconstitution of the Caenorhabditis elegans levamisole-sensitive acetylcholine receptor. Proc Natl Acad Sci U S A. **2008**; 105(47):18590–18595.
- 53. Michalski ML, Griffiths KG, Williams SA, Kaplan RM, Moorhead AR. The NIH-NIAID Filariasis Research Reagent Resource Center. PLoS Negl Trop Dis. **2011**; 5(11):e1261.
- 54. Wheeler NJ, Gallo KJ, Rehborg EJG, Ryan KT, Chan JD, Zamanian M. wrmXpress: A modular package for high-throughput image analysis of parasitic and free-living worms. PLoS Negl Trop Dis. **2022**; 16(11):e0010937.
- 55. Wheeler NJ, Zamanian M, Ryan KT, Gallo KJ. Multivariate screening of Brugia spp. adults. **2022** [cited 2022 Aug 29]; . Available from: https://protocolexchange.researchsquare.com/article/pex-1918/v1
- 56. Wählby C, Kamentsky L, Liu ZH, et al. An image analysis toolbox for high-throughput C. elegans assays. Nat Methods. **2012**; 9(7):714–716.
- 57. McQuin C, Goodman A, Chernyshev V, et al. CellProfiler 3.0: Next-generation image processing for biology. PLoS Biol. **2018**; 16(7):e2005970.
- 58. Altschul SF, Gish W, Miller W, Myers EW, Lipman DJ. Basic local alignment search tool. J Mol Biol. **1990**; 215(3):403–410.
- 59. C. elegans Sequencing Consortium. Genome sequence of the nematode C. elegans: a platform for investigating biology. Science. **1998**; 282(5396):2012–2018.
- 60. Ghedin E, Wang S, Spiro D, et al. Draft genome of the filarial nematode parasite Brugia malayi. Science. science.sciencemag.org; **2007**; 317(5845):1756–1760.
- 61. Abubucker S, Martin J, Yin Y, et al. The canine hookworm genome: analysis and classification of Ancylostoma caninum survey sequences. Mol Biochem Parasitol. **2008**; 157(2):187–192.
- 62. Jex AR, Liu S, Li B, et al. Ascaris suum draft genome. Nature. 2011; 479(7374):529–533.
- 63. Laing R, Kikuchi T, Martinelli A, et al. The genome and transcriptome of Haemonchus contortus, a key model parasite for drug and vaccine discovery. Genome Biol. **2013**; 14(8):R88.
- 64. Hunt VL, Tsai IJ, Coghlan A, et al. The genomic basis of parasitism in the Strongyloides clade of nematodes. Nat Genet. **2016**; 48(3):299–307.
- 65. Foth BJ, Tsai IJ, Reid AJ, et al. Whipworm genome and dual-species transcriptome analyses provide molecular insights into an intimate host-parasite interaction. Nat Genet. **2014**; 46(7):693–700.

- 66. Howe KL, Bolt BJ, Shafie M, Kersey P, Berriman M. WormBase ParaSite a comprehensive resource for helminth genomics. Mol Biochem Parasitol. **2017**; 215:2–10.
- 67. Katoh K, Standley DM. MAFFT multiple sequence alignment software version 7: improvements in performance and usability. Mol Biol Evol. **2013**; 30(4):772–780.
- 68. Capella-Gutiérrez S, Silla-Martínez JM, Gabaldón T. trimAl: a tool for automated alignment trimming in large-scale phylogenetic analyses. Bioinformatics. **2009**; 25(15):1972–1973.
- 69. Minh BQ, Schmidt HA, Chernomor O, et al. IQ-TREE 2: New Models and Efficient Methods for Phylogenetic Inference in the Genomic Era. Mol Biol Evol. **2020**; 37(5):1530–1534.
- 70. Yu G, Smith DK, Zhu H, Guan Y, Lam TT-Y. ggtree: an r package for visualization and annotation of phylogenetic trees with their covariates and other associated data. McInerny G, editor. Methods Ecol Evol. Wiley Online Library; **2017**; 8(1):28–36.
- 71. Dickinson DJ, Goldstein B. CRISPR-Based Methods for Caenorhabditis elegans Genome Engineering. Genetics. **2016**; 202(3):885–901.
- 72. Schwartz ML, Davis MW, Rich MS, Jorgensen EM. High-efficiency CRISPR gene editing in C. elegans using Cas9 integrated into the genome. PLoS Genet. **2021**; 17(11):e1009755.
- 73. Ghanta KS, Mello CC. Melting dsDNA Donor Molecules Greatly Improves Precision Genome Editing in Caenorhabditis elegans. Genetics. **2020**; 216(3):643–650.
- 74. Au V, Li-Leger E, Raymant G, et al. CRISPR/Cas9 Methodology for the Generation of Knockout Deletions in Caenorhabditis elegans. G3 . **2019**; 9(1):135–144.
- 75. Eroglu M, Yu B, Derry B. Efficient CRISPR/Cas9 mediated large insertions using long single-stranded oligonucleotide donors in C. elegans [Internet]. bioRxiv. 2022 [cited 2023 Feb 1]. p. 2022.09.26.509570. Available from: https://www.biorxiv.org/content/10.1101/2022.09.26.509570v1
- 76. Home [Internet]. CHTC. [cited 2023 Jun 19]. Available from: https://chtc.cs.wisc.edu/

Figures

Figure 1. Whole organism phenotypic effects of biogenic amines on free-living and parasitic nematodes A) Dose-responses of aminergic compounds on microfilariae motility over 48 hours. Each point represents the mean of two technical replicates within a plate for a total of 6 plates. Log2 fold change in movement compared to untreated controls, t-test (*p ≤ 0.05; **p ≤ 0.01, ***p ≤ 0.001). B) Effects of aminergic compounds on microfilariae cell viability over 48 hours as measured by cell toxicity stain (CellTox fluorescence). Percent change in fluorescence from untreated controls with each point representing a technical replicate, t-test (*p \leq 0.05; **p \leq 0.01, ***p ≤ 0.001). **C)** Effects of aminergic compounds on adult *Brugia spp.* movement over 48 hours as measured by optical flow. Each point represents an individual worm. Log₂ normalized movement compared to 0 hour motility within treatment groups, Wilcoxon-test (*p \leq 0.05; **p \leq 0.01, ***p ≤ 0.001). **D)** Effects of aminergic compounds on adult female *Brugia spp.* fecundity as measured by microfilariae output with each point representing an individual worm's mf output. Percent change of mf output from 0 hour fecundity within treatment groups and compared to untreated controls, t-tests (*p \leq 0.05; **p \leq 0.01, ***p \leq 0.001). **E)** Dose-response of aminergic compounds on C. elegans development over 48 hours. Each point represents an individual worm size. Worm size is compared to untreated controls, Wilcoxon-test (*p \leq 0.05; **p \leq 0.01, *** $p \le 0.001$).

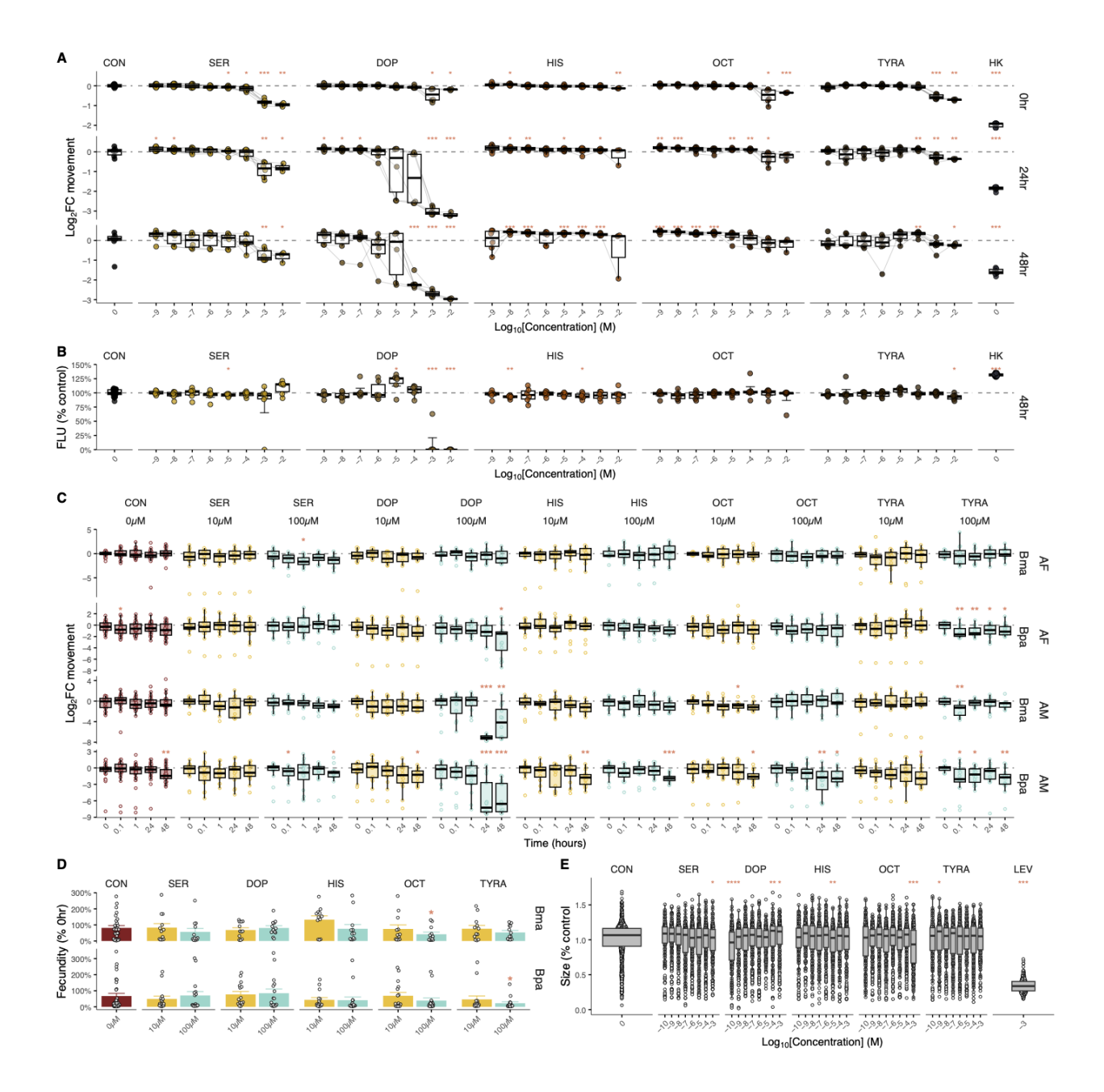


Figure 2. High throughput screen of A) 48 hr timepoint results for the 10 μM Screen-Well Neurotransmitter library screen against mf measuring motility and viability. Dashed lines mark the cutoff (z-score >1) for motility and viability hits. **B)** Clustering of hits by a z-score measure across viability at 48 hr and motility at three timepoints. **C)** 48 hr timepoint results for two 10 μM Screen-Well Neurotransmitter library screen against *C. elegans* measuring adult motility and, separately, larval development. Dashed lines mark the cutoff (z-score >1) for motility and development hits. Positive controls for motility were assigned z-score of 0 for development for plotting purposes. **D)** Clustering of hits by z-score measure across development at 48 hr and motility at three timepoints. **E)** The number of hits for each class of neurotransmitter in the library screen. Blue = *Brugia malayi* mf, green = *C. elegans*, both = brown, neither = cream. (ADR = adrenergic, DOP = dopaminergic, SER = serotonergic, OPI = opioids, ACH = cholinergic, HIS = histaminergic, iGLU = ionotropic glutamatergic, mGLU = metabotropic glutamatergic, GABA = GABAergic, ADN = purinergic and adenosine ligands). **F)** Dopaminergic hit profiles depicting which species was affected by the compound and the predicted compounds activity (based on mammalian data).

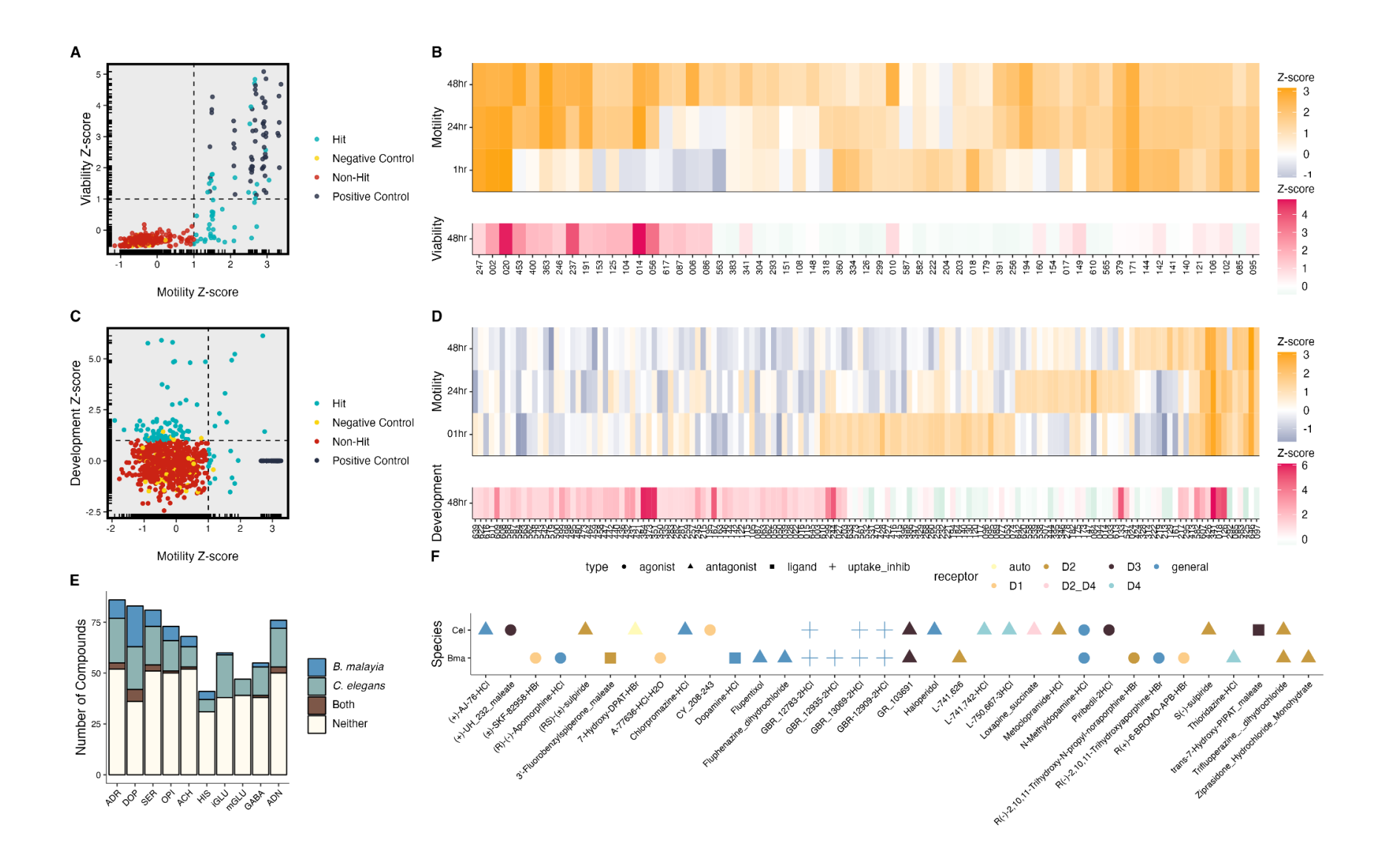


Figure 3. Homology-based searches identify 11 BA-GPCR and 5 BA-LGIC A) Phylogeny based on protein sequence alignment of characterized and putative nematode and human BA-GPCRs. *B. malayi* possesses three dopaminergic GPCRs (*dop-1*, *dop-2*, and *dop-5*). **B)** Phylogeny based on protein sequence alignment of characterized and putative nematode BA-LGICs. *B. malayi* likely possesses two dopaminergic LGICs (*Igc-53* and *Bm12502*).



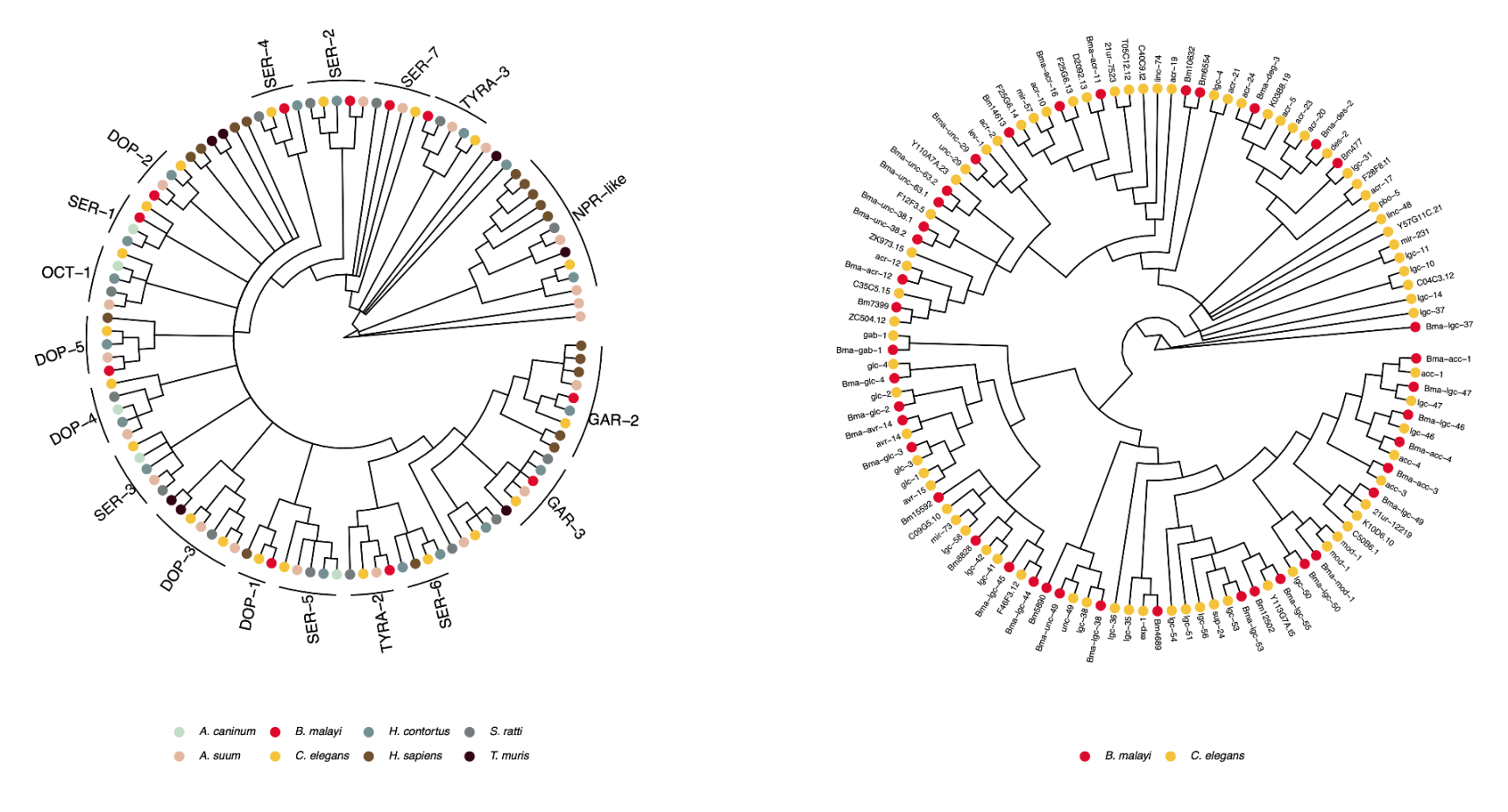
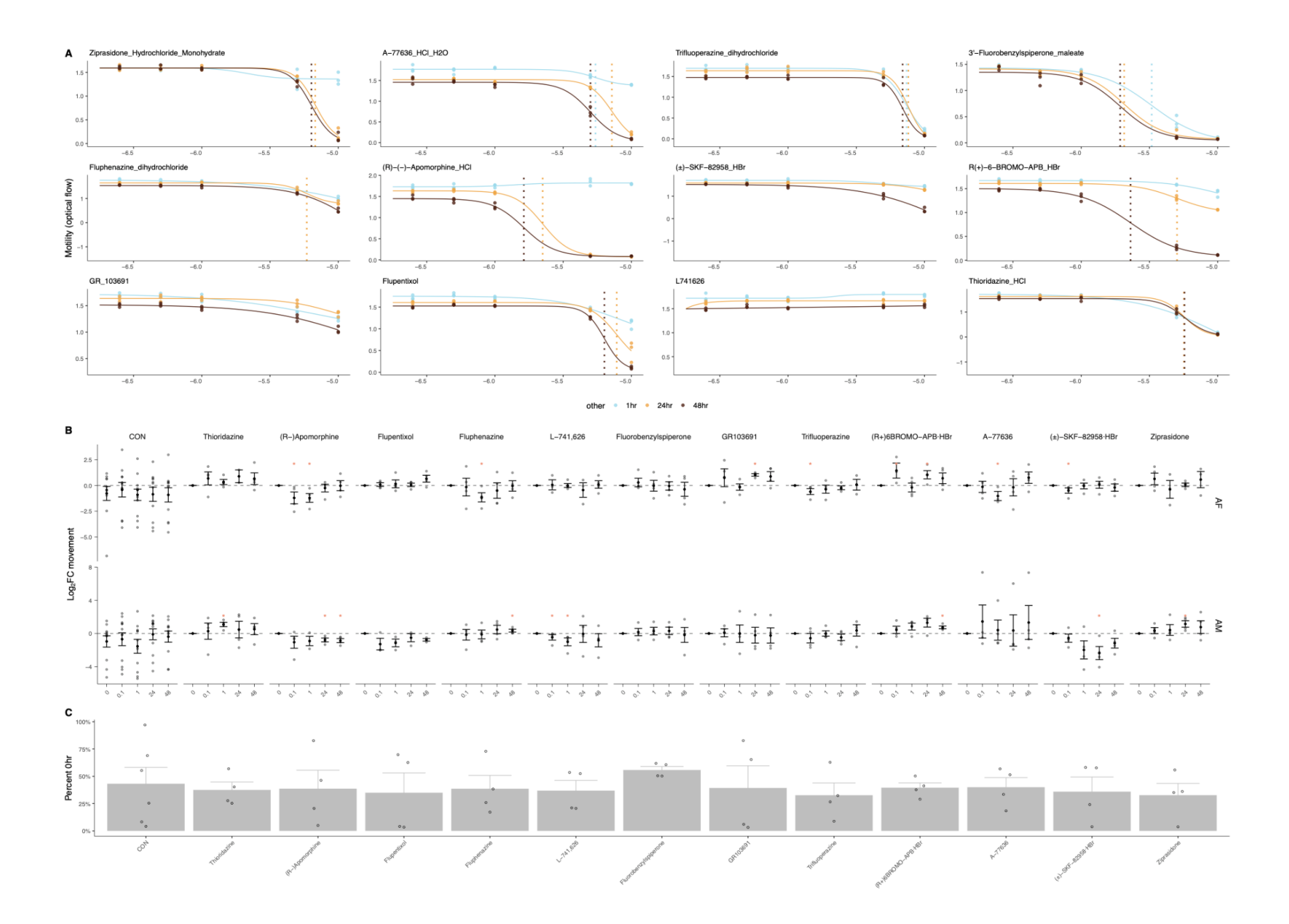


Figure 4. Dose-responses of dopaminergic compounds in *B. malayi* microfilariae and effects of 1 μM application on adults A) Five point dose-response (250 nM - 10 μM) of dopaminergic compounds measuring *B. malayi* mf motility at three timepoints (0 hr, 24 hr, 48 hr). Dashed vertical lines indicate ED50. (0 hr = blue, 24 hr = yellow , 48 hr = brown). B) Effects of 1 μM dopaminergic compounds on adult *B. malayi* motility, self-normalized to 0 hr motility over 48 hr. Each grey point represents an individual worm, black points represent the mean of worms in the treatment group. Log₂ normalized movement compared to 0 hour motility within treatment groups, Wilcoxon-test (*p ≤ 0.05; **p ≤ 0.01, ***p ≤ 0.001). C) Effects of prioritized dopaminergic compounds on adult female *Brugia spp.* fecundity as measured by microfilariae output with each point representing an individual worm's mf output. Percent change of mf output from 0 hour fecundity within treatment groups and compared to untreated controls, t-tests (*p ≤ 0.05; **p ≤ 0.01, ***p ≤ 0.001).



Supplemental Material

Supplemental file 1. Detailed reverse genetic approach methods and materials

Designing C. elegans LGC-specific CRISPR crRNAs

Guide RNAs were designed against C. elegans LGC receptors using the Benchling guide RNA design tool(Benchling reference) and design guidelines from previous C. elegans CRISPR gene editing approaches(Dickinson and Goldstein 2016; Schwartz et al. 2021; Ghanta and Mello 2020; Eroglu, Yu, and Derry 2022; Au et al. 2019). Potential crRNAs near the 5' end of each LGC receptor protein encoding sequence were identified using Benchling based on high On-Target and Off-Target Scores (>= 50.0). Guide RNAs with high scores for both were also assessed for total GC content (50-70%), avoidance of four or more consecutive T nucleotides, a G or GG immediately preceding the NGG PAM site, and unique 12bp sequence 3' to the PAM sequence for repair template purposes. Single-stranded oligodeoxynucleotide (ssODN) repair templates were designed for each Cas9 target site with 35 bp of homology flanking the double stranded break site and opposite strandedness of the guide RNA. Stop codons in each reading frame, including an Nhel restriction site for screening purposes, were added between the homology arms to cause premature truncation of the receptors. Synonymous point mutations were introduced in the crRNA and PAM site to prohibit any potential additional cutting by Cas9. All CRISPR-Cas9 reagents were ordered from Integrated DNA Technologies (IDT) (Coralville, IA, USA) with the recommended end modifications to enhance homology-directed repair. Table 1 contains the custom cdRNA and repair ssODN sequences chosen for each targeted LGC receptor.

Injection of co-CRISPR mix

The injection mix for microinjection into each gonad arm of *C. elegans* strain N2 was prepared by first combining the tracrRNA (0.9 μ I at 100 μ M) and crRNA targeting the LGC receptor (X μ I

at 0.4 µg/µl) into a PCR tube and incubated for 5 min at 95°C followed by 5 min at room temperature. A crRNA targeting *dpy-10* (0.37 µl at 0.4 µg/µl) was also added to implement a co-CRISPR strategy for detecting gene-editing events(Arribere et al. 2014). Cas-9 nuclease (IDT, #1081058) was added to the tracrRNA:crRNA and incubated at 37°C for 10 min. ssODNs were then added to the mixture and gently mixed by pipetting taking care not to introduce air bubbles. The injection mix was transferred to a 1.5 mL microcentrifuge tube and spun at 14,000 rcf for 2 min and then stored at 4°C until injection. The injection mix was made same day as microinjection into *C. elegans*.

Microinjection into C. elegans

Microinjections into *C. elegans* were completed using a FemtoJex 4x (Eppendorf, Hamburg, Germany) using glass filaments (#1B100F-4, World Precision Instruments, Sarasota, FL, USA) pulled on a Micropipette puller from Sutter Instruments (model P-87) (Novato, CA, USA). Pulled needles were filled with the co-CRISPR injection mix and affixed to a Zeiss AX10 microscope equipped with 10X and 40X objectives (Zeiss, Oberkochen, Germany). Young adult *C. elegans* L4 stage worms were mounted onto agarose pads with light halocarbon oil and each arm of the gonad was microinjected until the gonad was flooded with microinjection mix. Worms were recovered on NGM plates and incubated at 20°C.

Screening CRISPR-edited C. elegans

F1 progeny of microinjected worms were screened for the *dpy-10* roller phenotype were transferred to new, individual NGM plates (1 worm/plate) and allowed to lay the F2 progeny.

After all progeny had been laid, single worm genotyping was completed on the F1 hermaphrodite to identify editing within the desired LGC receptor using PCR amplification followed by *Nhel* restriction digest. Worm lysate was created by adding the F1 parental worm to a PCR tube containing 6 µl of lysis buffer (98 µl 2X lysis buffer and 2 µl 20 mg/ml proteinase K),

snap freezing at -80°C, and incubation at 60°C for 1 hr followed by head inactivation of the proteinase K at 95°C for 15 min. PCR amplification of the targeted LGC receptor region was completed by adding 2 µl of worm lysate to a PCR tube with 18 µl of master mix containing region specific primers (**Table 2**), 5X GoTaq Buffer (Promega, Madison, WI, USA) (1X), dNTPs (Promega, Madison, WI, USA) (0.2mM), forward and reverse primers (0.1 uM) and GoTaq Polymerase (Promega, Madison, WI, USA). Thermal cycling parameters were followed according to the GoTaq polymerase manufacturer specifications with an annealing temperature of 53°C and an extension time of 1 min for 35 cycles. The PCR products were incubated with *Nhel* (New England Biolabs, Ipswich, MA, USA) for 15 min prior to analyzing the resulting fragments through gel electrophoresis. Progeny from gene edited parental F1s were screened for homozygosity at the desired locus and backcrossed 5 times with *C. elegans* N2 to remove *dpy-10* edits and maintain the desired edit in the LGC receptor.

Supplemental Table 1. Custom cdRNA and repair ssODN sequences chosen for each targeted LGC receptor

Tar get	crRNA (5'->3')	Targ eted Exo n	Repair ssODN (5'->3')
Igc- 51	GCTCAGCAACAGT TTCACGG	Exon 2 of 8 total exon s	ATCGTACCAAATCGAACTGAACCATATGTGCGGCGCTATTCTAGGCTAGCTGAAGCTG TTGCTGAGCACACTGAGCTCCATCACA
<i>lgc-</i> 52	TAACTACCGTATCC GATCCG	Exon 4 of 9 total exon s	GAAATTTCGAAGATTCATCTGACACGGAGCTTCGGCTATTCTAGGCTAGCAGCGGATG CGGTAGTTGAGCCATATAGTACCATTTGG
<i>lgc-</i> 53	CATGATCGGCGGA GGGAAGG	Exon 2 of 13 total exon s	GTCGCTCTTTTCGGAACTTTTTACGTTTTCGGCCTCTATTCTAGGCTAGCTCCCTTCGC CGGTCATGTTGAGAAGATGGGATGTTTGG
Igc- 54	TCACCCTATACGG TCTGCAG	Exon 4 of 10 total exon s	CCTGCCGCATATTCAAAACTATTTTTTGTACACTGCTATTCTAGGCTAGCCAGACCATAT AGCGTGAAATCCGAAAGTTTCGATTTAGC
<i>lgc-</i> 55	GTTAGCGACTTGG CTCGCGG	Exon 3 of 12 total exon s	CTTCCTCCGAATCCTGTGATAATCCGAGTACACCGCTATTCTAGGCTAGCCTAGCCAGGTCGCTAACCACTGaaaataaaaattttg
Igc- 56	GCTATGTTAGCGA ACGATTG	Exon 4 of 10 total exon s	GCTTTTGCTATTCACAAAACACACATTCGGTGTACACAACTATTCTAGGCTAGCGCGTT CGCTGACATAGCTGTCTAATGACAAATTTG

Supplemental Table 2. PCR amplification primers for the targeted LGC receptor region

Target	Primers (5'->3')	Tm(°C)	Annealing (°C)
Igc-51	F: AAATGCACAAAACCGAGGCTC R: GCACATTAGGCTTTGGGGAC	58 58	53
Igc-52	F: AAATGCACTTCCAGAACCGGC R: GACAGTCGATGCCACATTCC	60 58	53
Igc-53	F: ATCATCATTCCGTCCCTCCG R: GCAGCACACTCAAGTACGTTG	59 58	53
Igc-54	F: CCGGCGAATGACACAATTTCC R: TCCATAGGCACGTGAGAAGG	59 58	53
Igc-55	F: GAGATGGTTTTGCGCGGATATC R: TGCATTGTGGAGCTCGATTGG	58 60	53
lgc-56	F: CTGTGGTAATTTGCACTGCCC R:CACCAAGAGTGATTCGAGCAGG	59 60	54

Chapter 5: CONCLUSION

5.1 Summary of key findings and importance

Vector-borne helminthiases are estimated to afflict hundreds of millions of individuals globally [1–4] but many of the parasites and their vectors that cause these infections are undermapped and the lack of crucial knowledge about the basic biology of these parasites have hindered disease treatment and control. This research continues to address these gaps by implementing surveillance of *Mansonella ozzardi* in the Colombian Amazon (chapter 2) and by profiling and characterizing aminergic (chapter 3) and dopaminergic (chapter 4) G protein-coupled receptors (GPCRs) in *Brugia malayi*. Using molecular and computational approaches, my research progresses the field's understanding of the basic biology and epidemiology of *Mansonella* and amasses critical information about *Brugia* biogenic amine GPCRs with the potential for anthelmintic discovery.

In chapter two, I implemented loop mediated isothermal amplification (LAMP) assays to comparatively benchmark diagnostic approaches for *M. ozzardi* in indigenous individuals in the Colombian Amazon region and used generalized linear models to begin to disentangle clinical and sub-clinical impacts of *M. ozzardi* on infected individuals. Our seroprevalence studies included 235 individuals and revealed the classical, gold standard diagnostic approach was severely under estimating *Mansonella* prevalence compared to LAMP assays using DNA from whole blood (13% compared to 40%, respectively). Genomic analysis confirmed the species and sequenced isolates clustered closely with other isolates from South America. Statistical models for *M. ozzardi* infection status did not significantly correlate to any reported symptoms or serology results and more data is needed to continue to explore pathogenicity and risk factors of infection. We established a cryopreservation technique that allows for lab-based studies of viable microfilariae and potentially the development of infectious stage larvae which may provide critical information on *Mansonella* anthelmintic drug responses. This research establishes novel information on *Mansonella* prevalence in Colombia, outlines methods for

molecular surveillance, and provides a framework to continue the study of this severely neglected parasite infection.

In chapter three, I show that GAR-3 is a cholinergic GPCR that is highly-expressed across the *Brugia* life cycle and I use novel spatial *in situ* techniques to localize receptor transcripts to critical parasite tissues which provide insight into receptor function. Using multivariate parasite assays and utilizing the model organism *C. elegans*, I profile responses to muscarinic and nicotinic compounds to deorphanize and pharmacologically profile *Bma*-GAR-3. Finally, I established a high-throughput assay (HTA) to screen parasite receptors expressed in *C. elegans* pharynx to measure phenotypic modulation under drug perturbation. This research provides information on the basic biology of *Brugia* by way of muscarinic neurotransmitter receptors that likely regulate critical physiological processes and establishes a platform for the continued studies of parasite and free-living nematode receptors.

In chapter four, I build off of my previous research on the muscarinic receptor, Bma-GAR-3, and expand my exploration of receptors mediating aminergic neurotransmission. I leverage a neurotransmitter library of 661 aminergic compounds in multivariate assays across both Brugia spp. and C. elegans. I prioritize a set of twelve dopaminergic compounds that have strong antiparasitic effects on B. malayi mf and screen this subset of compounds for adulticidal effects. This research seeds valuable knowledge on BA-GPCRs as drug targets, expands our understanding of helminth basic biology, and validates new methods for novel anthelmintic drug and target discovery.

5.2 Future directions

I have designed a research plan to continue the work in my fourth chapter. This plan includes 1) genetic screens in *C. elegans* to gain insight into receptors mediating phenotypic effects observed in HTA, 2) heterologous expression of receptors of interest in mammalian cell lines to

further pharmacologically profile and characterize these putative anthelmintic targets, and 3) spatio-temporal localization of lead receptors using methods defined in chapter 3.

5.3 Continued needs for the field

Helminth infections remain the most common infections worldwide with nearly two billion individuals infected and over five billion at risk [5,6]. Current treatment and control strategies are insufficient, relying on suboptimal anthelmintics and low sensitivity surveillance strategies or poor resolution disease mapping data. Current anthelmintics lack strong efficacy against some mammalian-dwelling life stages [7,8] and there are differential responses to anthelmintics across species [9–11]. Continued research on the basic biology of helminths can help break the cycle of 'lack of discovery' for anthelmintics and anthelmintic targets. This fundamental knowledge about druggable targets in helminths will help seed both whole-organism and target-based screening approaches and provide insight into interpreting the results of these screens. Higher sensitivity point-of-care diagnostics are needed for directing and monitoring treatment regimes, understanding co-endemicity, and accurate mapping of helminth infections. Molecular diagnostics provide a cost effective path forward for improving sensitivity and species specificity and can aid in mapping prevalence of both helminths and their vectors (where applicable).

Sanitation and improved water quality can facilitate eradication of these helminth infections. However, climate change threatens the success of current elimination programs and may roll back progress made over the last several decades [6,12,13]. Combined approaches of mass drug administration, climate initiatives, vector and environmental transmission control, and more sensitive diagnostics combined with advancements in drug target and anthelmintic discovery will help ensure continued progress toward elimination of helminth infections.

References

- Hotez PJ, Alvarado M, Basáñez M-G, et al. The global burden of disease study 2010: interpretation and implications for the neglected tropical diseases. PLoS Negl Trop Dis. 2014; 8(7):e2865.
- Mitra AK, Mawson AR. Neglected Tropical Diseases: Epidemiology and Global Burden. Trop Med Infect Dis [Internet]. 2017; 2(3). Available from: http://dx.doi.org/10.3390/tropicalmed2030036
- Bélard S, Gehringer C. High Prevalence of Mansonella Species and Parasitic Coinfections in Gabon Calls for an End to the Neglect of Mansonella Research. J Infect Dis. 2021; 223(2):187–188.
- 4. Lima NF, Veggiani Aybar CA, Dantur Juri MJ, Ferreira MU. Mansonella ozzardi: a neglected New World filarial nematode. Pathog Glob Health. **2016**; 110(3):97–107.
- 5. Pullan RL, Brooker SJ. The global limits and population at risk of soil-transmitted helminth infections in 2010. Parasit Vectors. **2012**; 5:81.
- 6. Blum AJ, Hotez PJ. Global "worming": Climate change and its projected general impact on human helminth infections. PLoS Negl Trop Dis. **2018**; 12(7):e0006370.
- 7. Laing R, Gillan V, Devaney E. Ivermectin Old Drug, New Tricks? Trends Parasitol. **2017**; 33(6):463–472.
- 8. Irvine MA, Stolk WA, Smith ME, et al. Effectiveness of a triple-drug regimen for global elimination of lymphatic filariasis: a modelling study. Lancet Infect Dis. **2017**; 17(4):451–458.
- 9. Hu Y, Ellis BL, Yiu YY, et al. An extensive comparison of the effect of anthelmintic classes on diverse nematodes. PLoS One. **2013**; 8(7):e70702.
- Francis H, Awadzi K, Ottesen EA. The Mazzotti reaction following treatment of onchocerciasis with diethylcarbamazine: clinical severity as a function of infection intensity. Am J Trop Med Hyg. 1985; 34(3):529–536.
- 11. Geary TG. Are new anthelmintics needed to eliminate human helminthiases? Curr Opin Infect Dis. **2012**; 25(6):709–717.
- 12. Okulewicz A. The impact of global climate change on the spread of parasitic nematodes. Ann Parasitol. **2017**; 63(1):15–20.
- 13. Short EE, Caminade C, Thomas BN. Climate Change Contribution to the Emergence or Re-Emergence of Parasitic Diseases. Infect Dis. **2017**; 10:1178633617732296.